Charlotte Björk Ingul

Quantification of regional myocardial function by strain rate and strain for evaluation of coronary artery disease

Automated versus manual analysis during acute myocardial infarction and dobutamine stress echocardiography

Doctoral thesis
for the degree of doctor medicinae

Trondheim, August 2006

Norwegian University of Science and Technology
Faculty of Medicine
Department of Circulation and Medical Imaging

NTNU
Innovation and Creativity

NTNU
Norwegian University of Science and Technology

Doctoral thesis
for the degree of doctor medicinae

Faculty of Medicine
Department of Circulation and Medical Imaging

ISBN 82-471-8095-2 (printed version)
ISBN 82-471-8094-4 (electronic version)
ISSN 1503-8181

Doctoral theses at NTNU, 2006:163

Printed by NTNU-trykk

Contents

1. Acknowledgements

The Faculty of Medicine, Norwegian University of Science and Technology, financed a four year scholarship from 2001 to the beginning of 2006. The research has taken place at the Department of Circulation and Medical Imaging and at the Section of Cardiology, Department of Medicine, St. Olavs Hospital, Trondheim University Hospital, where the patients were recruited and examined. A year from June 2004 to June 2005 was spent at the University of Queensland, Department of Cardiology, Princess Alexandra Hospital, Brisbane, Australia, financed by the Norwegian Research Council.

My main supervisor Stig Slørdahl was brave enough to ask an anaesthesiologist to enter a technical cardiology research field. With an endless enthusiasm he has supported me during the study time and let me go my own ways. He has always responded my questions instantly and given me support on all levels.

Asbjørn Støylen, my co supervisor, has been my constant source of expert knowledge in the field (and cardiology in general) and hand on support. He taught me everything I needed to know about SRI, echocardiography and especially DSE, a time-consuming process. His ideas have been the red line I have followed and when I entered my own he was open to support. He even took the long way to Australia.

Hans Torp, my technical supervisor, financed the first six months of my research. He has been my inspiration for trying to understand the technical aspects of ultrasound and has supported me with students during the development of an automated analysis of SRI.

Svein Arne Aase whom I have worked closely with at the Institute, has been invaluable with his technical support and advancement of the automated method including automatic timing events.

Sigrid Berg and Anna Leivestad who after my initiation created the first version of the automated analysis.

Knut Bjørnstad who did the WMS for the DSE study and Rune Wiseth for the angiographic measurements.

Research nurses Eli Granviken and Ann-Elise Antonsen for being constant source of helpfulness and assistance in the patient studies.

To the cardiology department in general, where I did my last training for my specialisation in anaesthesiology. Without the positive atmosphere and kind colleagues I would never have entered this research field.

Tom Marwick, a brilliant cardiologist and researcher, was my supervisor in Australia and gave me unique knowledge in the evaluation of stress echocardiography and access to their large DSE database. This collaboration resulted in the two last manuscripts with a number of patients impossible to obtain at St Olavs Hospital. He taught me never to stop, which led to new perspectives and knowledge. His intensity and presence with his PhD students was overwhelming. I also want to thank his hardworking group and the sonographers for doing all the images for the studies.

Siri Malm, my dear friend and colleague, whom I through the years have shared joy and frustration has been of great support.

I also want to thank Vidar Lundberg and Jørgen Mæhle (GE Vingmed) for their technical assistance.

Finally and most important Øyvind, my dear husband, who has been extremely patient, supportive and always there when needed. My lovely sons Christian and Fredrik have always been fascinated by the ultrasound images, but have suffered from a mother being away too much.

2. List of papers

Paper I

Bjork Ingul C, Stoylen A, Torp H, Skjaerpe T, Slordahl S. Recovery of stunned myocardium in acute myocardial infarction quantified by Strain Rate Imaging. A Clinical Study. J Am Soc Echocardiogr 2005;18(5):400-9.

Paper II

Bjork Ingul C, Torp H, Aase S, Berg S, Stoylen A, Slordahl S. Automated Analysis of Strain Rate and Strain; Feasibility and Clinical Implications. J Am Soc Echocardiogr 2005;18(5):410-7.

Paper III

Bjork Ingul C, Stoylen A, Slordahl S, Wiseth R, Burgess M, Marwick T. Application of Strain Rate Imaging with Automated Analysis to Dobutamine Stress Echocardiography: An Angiographic Comparison.

Paper IV

Bjork Ingul C, Rozis E, Slordahl S, Marwick T. Incremental Value of Strain Rate Imaging to Wall Motion Analysis for Prediction of Outcome in Patients Undergoing Dobutamine Stress Echocardiography.

3. Abbreviations and definitions

AMI - acute myocardial infarction

AUC - area under the ROC curve

AVC - aortic valve closure

CAD - coronary artery disease

CI - confidence interval

CV - coefficient of variation

DSE - dobutamine stress echocardiography

fps - frames per second

LV - left ventricle

MI - myocardial infarction

PSI - postsystolic strain index= (peak strain)-(end-systolic strain)/ peak strain

PSS - postsystolic shortening

QCA - quantitative coronary angiography

ROC - receiver operating curve

ROI - region of interest

SD - standard deviation

S_{es} - end-systolic strain

S_{peak} - peak strain

SR - strain rate

SRI - strain rate imaging

SR_s - peak systolic strain rate

TDI - tissue Doppler imaging

t_{SRs} - time to peak systolic strain rate

WM - wall motion

WMS - wall motion score

WMS - wall motion score index

4. Introduction

Echocardiography has become an important diagnostic tool in coronary artery disease (CAD). Conventional two-dimensional echocardiography for assessment of regional myocardial function at rest or at stress test (exercise or pharmacological) is a subjective technique limited by the visual assessment. To be able to quantify the complex motion of the cardiac cycle, tissue Doppler imaging (TDI) was introduced [1-3] including the modalities of myocardial velocity-, displacement-, strain rate- and strain imaging. Doppler myocardial velocities can detect abnormal regional function, but due to tethering to adjacent myocardial segments, the exact position of the ischemic segment within a cardiac wall cannot be determined. Velocity data alone is also influenced by overall heart motion and rotation, and detect motion rather than regional deformation. Myocardial velocity is more a global measurement of the ventricle than a regional.

A regional measurement of deformation, strain rate imaging (SRI), was developed to overcome the limitations of velocities at our Department by Heimdal et al. [4]. SRI is obtained by the use of velocities and includes the modalities of strain rate and strain. Strain is a measure of tissue deformation and strain rate deformation rate. As the ventricle contracts, muscle shortens in the longitudinal and circumferential dimensions (a negative strain) and thickens or lengthens in the radial direction (a positive strain). Strain rate measures the time course of deformation, and is the primary parameter of deformation derived from tissue Doppler. SRI is not affected by tethering or aliasing.

SRI has been shown to quantify regional myocardial function in experimental studies with sonomicrometry [5], as well as been validated against MRI [6] and in several clinical studies [7-9]. It has also been established that SRI as a clinical application can diagnose viability [10, 11] and some cardiomyopathies [12-14]. Two small studies have confirmed that the use of SRI during dobutamine stress echocardiography (DSE) is feasible and more sensitive than wall motion score (WMS) [15-17]. Application of tissue Doppler during cardiac resynchronization therapy has shown contrary results whether velocities or SRI is the optimal method. Normal values for SRI parameters have not yet been established in a large population.

The ejection of blood during left ventricular (LV) contraction is caused by the apex-to-base (longitudinal) shortening with secondary myocardial wall thickening in radial direction due to incompressibility of the heart. Systole is also a function of LV torsion due to oppositely directed apical and basal rotation. This necessitates complex myofibre rearrangements during systole. The myofibres within the LV wall are organized in a helical pattern from base to apex by obliquely running sheets of fibres. The fibre orientation of the subendo- and subepicardium is mainly longitudinal, and circumferential in the mid-myocardium. Longitudinal deformation can be measured by SRI because of the structure of the subendocardial muscle fibres, which are the most difficult to perfuse with blood distributed from the epicardial coronaries.

Due to the limitations of SRI being highly dependent on insonation methodology, acquisition frame rate, and noise component in the data acquired, it has been slow to emerge as a clinical routine method. Any noise in the velocity data set will be amplified

during strain rate calculation causing a low reproducibility. Furthermore manual analysis, especially if tracking of the tissue is used, is time-consuming.

Other techniques for quantifying regional myocardial function have recently been introduced to overcome the angle dependency of SRI. Strain rate and strain are calculated from the speckle pattern in the grey scale images. The clinical utility of that method has not yet been shown.

This thesis has concentrated on longitudinal assessment of regional function as radial function is limited to a few segments of the parasternal long- and short-axis views. We introduced an automated method for the analysis of stress echo based on a combination of the velocity gradient in tissue Doppler images and the speckle pattern in the grey scale images.

5. Background

5.1 Tissue Doppler Imaging

Observer expertise is required for acceptable accuracy of stress echocardiography and visual assessment of asynchronicity is limited to 70-100 ms [18, 19]. However, this is in real time assessment. As most evaluation is done in post processing, with the possibility for reduced replay speed, or even stepped frame by frame analysis, the real temporal resolution of B-mode is limited only by the frame rate. However, while B-mode has a frame rate of 30-70 frames per second (fps), tissue Doppler has a potential frame rate of at least 150, even in full sector.

Tissue Doppler signals from the myocardium are obtained by inverting the filter settings for blood flow Doppler by selecting signals with low velocities and high peak values. The colour Doppler myocardial signal is usually superimposed on the two-dimensional grey scale image. The pixels are colour coded and represent numerical velocity. TDI measures velocities by the Doppler shift of reflected ultrasound. Myocardial velocities can be obtained from either pulsed Doppler spectral display or mean velocities extracted from colour Doppler mode. Longitudinal velocities can be measured from the three apical views and radial velocities from the parasternal views.

5.2 Strain rate imaging

Strain rate can be obtained as the spatial derivation of the velocity gradient along the ultrasound beam. Strain rate can be calculated by taking the velocity difference between two neighbouring points in the tissue (v1 and v2) and divide them by the distance between the points (L, which is the offset length or strain length): strain rate = (v1-v2)/L, meaning that the unit of strain rate becomes s^{-1}. It can be shown that this is equal to the rate of deformation, i.e. the strain rate. Longitudinal rate of deformation changes are expressed as negative strain rate values during systole (rate of shortening), positive strain rate values during diastole (rate of lengthening) and zero if there are no changes. Strain is measured by temporal integration of strain rate and is a dimensionless quantity (expressed in %). Strain measures the local deformation, relative to its initial length.

The disadvantage of strain rate is the unfavourable signal to noise ratio as the signal is a gradient between two points and noise from both points will be added, resulting in a noisy signal, which will affect the reproducibility of the method. However strain is less noisy, because the curves are smoothed during the integration, thus omitting the majority of the noise. On the other hand strain has problems related with drift from the baseline because of the integration process. In normal myocardium the peak of strain rate is measured in the first third of the cardiac cycle and strain at the end of systole. Urheim et al. demonstrated in an animal model that volume loading markedly increased peak strain and peak systolic strain rate (SR_s), with unchanged peak systolic elastance [5]. An experimental study on normal myocardium demonstrated the correlation

between SR_s and dP/dt (an index of contractile function), whereas peak strain correlated best with changes in stroke volume and, therefore, was more closely related to changes in global hemodynamics than changes in contractility [20]. Tissue Doppler measures only one component of the true velocity vector and the velocities along the ultrasound beam are therefore angle-dependent as all secondary measures based on Doppler velocities. Strain rate is even more so; in an experimental study Heimdal et al. showed a 46% reduction in SR_s with an angle of 25 degrees between the ultrasound beam direction and the direction of the myocardium [21]. In a one-dimensional object, the only possible deformation is lengthening or shortening, which limits the measurement of radial, circumferential and longitudinal function in the same segments. However, the heart is three-dimensional and deformation is described by nine strain components. The three normal strain components represent the wall thickening/thinning (transmural strain), longitudinal shortening/lengthening of the wall (longitudinal normal strain) and circumferential shortening/lengthening of the wall (circumferential normal strain).

A speckle pattern is produced by the interference of reflected ultrasound. Each region of the myocardium has a unique speckle pattern because of the random distribution of the backscattered signals. A search algorithm is used to find the matching kernel region (an area with a unique speckle pattern) in a search area from frame to frame. The position where the highest similarity of the kernel region is found determines the displacement relative to its original position. Tracking the speckle patterns has been shown effective for angle independent imaging of blood flow and tissue motion [22, 23]. Strain by speckle tracking has recently been validated against ultrasonomicrometry [24] and for estimation of regional LV rotation and torsion [25-27].

Speckle tracking and two-dimensional strain only uses the grey scale data and requires a sufficient frame rate, dependent on the image quality, usually around 50 fps to be able to follow the grey scale pattern from frame to frame. Two-dimensional strain by RF data has also been introduced [28]. Advantages are angle independency, the ability to track in two directions, tracking along the wall and not along the ultrasound beam, and improved lateral resolution.

5.3 Automated analysis

Most prior related research on automated methods in echocardiography has focused on endocardial border tracking to assess regional LV function in the grey scale images, or by the RF signal. Detection of both endocardium and epicardium has been used in an attempt to automatically evaluate wall thickening [29]. Automated edge detection has been based on the detection of the blood pool-endocardial border as a discontinuity in integrated backscatter displaying the endocardial motion in real time [30]. Colour kinesis is an extension of this technology, which in addition generates for each frame a binary blood-tissue mask image in which each pixel is classified as either blood or tissue.

The potential clinical use was quantitative diagnosis of regional wall motion (WM) abnormality by colour-coded movement of the walls [31]. Online quantification of

regional WM with automated segmental motion analysis was a further development of colour kinesis [32]. Even though there has been a great deal of interest in automatic border identification methods, the utility of the method so far has not been clear and these methods are not widely used in clinical practice.

A further development of the grey scale images using the speckle pattern matching techniques was introduced in 2004 as a real-time automatic echocardiographic assessment of cardiac function [33, 34]. The manual input was tracing a line along LV endocardium and strain rate /strain and tissue tracking were measured with a high accuracy in patients with previous myocardial infarctions (MI). The B-mode frame rate was high (80 fps) compromising the line density resulting in reduced spatial resolution. Speckle tracking in general is limited by the quality of the echocardiograms. Another speckle method with automated tracking system was found to correlate well with myocardial strain by sonomicrometry [35]. The first point in the B-mode image has to be selected manually in the first frame.

5.4 Myocardial infarction

The first clinical study on SRI was a feasibility study by Heimdal et al. demonstrating the use of SRI for regional dysfunction in six patients with MI [4]. Another initial study by Stoylen et al. found a good correspondence between semi-quantitative WM from colour strain rate images (curved M-mode) and grey scale WM in patients with a MI within a week [36]. They have also demonstrated the use of SRI to identify the infarcted-related artery identified by angiograms in acute MI, both semi-quantitatively and quantitatively by strain rate traces [7]. In a study on transmural infarcts SR_s, systolic strain and early diastolic strain rate showed pronounced reduction in chronically infarcted regions compared to normal segments [37]. A clinical validation study of strain in patients with acute MI found a good correlation between echocardiography and MRI [6]. Tissue Doppler with a high temporal resolution has given a new insight into the mechanical events of the cardiac cycle. Acute ischemia induces sequential changes in the contraction pattern of which the longitudinal changes can be quantified by SRI. In early systole, strain rate and strain traces will initially show positive values representing the early systolic lengthening, followed by a reduction in the peak value and a delayed strain rate peak, showing decreased contractility [8, 38]. Thereafter delayed contraction is represented by an extra peak after aortic valve closure (AVC), post systolic shortening (PSS). Typical peak values of acute and chronic ischemia are $SR_s < -1\ s^{-1}$ and end-systolic $S_{es} < -15\%$.

Pulsed wave tissue Doppler velocities were used by Garcia-Fernandez et al [39] in an experimental model of acute ischemia, demonstrating that up to 40% of the segments may have measurable regional diastolic motion abnormalities whereas transmitral diastolic Doppler inflow pattern remained normal. The same group showed in a clinical study that the regional diastolic WM was impaired in ischemic myocardial segments, even when systolic contraction was preserved [39]. However the clinical importance of

a suppressed diastolic function in the initial phase of an acute MI is not fully clear, but could be a sensitive marker.

5.5 Dobutamine stress echocardiography and the diagnosis of coronary artery disease

DSE is a sensitive and specific test for the diagnosis of CAD and has been validated in numerous studies [40-42]. The conventional method is based on visual assessment of stress-induced changes in WM and other semi-quantitative approaches such as ejection fraction and LV end-systolic volume has been used. They are markers of the extent and severity of disease and can identify patients at high risk of cardiovascular events. However, the technique is demanding, both to perform and interpret and limited by relaying on the development of stress-induced abnormalities of wall motion and thickening. Only trained experts have a high enough accuracy [18]. In addition, the variability of interpretation of stress echocardiography increases in between centres [43, 44].

DSE predicts presence of significant CAD by detection of ischemic myocardium during stress. DSE is also an independent predictor of cardiac death with an increasing risk of death with the extent of abnormal wall motion [45, 46]. Patients with a negative dobutamine stress test have a very low risk of cardiac events (1.4%/year) and cardiac death (0.7%/year) [47].

Digitized side-by-side synchronized reading [48] as well as second harmonic imaging [44] has improved accuracy and reduced variability, but the method remains expertise dependent [49]. The extent of coronary disease may be underestimated as the systolic wall motion abnormalities occur late in the ischemic cascade compared to other techniques that pick up earlier changes involving perfusion or diastolic function.

To improve the accuracy of stress echocardiography different techniques have been introduced; myocardial contrast perfusion imaging [50, 51], three dimensional echo [52] and methods to quantify regional wall motion [53].

TDI has been introduced as a quantitative and more objective method for assessing myocardial function in DSE. Tissue Doppler velocities have been shown to increase the diagnostic accuracy of DSE, but due to the tethering effect ischemia can be diagnosed but not located [49, 54-56]. SRI is unaffected by tethering and heart translation making the method applicable to diagnose the presence of coronary disease, which might exceed the accuracy of scintigraphy and other non-invasive techniques. Table 1 summarizes the experimental and clinical studies combining DSE and SRI.

Table 1. Clinical and experimental dobutamine stress echocardiography studies using SRI for the diagnosis of coronary artery disease

Author	Exp/ clin	Number	Feas/viab/ ischemia study	Reference method	SRI parameter	Cutoff value	AUC/ Feas	Sens	Spec
Kowalski	Clin	22	Feasibility	Angio					
Voigt	Clin	44	Ischemia	Angio/	PSI	>0.35	0.90	82	85
				SPECT	CAMM SR			86	89
Hanekom	Clin	207	Ischemia	Angio	SR_s	-0.95	0.80	96	62
Bjork Ingul	Clin	197	Ischemia	Angio	SR_s	-1.3	0.90	89	93
Abraham	Clin	60	Ischemia		TR	>20%	/90%	92	75
Armstrong	Exp	8 dogs	Ischemia		Peak strain	↓ 8%			
Jamal	Exp	16 pigs	Contr.res.		SR_s				
Weidemann	Exp	11 pigs	Ischemia	P.elastance	SR,S,PSS				
Miyasaka	Exp	7 pigs	Ischemia		Radial SR_s	4.84	1	100	100
Greenberg	Exp	7 dogs	LV contr.	P.elastance	SR,S				
Yip	Exp	14 pigs	Ischemia	RMBF	SR_s			81	91
					TR			65	91
Hanekom	Clin	55	Viability	Angio	Viability m.		0.88	82	80
Hoffman	Clin	37	Viability	PET	SR_s		0.89	83	84
Bjork Ingul	Clin	700	Prognostic		Mean SR_s	>-2	0.73	75	60

AUC - area under the curve, angio - angiography, clin - clinical, contr. res. - contractile reserve, exp - experimental, feas - feasibility, p.elastance - peak elastance, PET - positron emission tomography, PSS - postsystolic shortening, RMBF - regional myocardial blood flow, sens - sensitivity, spec - specificity, SR - strain rate, SRI - strain rate imaging, SR_s - peak systolic strain rate, S_{es}- endsystolic strain, SPECT - myocardial perfusion scintigraphy ,TR - time to onset of regional relaxation, viab. - viability, viability m.- viability model, ↓ 8% - decrement by 8% after 90 seconds occlusion. Paper III is the reference for ischemia study (Bjork Ingul) and paper IV for the prognostic study (Bjork Ingul). References to the studies above [10, 11, 15, 17, 57-64].

Low-dose dobutamine challenge cannot only differentiate between acute ischemic and stunned myocardium, but also between chronic transmural infarction and non-transmural infarction [65, 66]. A non-transmural infarction is characterized by markedly reduced peak systolic strain rate/strain at rest and some PSS. During a low-dose dobutamine challenge a non-transmural infarct will exhibit an ischemic response, i.e., an increase in PSS associated with a reduction or no change in peak systolic strain rate /strain [65]. A transmural infarction is characterized by either no measurable systolic deformation or the presence of abnormal thinning/lengthening at rest, with no inducible increase in thickening/shortening during a dobutamine challenge [65]. The transmural extension of the scar could be defined by the regional deformation response with the lower the systolic deformation the greater the transmural extension of scar in the region at risk [65].

6. Aims of the study

1. To evaluate the potential of SRI in prediction of recovery of function after an acute myocardial infarction (AMI) by conventional manual measurement and to follow the time course of these changes

2. To develop an automated method of analyzing SRI and assess the feasibility, repeatability and accuracy in normal subjects and patients with AMI

3. To test the ability of SRI to predict the presence of significant CAD, to decide the optimal variable of SRI and normal values in a large DSE population using the automated method.

4. To investigate the prognostic potential of using SRI in DSE for prediction of mortality compared to conventional grey scale WM analysis

7. Material and methods

7.1 Study subjects

Patients were included from two different centres; St. Olavs Hospital, Trondheim University Hospital, Trondheim, Norway (paper I, II, III) and Princess Alexandra Hospital, Brisbane, Australia (paper III, IV). The Brisbane populations were all recruited from a DSE database and WM previously scored by Dr. Marwick. Only patients with coronary angiography done within six months after DSE were included. The tissue Doppler data was then analyzed by me. The patients from Trondheim were included consecutively after having an angiography performed and underwent a DSE within three months (by either Dr. Støylen or myself). Patients who underwent the test for study purposes gave written informed consent and the study was approved by the respective ethics committees.

In total there were 61 patients defined as normal based on a normal angiography, normal resting echocardiography and a negative response to DSE (12 had a false positive response) and of these patients, 30 were recruited in Trondheim and the remaining in Brisbane. They were initially referred to angiography because of suspected CAD. The 30 normal patients from Trondheim were used in the studies in both paper II and III.

For paper III, the normal and low risk populations were originally divided into four groups; subjects younger than 50 years with low probability of CAD, subjects older than 50 years with low probability of CAD, normal Trondheim subjects and normal Brisbane subjects. We found no significant differences between the groups in SRI values (Table 2).

Framingham score was used to define patients at low risk (<1%/year) of CAD and 61 patients were included, all from Brisbane. Mean Framingham score was 3.7. These patients did not have coronary angiography performed. A total of 76 patients had an angiography with >50% narrowing of at least one major vessel by quantitative coronary angiography (QCA) and a DSE with normal resting function. The majority (60) of these patients were recruited from Trondheim. Patients with left bundle-branch block, cardiomyopathy, severe valvular heart disease, ongoing atrial fibrillation/flutter were excluded from the DSE studies. The infarct population consisted of 30 consecutive patients with first-time AMI, admitted to the coronary care unit in Trondheim. They were examined day one, seven and 90. Hemodynamically unstable patients were excluded. Four patients were excluded during the study; three had coronary artery bypass surgery and one died during the observation period, thus the final study population consisted of 26 patients. The infarct material was also used in the method study (paper II).

A sub-study was done for paper II in order to evaluate the influence of B-mode frame rate on under-sampling and precision in speckle tracking (method 3), further analysis was done in ten healthy individuals (mean age 28 ± 6 years, 5 women).

No patients had coronary angiography for study purposes alone. Only six patients of a total of 868 (0.7%) were excluded due to poor image quality (1 patient in paper III because of emphysema and no window, and 5 patients in paper IV). The number of women included was 345 (40 %).

Table 2. A comparison of four different populations with a normal response to DSE and the three different methods on calculating strain rate /strain

	Segment length method SR_s		Static velocity gradient method		Dynamic velocity gradient method	
	Rest	Peak	Rest	Peak	Rest	Peak
Low prob <50 (n=30)	-1.37	-2.31	-1.45	-2.67	-1.45	-2.61
Low prob >50 (n=30)	-1.33	-2.16	-1.41	-2.60	-1.41	-2.51
Normal Trond. (n=31)	-1.27	-2.49	-1.35	-2.77	-1.37	-2.85
Normal Brisb. (n=22)	-1.33	-2.23	-1.47	-2.46	-1.42	-2.35

Brisb. - Brisbane, DSE - dobutamine stress echocardiography, low prob. - low probability for coronary artery disease based on Framingham score, SR - strain rate, S - strain, SR_s - peak systolic strain rate, Trond. - Trondheim.

7.2 DSE protocol

After obtaining a resting echocardiogram in parasternal and apical views a standard DSE protocol was performed with incremental dobutamine infusion rates of 5, 10, 20, 30, 40 μg/kg/min for 3 minutes at each dose. Patients who did not achieve 85% of the age-predicted maximal heart rate (220-age) were given atropine until target heart rate was achieved. In Brisbane the patients were given atropine in 0.3 mg increments up to 1.2 mg and in Trondheim initially 0.5 mg and then 0.25 mg up to a maximum of 1 mg. Adjunctive sustained handgrip was added at peak stress in Brisbane if the patient failed to reach target heart rate. Cardiac rhythm and blood pressure were monitored before and during test. Criteria for terminating the test were: severe ischemia evidenced by extensive new wall motion abnormalities, horizontal or downsloping ST segment depression > 2 mm, ST segment elevation > 1 mm in patients without prior myocardial infarction, severe angina; systolic blood pressure > 240 mmHg or < 100 mmHg, serious ventricular arrhythmia, patient intolerance or serious side effects due to dobutamine. The test was considered non-diagnostic if the patient failed to achieve target heart rate without inducible WM abnormality.

7.3 Coronary angiography

Coronary angiography was performed using standard techniques. The angiograms were evaluated by a single observer blinded to the echocardiograph results. Segmental disease was evaluated using a previously described 15-segment American Heart Association model of the coronary tree [67]. Stenosis severity was measured by QCA, using an automated edge detection system (Philips Medical Systems, Eindhoven, the Netherlands). A maximal lumen diameter stenosis of >50 % in any plane was classified as significant. A fixed pattern of correspondence between coronary arteries and walls was used because of the difficulties in accounting for the exact coronary distribution.

7.4 Echocardiographic image acquisition and analysis

The studies were acquired using either a Vivid 5 ultrasound scanner (paper I, II, IV) or a Vivid 7 scanner (paper I, II, III) (GE Vingmed Ultrasound, Horten, Norway). A 2.5-3.5 MHz phased array transducer was used. Recordings were done from parasternal and the three standard apical planes; four-chamber, two-chamber and long-axis. Either one cineloop (paper I, IV) or three cineloops were recorded (paper II, III) simultaneously both in tissue second harmonic mode and tissue Doppler mode from the three apical planes. A complete echo/Doppler study was also recorded for all studies, including parasternal long-axis and short-axis. The pulse repetition frequency (prf) was between 1-1.5 kHz to avoid aliasing. Stress images were recorded at baseline, low-dose, peak and at recovery (paper IV) in a digitized quad-screen format. Echo data was stored digitally and subsequently analyzed offline.

Paper II included an additional B-mode frame rate study. Recordings were made at 70 fps and reduced to 35 fps by removing every second frame in grey scale data in apical four-chamber, two-chamber and long-axis views. The sector angle was set to 60 ° with equal frame rates for B-mode and tissue Doppler images. In all, 160 segments were analyzed and the feasibility for SR_s was 84 %/83 % and for S_{es} 81%/80% (70/35 fps). For 70 fps, SR_s was -1.12 (0.31) s^{-1} and S_{es} -18.7 (5.1) %, compared to 35 fps where SR_s was -1.13 (0.42) s^{-1} and S_{es} -19.1 (5.3) %.

Ejection fraction was measured by endocardial tracings from four-chamber and long-axis planes and Modified Simpson's method used for the calculations (paper I).

The mean frame rate for tissue Doppler (Vivid 7) was 155 fps (range 109 to 209). For B-mode on Vivid 7 it was 49 fps (36-70). The mean frame rate on Vivid 5 was 133 fps (130-147), the same as for B-mode and tissue Doppler. Table 3 summarizes frame rate, number of beams and samples along the ultrasound beam for each paper.

Table 3. A summary of the ultrasound characteristics (frame rate, number of beams and samples) for grey scale and tissue Doppler images

	Paper I	Paper II	Paper III	Paper IV
2D frame rate	83 (36-133)	63 (26-146)	42 (25 to 62)	97 (75 to 133)
tissue Doppler frame rate	152 (109 to 208)	154 (85-209)	150 (92 to 225)	97 (75 to 133)
beams 2D	53 (35-75)	64 (29-111)	93 (52-127)	41 (20-87)
beams tissue Doppler	11 (8-20)	12 (8-24)	15 (8-24)	16 (10-28)
samples 2D	393 (356-421)	393 (323-453)	398 (323-486)	414 (188-486)
samples tissue Doppler	140 (128-172)	149 (122-186)	181 (119-296)	151 (102-258)

2D - two dimensional, frame rate in frames per second, beams - number of ultrasound beams, samples along ultrasound beam.

7.5 Grey scale analysis, echo variables and definitions of segments

Commercially available software was used for the analysis in paper I and for comparison in paper II (EchoPAC PC ^{TM}, GE Vingmed Ultrasound, Horten, Norway).

An experienced observer interpreted the two-dimensional grey-scale echo images according to the American Society of Echocardiography 16-segment model [68, 69] in a 1-4 scale: normal (1), hypokinetic (2), akinetic (3) or dyskinetic (4). Brisbane used severely hypokinetic (2.5) in addition. Wall motion score index (WMSI) was calculated as the average WMS of the number of measurable segments. The observer was blinded to all clinical data except in paper IV.

Paper I defined infarcted segments as segments with WMS >1, corresponding to a location defined by ECG and angiography. The border zone was defined as segments with normal WMS and SR_s between -0.5 s^{-1} and -1.0 s^{-1}, localized between normal and infarcted segments. In a previous study by Stoylen et al. [7] they found that SR_s in normal segments was -1.2 s^{-1} and -0.75 s^{-1} in segments with WMS 2. The cut-off for the normal segments in this study was placed in between these values, as strain rate has a high variability, and normal values have to be defined in rather wide confidence intervals. Return to normalization of SR_s was therefore defined as SR_s value greater than -1.0 s^{-1}. A study was classified as abnormal at rest if there was dyssynergy with or without ischemia at peak.

The number of ischemic segments and scarred segments at peak were also compared. A negative study was characterized by a normal response in all segments.

7.6 Manual analyses

For each segment, a stationary region of interest (ROI) was manually set in early systole in the mid-wall portion of each segment. The size of the ROI was 5 mm laterally and longitudinally adjusted to cover the length (mean 20 mm) of the segment. The velocity gradient was calculated based on several velocities within the ROI. The offset length was 10-12 mm, depending on the noise level. In the basal segments, the ROI was set to avoid the aortic valve plane, and in apical segments the lower third was used to avoid unsuitable angle deviation exceeding 30^0. If artefacts were seen on the B-mode image, the size and position of the ROI was adjusted to avoid these. Linear regression of velocity data and the slope of the velocity gradient were used for the strain rate calculation. Eulerian strain rate was integrated to Lagrangian strain (Figure 4). AVC was used as a time marker for end-systole and was derived from tissue Doppler velocity, pulsed wave, and a sample volume was placed in the basal septal segment in an apical four-chamber view [38, 70].

7.7 Customized software

7.7.1 Automated identification of myocardial segments

For the automated measurements we used a customized post processing system programmed in an engineering interface (GcMat, Vingmed, Horten, Norway) that runs under Matlab (Math Works Inc., USA) (Figure 1). The method was based on using tissue Doppler to track a set of candidate points in all of the ultrasound frames in a cardiac cycle. The points were positioned in the first frame and for the consecutive frames velocity, distance from the probe and grey-scale value stored. First the apex and two points defining the atrioventricular plane, in an apical view, were identified automatically [71]. Secondly an automatic endocardial border detection, using snake algorithm (dynamical programming), positioned 40 points in the endocardium [71]. Then in each wall of the ventricle three segments were defined automatically using two of the points from the endocardial detection. The two points were positioned three mm into the myocardium. In the apical view a total of seven points were displayed on the image, subject to manual adjustment, and tracked. A speckle tracking method, using a pattern matching algorithm of the grey scale data [22] combined with tissue Doppler velocities, was applied to kernels at the segment borders. This enabled the motion of the myocardium to be followed in two dimensions throughout the cardiac cycle, axially (along the ultrasound beam) by tissue Doppler data and laterally by speckle tracking. Tracking by tissue Doppler limited the search area to a sector extending in the lateral direction and thus reduced the time for the speckle search. To avoid drift, the tracking algorithm was applied both forward and backward, and the results were averaged. The position of the kernel regions could be adjusted manually if the tracking was poor. The displacement of the kernel regions was used to check the tracking (Figure 1). The search procedure resulted in tracking of segment position, segment orientation and segment length throughout the cycle.

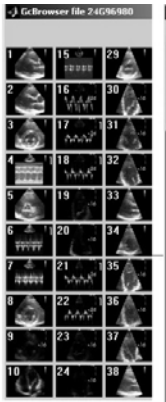

1. GC Browser

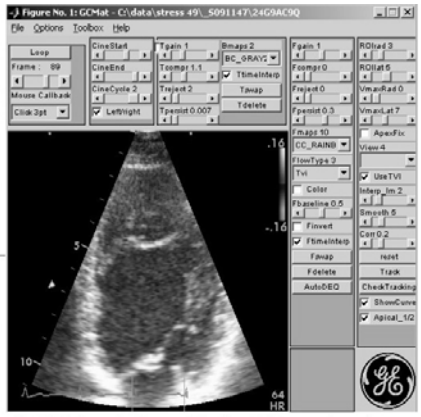

2. GCMat window with the different functions

3. Autodeq divides the ventricle in 6 segments

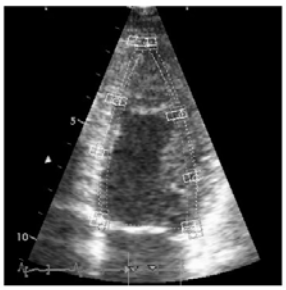

4. Each point is tracked throughout the cardiac cycle

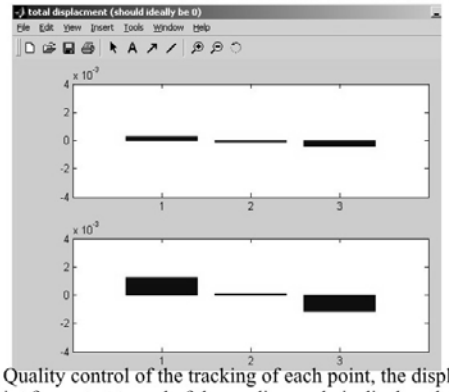

5. Quality control of the tracking of each point, the displacement for each point from start to end of the cardiac cycle is displayed above

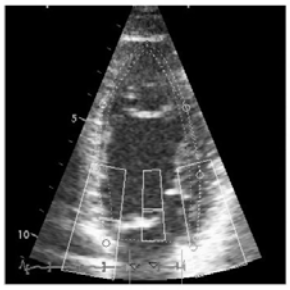

6. AVO and AVC are automatically chosen

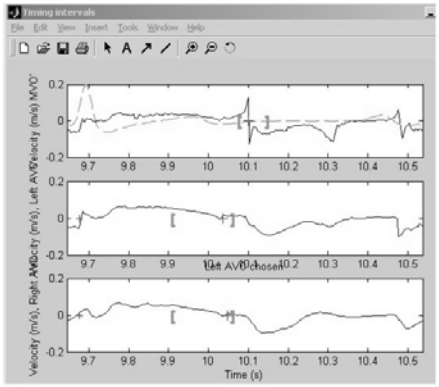

7. Left or right AVC is chosen automatically

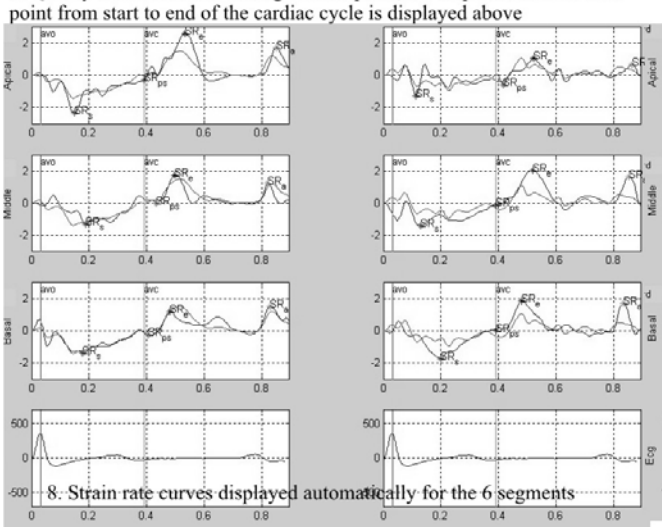

8. Strain rate curves displayed automatically for the 6 segments

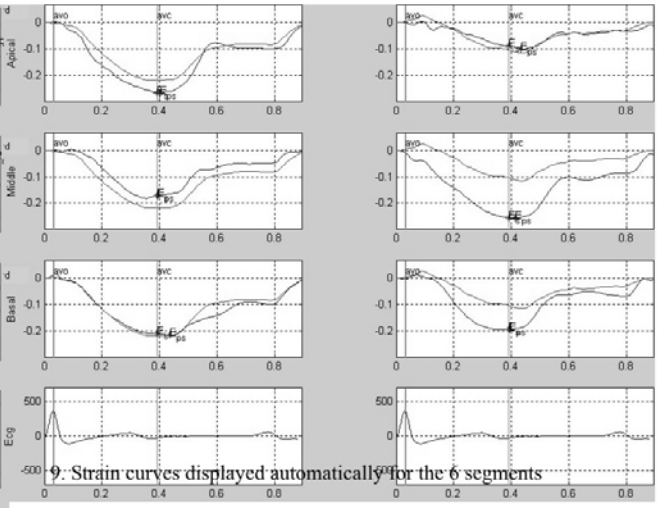

9. Strain curves displayed automatically for the 6 segments

Figure 1. The automated method is illustrated in this figure. Apex and the two points of the mitral ring is detected, a line is then drawn along the mid myocardium, and divided into six segments (4). This can be done fully automated, subject to manual correction, or the points can be placed manually from the beginning. The kernel positions are then tracked automatically throughout the cycle and the quality of the tracking is checked by the total displacement at end cycle (5). AVC is then detected from the tissue Doppler data, subject to manual correction (6). Velocity gradient method or segment length method is chosen to calculate strain rate/strain and then by choosing analyse, strain rate and strain curves are automatically produced (8, 9). Numerical values for the following parameters are stored in a worksheet; peak systolic strain rate, postsystolic shortening, time to peak systolic strain rate, E-wave by SR, time to peak E, A-wave by strain rate, end-systolic strain, strain postsystolic shortening, peak velocity of basal segment, AVC, AVO, heart rate and displacement of AV-plane.

7.7.2 Averaging

The following settings were used; strain length (distance for velocity gradient calculation) 10-15 mm for the tissue Doppler method, axial averaging 1 mm and temporal averaging 10 ms. The optimal temporal averaging for strain rate was simulated in a cardiac cycle with stepwise temporal filtering increasing with 10 ms steps from 0 to 60 ms (Figure 2). Information was taken from only one beam as the spatial resolution is rather poor with increasing depth. The distance between beams is illustrated in figure 3. Vivid 7 data captures B-mode and tissue Doppler data simultaneously. However Vivid 5 does not allow simultaneous acquisition of B-mode and tissue Doppler data resulting in a difference in acquisition time, but this was compensated by temporal interpolation in the speckle tracking algorithm.

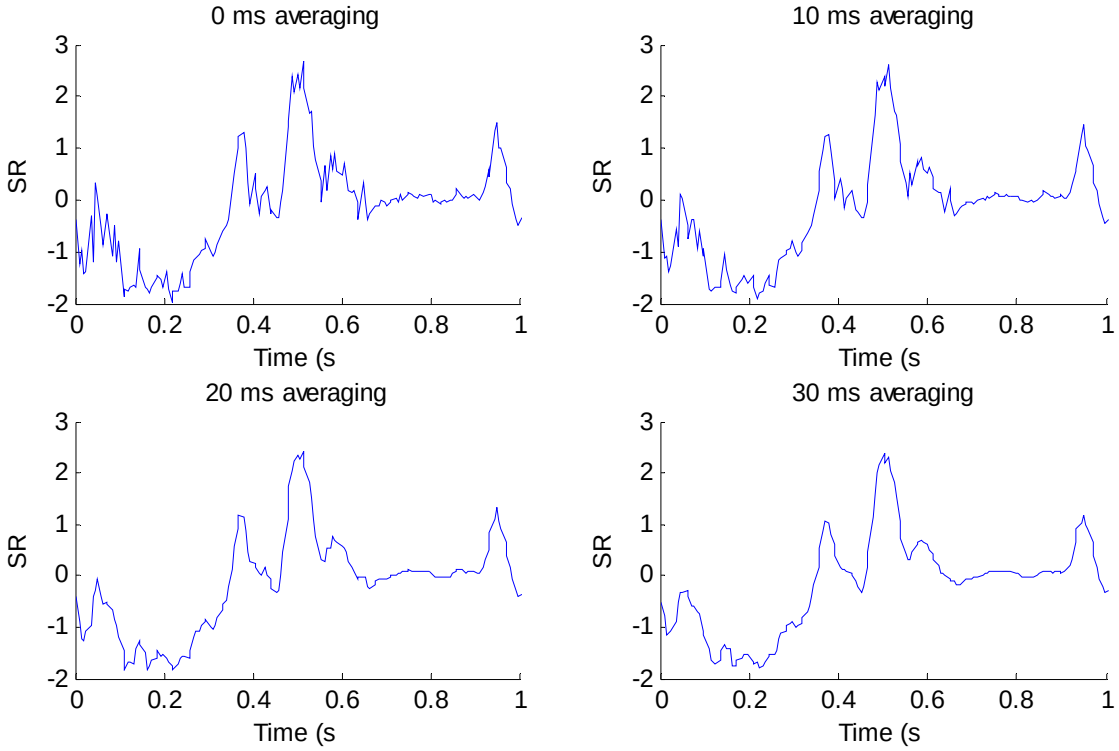

Figure 2. The effect of temporal averaging on strain rate. Top left figure illustrates an unsmoothed strain rate trace with no temporal averaging resulting in a noisy signal. Top right figure with a 10 ms averaging is smoother compared to 0 ms, but at 20 ms there is a reduction in peak systolic strain rate (bottom left figure). Bottom right at 30 ms shows an even smoother trace with further reduction in peak values.

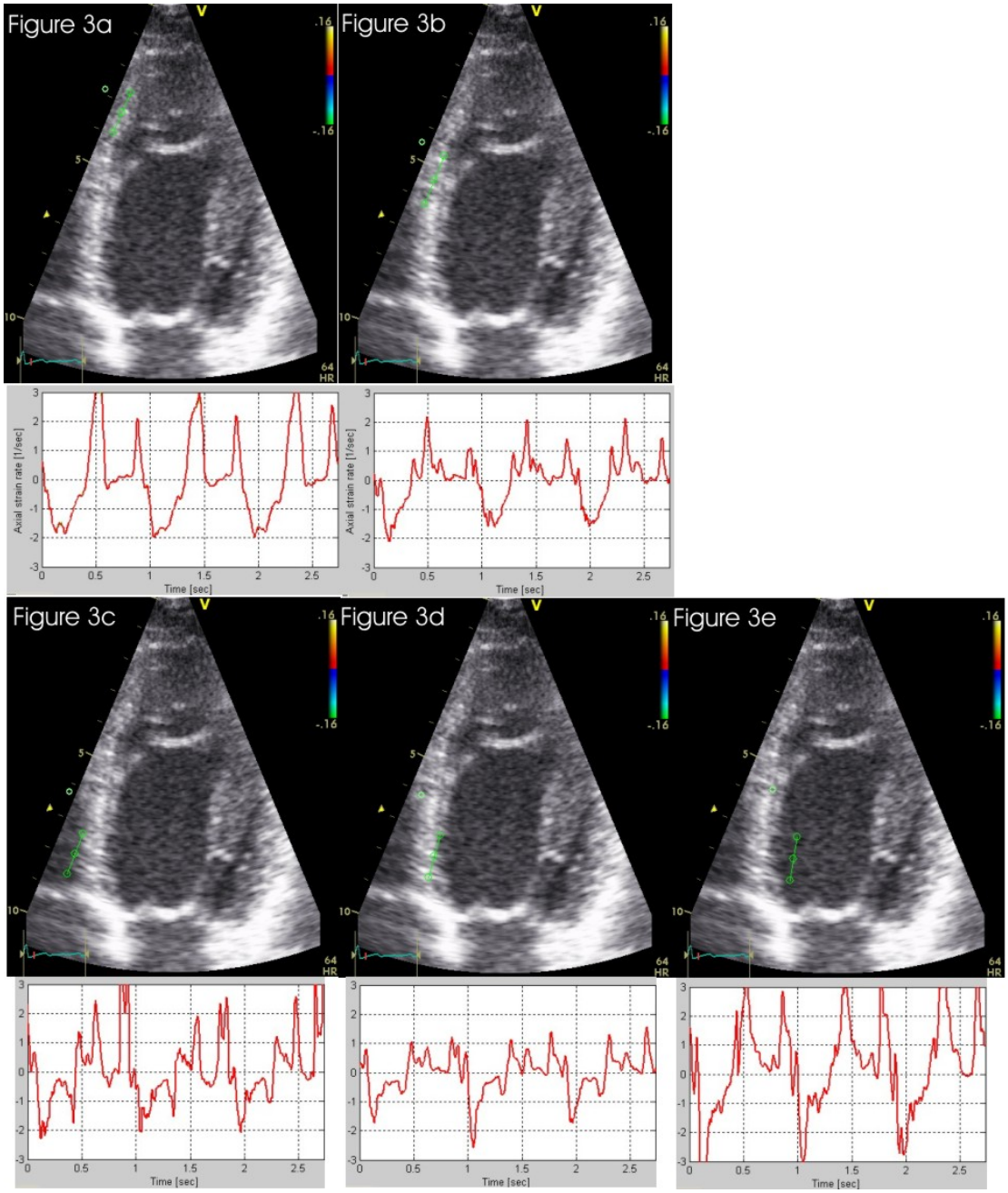

Figure 3. The green line shows the direction of the ultrasound beam and the length of the line is the offset length for strain. The images are frozen in the beginning of systole. In figure 3a, the ROI is set in the apical septum with perfect alignment and the strain rate trace is displayed. In figure 3b, the ROI is set in the mid septum with good alignment. Figures 3c-e illustrates the effect of poor spatial resolution. In this image with 10 tissue Doppler beams, the angle increment (theta) is 0.08 radians and the segment analyzed is 16 cm (radius) from the transducer, the lateral distance (arc length) between the closest beams is 1.27 cm. This makes it rather unlikely that the endocardium and epicardium can be distinguished in the basal segments. Even though the beam in figure 3e is in the blood pool and the beam in figure 3c in the right ventricle, the strain rate traces still look reliable, but should not be used as they have no information on the deformation of the myocardium. The ultrasound beam is in the myocardium in figure 3d.

7.7.3 Methods

SRI parameters were measured in three different ways; either by using velocity data or segment length variation, but tracking was performed in the same way (no tracking in method 1).

Method 1 (*static velocity gradient method*); a stationary ROI was placed automatically in the centre of the defined segment at end-diastole. Strain rate was calculated from the velocity gradient along the ultrasound beam [4] at a fixed position in space (with the same correction as in method 2). Tracking was not utilized in this method, only automated segmentation and ROI placement.

Method 2 (*dynamic velocity gradient method*); a ROI was placed automatically in the centre of the segment at end-diastole, and the mid-point of the segment was tracked throughout the cardiac cycle as described. Strain rate was calculated from the velocity gradient along the ultrasound beam and strain calculated as the temporal integral of strain rate, corrected from Eulerian strain rate to Lagrangian strain, though both being angle dependent (Figure 4).

Method 3 (*segment length method*); strain was calculated directly from the variation of the segment length using the tracked end points: strain = $(L-L_0)/ L_0$. Strain rate was calculated as the temporal derivative of Lagrangian strain, with correction to Eulerian strain rate (Figure 4). This enabled angle-independent measurements of strain rate and strain.

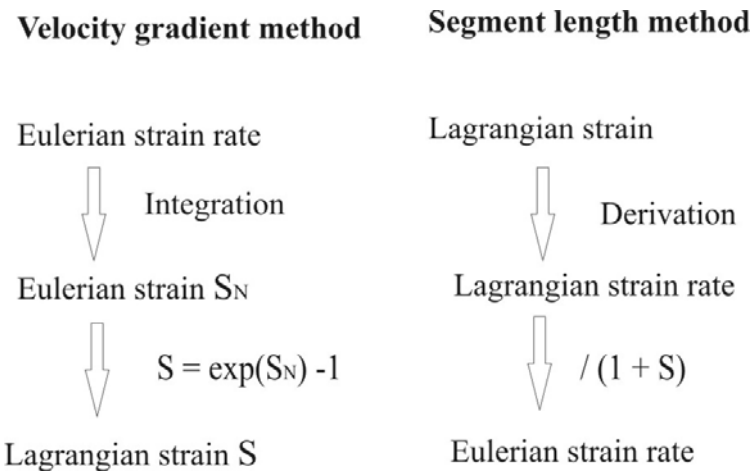

Figure 4. The segment length method calculates strain rate as the time-derivate of strain, but the velocity gradient method calculates strain rate as the velocity-gradient. Eulerian strain rate is used because it is the same as "Myocardial velocity gradient". Eulerian strain rate will give a 15% higher absolute value in end-systole, if strain = 15%. (Eulerian strain rate uses a fixed reference segment length) and a maximal increase of 20%. Therefore a correction factor is applied for the segment length method and the strain rate value is divided with a correction factor (1 + strain).

7.7.4 Aortic valve closure

The timing of aortic valve closure (AVC) was defined from the Doppler spectrum of aortic flow, pulsed wave, in the apical four-chamber view and adjusted to the heart rate in the actual image being analyzed (paper II).

In paper III and IV, the timing of AVC was automatically defined by an algorithm developed at our department, using tissue Doppler imaging [72]. AVC is an abrupt mechanical event, and as the open aortic valve suddenly closes, there is a slight motion away from the ultrasound probe, stopping with a slight "bounce" at the time of the AVC, shifting from negative to positive velocity [73]. AVC can be observed as a notch in the three apical views in tissue Doppler imaging velocity/time curves occurring after ejection, but before early relaxation. Aortic valve opening was then detected and the same algorithm was used, but in a search interval between 15 to 120 ms from the start of the QRS-complex. The highest acceleration in the defined search area was chosen as aortic valve opening. The values were stored and displayed automatically in all curves. The AVC value was stored and displayed automatically in all curves (Figure 1).

7.8 SRI variables

Peak systolic strain rate (SR_s) was determined as the maximal negative strain rate value during ejection and values described in magnitude. PSS was defined as myocardial segment shortening after AVC. Peak postsystolic strain rate (SR_{ps}) was measured as the first negative wave after end-systole, and the cut-off between normal and pathological SR_{ps} was empirically chosen as -0.2 s^{-1}. Time to peak systolic strain rate (t_{SRs}) was measured from aortic valve opening to maximal negative SR value during ejection time. Peak strain rate of early diastolic filling (SR_e) was measured at the peak of the first positive wave following isovolumic relaxation. If more than one peak was seen, they were compared with mitral flow, and the SR_e peak consistent in time with the E-wave of mitral flow was chosen as the correct. The onset of diastole (early filling), E-wave, was measured by pulsed wave Doppler flow in the mitral valve at the level of the tip of the mitral valve leaflets in the apical four-chamber view. Peak strain rate of late diastolic filling, the A-wave (SR_a), was measured as the first positive wave occurring after the P wave on the ECG. End-systolic strain (S_{es}) was measured at AVC. Peak strain (S_{peak}) was measured as the greatest value after end-systole. Post-systolic strain was calculated as the difference between S_{peak} and S_{es}. A post-systolic strain index (PSI) was calculated; $(S_{peak} - S_{es})/ S_{peak}$ [9]. Delta strain rate and delta strain were measured as the difference between baseline and peak level value of DSE.

Measurements were made in 18 segments all blinded from WM results, clinical data and angiographic results.

In paper III; coronary territories were identified as abnormal if any constituent segment has SR_s less than the specified minimum value. All segments supplied by a stenosed coronary artery were labelled "at risk" and the presence of a minimum SR_s value less than the normal range defined the territory as abnormal.

In paper IV; SR_s, S_{es} were either expressed as the segmental value; the number of segments at risk per patient (using a cut-off) or the mean value, which was defined as the risk per patient with mean value (average of all segments measured) less than cut-off.

7.9 Derivation of cut-off values of SR_s, S_{es} and WMSI

In paper III the material was randomly divided. Half of the material was used to define the optimal cut-offs of segments at risk for ischemia using receiver-operating characteristics analysis (ROC-curves) with respect to SR_s, S_{es} and WMSI. The optimal cut-off value was defined as the point with the highest sum of sensitivity and specificity. The remaining half of the material tested these cut-offs. The same was applied to paper IV were half of the material was used to define patients at low and high risk of mortality.

7.10 Statistics

Measurements are presented as mean ± standard deviation (SD). Student's t-test was used for comparison of two variables. For assessing the relationship between variables, Pearson's correlation coefficient was used, and validity of parametric analysis was confirmed by Spearman's rank correlation coefficient. Multiple linear regression was used to test predictors of recovery of myocardial function. One-way analysis of variance (ANOVA) was used to compare mean values between the analysis methods, the patient groups and the time series. Scheffe's method was used to correct for multiple comparisons (Bonferroni's method in paper 1). The area under the ROC curve (AUC) was used for comparison of sensitivity and specificity between methods and variables. McNemar's test was used for paired categorical data. Multivariate analysis was used to establish which parameters were independent. The method of Bland and Altman was used for variability analysis. For intra- and interobserver variability, Bland and Altman 95% limits of agreement and coefficient of variation (CV) were used. Cox models were used to estimate the univariate hazard ratio of event for each variable. Multivariate analyses were determined by the Cox proportional hazards model. A forward stepwise Cox proportional hazard regression model was used to investigate the incremental value of echo variables on clinical variables. Kaplan Meier survival curves were used to estimate the time to death. Log-rank test compared differences between survival curves. A value of $p < 0.05$ was considered statistically significant.

8. Summary of papers

Paper I: Strain rate imaging and recovery of infarcted myocardium

In this study, we compared wall motion, SR_s and S_{es} in 26 consecutive patients with first-time AMI at day one, seven and 90. Initial dyskinesia was seen in 25% of the segments. SR_s was -0.45 s^{-1} and S_{es} -4 %. On the contrary there were no significant changes in S_{es}. An improvement of regional contractility could be seen in the infarcted segments with an increase of SR_s after one week (-0.45 to -0.68 s^{-1}), with no further changes. The same conditions applied to the border zone segments. WMSI showed no significant change the first week, but between one week and three months there was a significant decrease from 1.43 to 1.28. Hyperkinesia was reduced during the first week in the normal segments demonstrated with a decrease of SR_s from -1.41 to -1.31 s^{-1}. Systolic strain showed similar results as SR_s. PSS was present in 60% of the infarcted segments, but did not predict improvement of function.

Paper II: The use of automated analysis in strain rate imaging

This was a method study of a combined use of tissue Doppler and speckle tracking, using a customized post processing system with automated methods of analyzing SRI in 60 patients (30 with MI and 30 normal). SRI parameters were measured in three different ways; either by using velocity data (with or without tracking) or segment length variation. The timing of AVC was automatically detected by using tissue Doppler. SR_s and S_{es} were measured in each segment simultaneously and identified automatically. Standard manual analysis was used as reference. Automated analysis of strain rate and strain was quicker than manual analysis, 2 minutes versus 11 minutes per patient. Accuracy varied between 94% and 96% for the automated methods compared to 96% for the manual method. Values for SR_s were reduced with the method based on segment length variation compared to the velocity gradient methods.

Paper III: Automated strain rate imaging during DSE

In this study SRI was combined with DSE in 198 patients - 76 with and 61 without CAD at angiography, and 61 at low risk of CAD. The automated method was used for analysis of SRI variables. Results were compared with independent WMS by an expert reader. The material was randomly divided into two groups and six SRI variables were analyzed by the automated software. Group 1 established optimal cut-offs for detection of CAD. The optimal variable was SR_s with cut-off -1.3 s^{-1} (AUC 0.90). Group 2 tested the accuracy and the use of SR_s permitted a higher sensitivity/specificity (89%/93%)

than was obtainable with WMS (75%78%). The normalcy of SR_s using the same cut-off was 82%. At peak stress, SR_s was greater in the normal segments compared with segments supplied by stenosed vessels (-2.6 ± 0.9 vs. -2.3 ± 1.1 s^{-1}). For patients without CAD, strain rate was homogeneous across age groups and hemodynamic conditions apart from beta-blocker therapy.

Paper IV: Strain rate imaging and prediction of mortality

All patients that underwent DSE for evaluation of known or suspected CAD during a two year period were included in this study (n = 787). The final study population consisted of 646 patients. Total mortality was identified over 7 years of follow-up (mean 5.2 years ± 1.5 years). SR_s and S_{es} were analyzed by the automated method. Ischemia was detected in 45% of the patients and 39% had a previous MI. Death occurred in 17% of the patients during follow-up. The mortality rate for patients with normal DSE was 2% and for patients with ischemia 5% (both without previous MI). The optimal variable was found by averaging all segments (mean SR_s) with an AUC of 0.73 and cut-off -2 s^{-1}. AUC for the other optimal cut-offs was 0.62 for mean S_{es}, 0.73 for segmental SR_s and for WMSI 0.62.They were all independent predictors of mortality, but in a multivariate analysis only mean SR_s (hazard ratio 2.5) was predictive. Kaplan-Meier survival curves distinguished significantly between low and high risk of mortality for all four variables. Mean SR_s also provided incremental value to WM analysis and clinical data by an increase in overall chi-square from 37 to 59.

9. Discussion

9.1 Myocardial infarction

We showed in paper I that quantification of recovery of function in infarcted segments was superior compared to WMSI. The regional systolic function is impaired in the normally perfused myocardium immediately adjacent to an acutely ischemic region. We found that segments in the peri-infarct area retained some of the function, but contractility was not normalized. The area of the border zone in experimental studies varies widely with region, segment orientation and size of culprit vessel. The clinical importance of the border zones lies in changes of the wall mechanics, which could affect the remodelling process and hypertrophy.

Both early peak and late diastolic strain rate were reduced in paper I, but with less reduction initially and less improvement during follow-up compared to systolic function. Other studies support the reduction of early diastolic strain rate [8, 74].

9.2 Myocardial stunning

In the initial phase of an AMI, it is impossible to differentiate between ischemic myocardium with an inadequate flow and stunned myocardium with adequate reserve, as both show similar abnormal deformation pattern at rest. Experimental studies found that strain rate/strain patterns in stunned myocardium at rest resembled those during severe hypoperfusion. Derumeaux et al. [75] have demonstrated that systolic myocardial velocity gradient partially recovered after the first minutes after reperfusion in stunned myocardium. In paper I, we could follow the regional changes in the ischemic segments and observed an increase in peak systolic strain rate/strain after a one week recovery period, indicative of regress of stunning. This is a promising finding for the follow-up of patients and the need for intervention.

9.3 Postsystolic shortening

Postsystolic thickening or shortening is a phenomenon that occurs after AVC as a shortening of the myocardium accompany decrease in maximal systolic thickening. PSS after AMI has been proposed as a marker of viable tissue and a sensitive marker of ischemia. Experimental studies have confirmed that with increasing severity of acute ischemia, there is a progressive reduction in maximal systolic strain rate/strain with a concomitant increase of PSS [76]. It has also been demonstrated that PSS often disappears after reperfusion in severely infarcted myocardium, probably as a result of the increased stiffness caused by severe oedema, contracture, and cellular and hemorrhagic infiltration [77]. Skulstad et al. found that PSS is a relatively non-specific

mechanism of ischemic myocardium and may occur in dyskinetic segments by an entirely passive mechanism. However, in segments with systolic hypokinesia or akinesia, PSS is a marker of actively contracting myocardium [78]. If PSS itself really is an active process, has not yet been established. In paper I, we showed the presence of PSS in 73% of mid-infarct segments, 60% in infarct segments, 29% in border-zone segments and in 5% of the remaining segments. Most of the PSS had disappeared in the border-zone segments after one week compared to a reduction of half in the infarcted segments at three months. The degree of PSS has been proposed to predict recovery of function; however our data did not support that. As PSS is a non-specific finding it should be evaluated together with deformation indices. Lyseggen et al. proposed in an experimental study that the ratio between systolic lengthening and combined late and postsystolic shortening (L-S ratio) was able to identify active myocardium in dyskinetic segments. However, after 15 minutes of absolute ischemia, the myocardium had become absolutely passive, although remaining viable. Reperfusion of viable myocardium caused a reduction of the L-S ratio, reflecting recovery of function [79]. Another animal study found that in the presence of reduced regional systolic deformation, a higher rate of PSS than systolic shortening identifies acutely ischemic myocardium [80]. Other ratios such as PSI will be discussed under optimal parameters. In healthy individuals, PSS can be found in as much as a third of the segments, but with normal strain rate/strain values [81]. The same study found strain rate/strain to be reduced in infarcted segments, but PSS was more common (79%), with greater values and later peak [81]. In paper I, a cut-off between normal and pathological PSS of >-0.2 s^{-1} was used for strain rate and others have proposed pathological PSS to exceed >20% of the total strain [81], together with a reduction of systolic function.

9.4 Stressechocardiography and SRI

9.4.1 Strain versus strain rate

In normal subjects stroke volume increases from baseline to 20 μg/kg/min and reaches a plateau or decreases with higher doses of dobutamine [82]. Cardiac output increases throughout the infusion, which is primarily mediated by increased heart rate at higher doses. An experimental study showed at varying inotropic states that SR_s correlated well with LV dP/dt_{MAX} as an expression of contractile function ($r = 0.82$; $p< 0.001$) and systolic strain correlated best with global ejection fraction ($r = 0.87$; $p< 0.001$). Strain is more load dependent compared to strain rate which is more related to local contractile function and thus less dependent on changes in preload or afterload [83]. A mathematical model by Claus suggested that SR_s would increase with increasing preload provided preserved contractile reserve, whereas SR_s will decrease both with increasing ventricular size and with increasing afterload [84]. However, there is still a need to further investigate the precise interaction of changes in strain rate and strain versus changes in preload and afterload in clinical practice. Another experimental study found that strain rate was relatively independent of heart rate as SR_s remained constant during atrial pacing increase in heart rate compared to strain that decreased as well as

stroke volume [85]. The first clinical DSE paper was a feasibility study and they demonstrated a continuous increase of SR_s in normal segments from baseline, reaching the highest values at the peak dose [15]. Furthermore, for strain there was an initial slight increase at low-dose, but no further increase with increasing dose. The biphasic strain response to dobutamine infusion is probably an effect of initial increase in stroke volume. Cardiac output increases further with higher doses of dobutamine by an increase in heart rate, as the stroke volume remains constant or falls. Paper III demonstrated an initial increase in strain at low-dose and then a small decrease at peak, which probably represents a fall in stroke volume. In the study in paper III, different heart rate groups were compared at peak stress and strain rate increased to heart rate 140 with no further significant increase (Figure 5). S_{es} was similar in the four heart rate groups at peak (Figure 5).

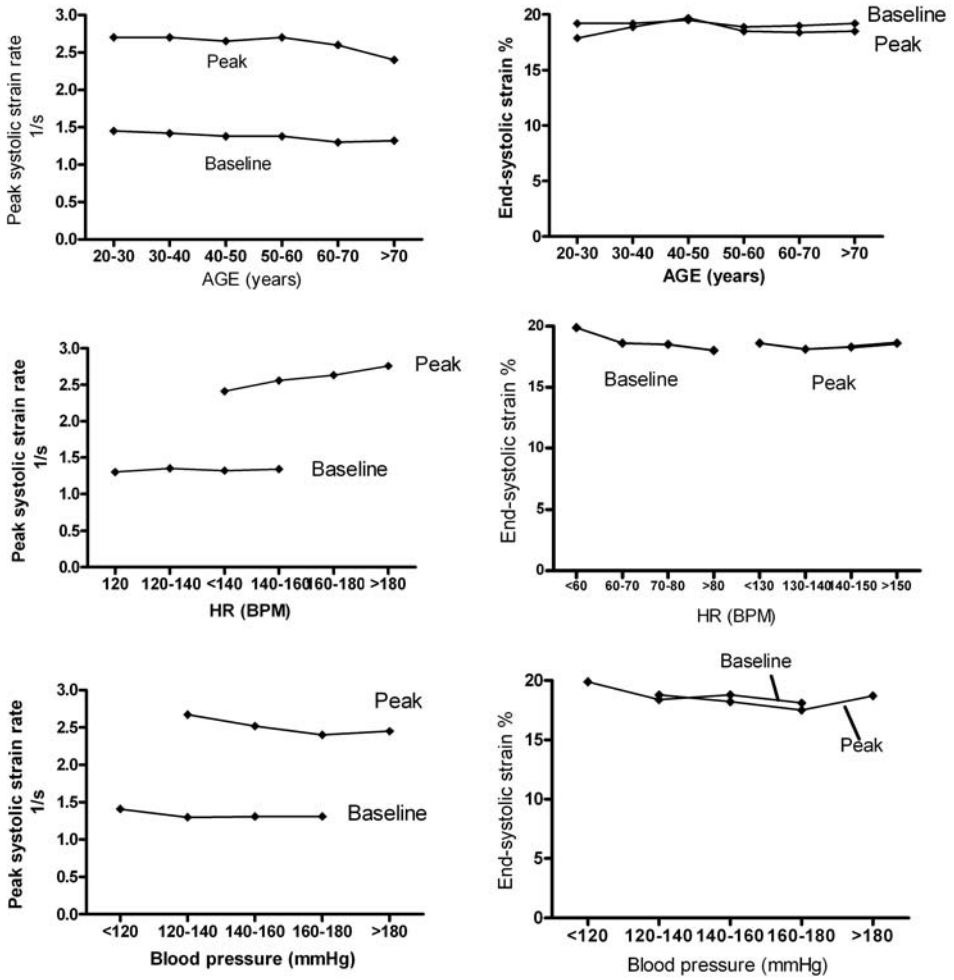

Figure 5. The effect of age and hemodynamics at baseline and peak dobutamine stress echocardiography for peak systolic SR (strain rate) and end-systolic strain in absolute values in normal subjects with a negative DSE (n = 122). For age, all values were non significant for SR and strain. Peak systolic SR was significantly reduced at peak for systolic blood pressure >160 mmHg ($p < 0.05$). At peak, SRs was significantly reduced ($p < 0.01$) at heart rate (HR) <140, but with no difference for end-systolic strain.

9.4.2 Peak value versus timing

An evaluation of the regional myocardial function by SRI can be performed by measuring strain rate/strain peak values or by timing reciprocating events within the cardiac cycle. Regional mechanical events should be able to be accurately timed with SRI, because of the high temporal resolution. However strain rate is a noisy method because any random noise in the velocity data will be amplified in the derivation process from the velocity gradient. Strain is less noisy as the integration of the strain rate curves over time acts as a low pass filter [86]. The peak value of the strain rate /strain curves can be affected by the insonation angle. A deviation of more than 15 degrees will reduce the peak value, provided that the velocity is perpendicular to the myocardium and the LV is normal. A deviation of more than 90 degrees, wall thickening/thinning will be measured instead of longitudinal shortening/lengthening and the values shift from negative to positive. Even if the angle deviation is small the calculation of the velocities is prone to small errors as the true motion of the myocardium is unknown. Out of plan motion, radial (lateral) motion and torsion all affect the estimate of the velocities. Attempts to correct for the angle dependency have so far not been successful [87]. The timing of cardiac events is probably less affected by the angle dependency and might be more robust, especially regional phase changes from contraction to relaxation patterns. The shape of the traces and the strain rate profile illustrated by curved M-mode are other interesting semi-quantitative indexes. As discussed above strain rate and strain traces offer several parameters to be measured and paper III and IV sought to evaluate the optimal parameter for DSE. Our and other's findings are discussed below.

9.4.3 Peak stress influence on measurements

At peak stress the velocities increase with a subsequent potential of more out of plane movement. Higher heart rate influences the duration of cardiac events and at a heart rate above 100 beats/minute, the diastases will disappear and the E and A-wave fuse. Systole shortens with a further increase in heart rate and is more affected by the temporal resolution, because the numbers of frames decrease with increase in time course. The tracking of the ROI will also be affected of the reduced frame rate as the motion between each frame will be larger. In addition, the physiological effect with increased breathing and translation of the heart will also influence the measurements. In some cases, the stress test may be negative because of lack of ischemia rather than failure of recognition of regional left ventricular dysfunction [88]. Over interpretation in the inferior wall is a well known cause of false positive DSE, which is illustrated in Figure 6.

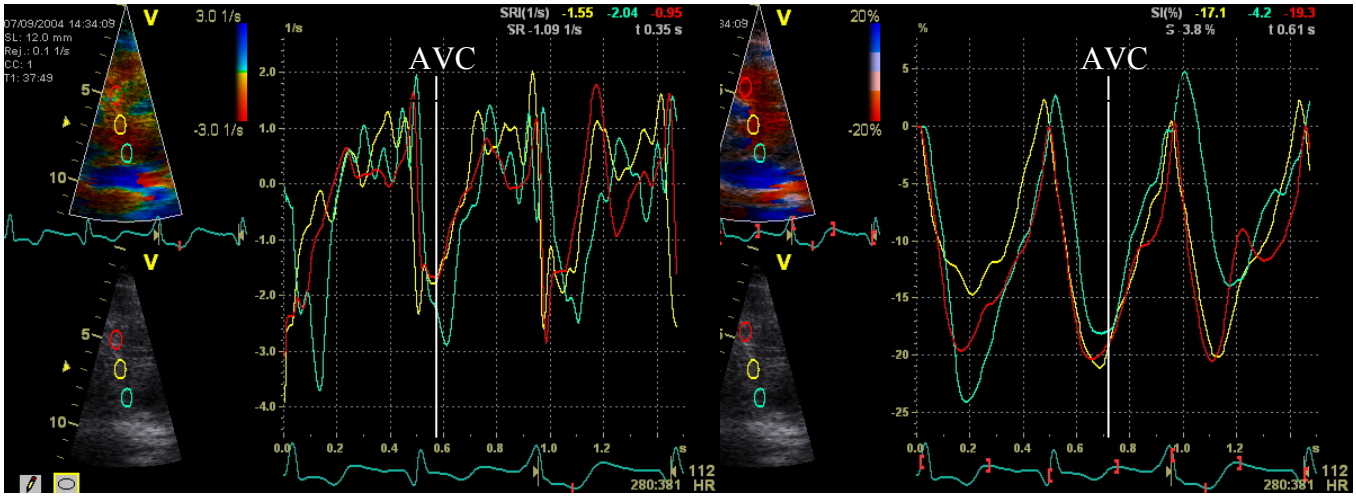

Figure 6. An example of a false positive interpretation by WM in grey scale images showing ischemia in basal and mid inferior segments read by an expert. Left image shows 3 cineloops and 3 strain rate traces at peak stress of basal inferior, mid inferior and apical inferior segments with normal peak systolic strain rate values between -1.8 and -2.5 s^{-1}. Right image shows the strain traces from the same segments at peak stress. Angiography showed normal coronary arteries.

9.5 Optimal SRI parameters for the detection of stress induced ischemia

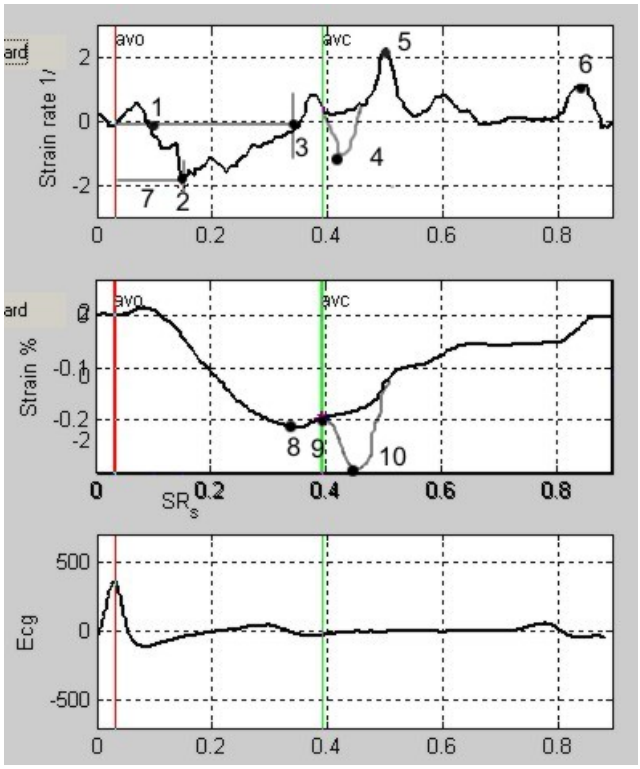

Figure 7. Top image shows strain rate trace, middle image strain trace and bottom image an ECG. The curve is from a normal subject and the grey part of the curves to illustrate PSS. Avc = aortic valve closure, avo = aortic valve opening

Strain rate parameters

1. Time to onset of shortening
2. Peak systolic strain rate
3. Time to end of shortening
4. Postsystolic shortening
5. Peak early diastolic strain rate (E-wave)
6. Peak late diastolic strain rate (A-wave)
7. Time to peak systolic strain rate

Strain parameters

8. Peak systolic strain
9. End-systolic strain
10. Postsystolic strain

1. Time to onset of the shortening (strain rate)

By a delay in the time to onset of the shortening in the strain rate traces one should be able to detect an initial elongation in an acute or chronically infarcted segment. We found in paper I that only 25% of the acutely infarcted segments showed an initial lengthening, which limits the use of this parameter.

2. Time to peak systolic strain rate

In a normal segment the contraction occurs in the first third of systole and at peak stress close after isovolumetric contraction (IVC). A delayed contraction is shown during ischemia and the time to peak systolic strain rate (t_{SRs}) would theoretically be a sensitive marker.

We studied thirty healthy subjects with a normal coronary angiography and normal resting echocardiography and t_{SRs} was measured from start of ejection to peak of strain rate and values expressed as percentage of ejection time [89]. The manual method was used. T_{SRs} could be measured in 90% of the segments. In all segments, the value of t_{SRs} was 34 (17) % and there was no significant difference between basal, mid or apical level, nor between the walls, except septum (see table 4). We found that the variability of t_{SRs} is too high in normals to be used as an index of regional myocardial function. The variability of t_{SRs} may partly be due to artefacts, but also demonstrates the physiological variation in deformation patterns in normal ventricles.

Table 4. Time to peak systolic strain rate on segment and wall level

Segment level/wall	t_{SRs} in % of ejection time	t_{SRs} range in % of ejection time	SR_s (SD) s^{-1}
Basal segments	36,0(17,2)	21–58	-1,41(0,41)
Mid segments	34,2(18,4)	14-54	-1,28(0,40)
Apical segments	32,6(15,9)	19-49	-1,22(0,37)
Septal wall	31,6(16,4)	13-73	-1,25(0,33)
Lateral wall	38,3(16,9)	14-66	-1,33(0,46)
Inferior wall	33,2(14,8)	14-51	-1,34(0,39)
Anterior wall	36,8(20,5)	14-74	-1,29(0,39)
Inferiolateral wall	35,0(20,1)	7-83	-1,47(0,49)
Anterioseptal wall	35,8(16,2)	14-57	-1,26(0,32)

$t_{SR\,s}$- time to peak systolic strain rate, SR_s - peak systolic strain rate

Paper III showed that t_{SRs} did not perform well at peak DSE either with an AUC of 0.69 for the velocity gradient method giving a sensitivity of 83%, specificity 74% and accuracy 78% (AUC 0.78 for segment length method). Even though variability was high there was a significant difference between rest and peak stress ($p<0.01$). These findings are confirmed in an earlier study with the t_{SRs} of 31 ± 23 % of ejection time at rest and 31±43 % of ejection time at peak in non-ischemic segments. In the same study t_{SRs} differed significantly between ischemic (55 ± 38%) and non-ischemic segments ($p<0.05$). The higher variability with t_{SRs} could also be an effect of too low temporal resolution. Increases in frame rate increase the sample points and might reduce the variability.

3. Time to end of shortening

The time point of regional transition from contraction to relaxation is delayed in ischemic segments in the presence of PSS, wherein relaxation starts later compared to non-ischemic segments. Abraham et al. studied the time to onset of regional relaxation (TR) with an automated analysis program. Automated TR measurements were feasible in more than 90% of the segments and the intra- and interobserver variability were low (6% and 9%, respectively). A percent change of less than 20% in TR identified patients with an ischemic response during dobutamine infusion (sensitivity 92%, specificity 75%). Other studies have been either concordant with an AUC of 0.80 [17] or unconcordant with an AUC of 0.62 using the same cut-off value [57]. We did not measure this variable in our studies.

4. Peak systolic strain rate

Even though the strain rate signal is noisy and peak value dependent upon angle, SR_s was our most accurate parameter to identify ischemia (AUC 0.90) with a cut-off value of $< -1.3\ s^{-1}$. This resulted in a sensitivity and specificity of 89 and 93%, respectively. In comparison with WM, SR_s increased the sensitivity significantly. However, the specificity was not significantly increased (only in value), an unexpected finding since

the visual assessment on subtle and transient changes in regional contractility is limited and would affect specificity. An increased sensitivity is in contrast to a study on 16 patients with false-negative results of DSE, where they found that strain rate and strain failed to increase the sensitivity of DSE [88]. Their most likely explanation was that the segments with false-negative results actually lacked induced ischemia rather than under interpretation of wall-motion abnormalities. SR_s did not perform as well in two other studies (AUC 0.74 and 0.80) [17, 57]. The last study included abnormal WM at rest and both the cut-off value (< -0.95 s^{-1}) and specificity (57%) differed markedly form our results.

5. Increment of strain rate and strain

The change in strain rate or strain did not perform as well as SR_s and S_{es}, because of the difference between two measurements being sensitive to measurement errors of both. The AUC for delta strain and delta strain rate was 0.79. The accuracy was 72% for delta strain and 71% for delta strain rate, especially the specificity was low 54% and 66% respectively.

6. Postsystolic shortening

PSS has been shown to be a sensitive marker of ischemia [90-92], but can also be seen in healthy individuals in as much as a third of the segments at rest [81]. However, the development or increase in PSS at peak stress might be a sensitive marker of inducible ischemia as there is a reference value at baseline. Voigt et al. found that PSS at peak stress was found in all of the ischemic segments and in almost half of the non-ischemic segments [17]. Paper III showed that PSS was present in 32% of the segments at rest (no WM abnormality) and in 40% at peak (both ischemic and non-ischemic segments). PSS as a sole index does not seem specific enough.

7. End-systolic strain

End-systolic strain has been the most studied parameter in experimental and clinical settings. As the curves are less noisy it is an easier parameter to measure, but we found S_{es} to be less feasible compared to strain rate because of drift of the curves. S_{es} performed well at peak DSE, even though it estimates the regional magnitude of deformation and does not take into account the temporal resolution. It was the second best parameter with an AUC of 0.87 (cut-off <-9%) and accuracy 84%. Other studies found this parameter weaker with AUC of 0.65 and 0.62 (cut-off value <-10%) [17, 57].

8. Peak systolic strain

Peak systolic strain reflects the maximum length change during the entire cardiac cycle. Voigt found this parameter of less clinical value than S_{es} [17].

9. Post-systolic index (PSI)

A clinical angioplasty study defined this ultrasonic strain index as the ratio of PSS to maximal segmental deformation [93]. PSI could in this non DSE study differentiate acutely ischemic segments from normal and other dysfunctional segments with an AUC of 0.94. PSI has been proposed as the optimal parameter in several studies for detection of ischemia during DSE with reported AUC of 0.90 (cut-off 0.35 sensitivity 82%, specificity 85%) and 0.61 (cut-off 0.25) [17, 57]. In paper III, PSI closely followed S_{es} with an AUC of 0.86 (cut-off 0.27) and with 83% accuracy. This might be the most robust of the SRI parameters, but in daily clinical practice it is inconvenient to calculate a ratio.

10. Curved anatomical M-mode of strain rate (CAMM)

This is a semi-quantitative parameter and most information is obtained from the strain rate curved m-mode. We always start the quantitative analysis with a CAMM which gives an overview of the quality of the data, presence of reverberations, the extent of ischemia and the timing between the walls. The use of CAMM has only been explored in one clinical DSE study and they found that the use of CAMM (strain rate) increased the sensitivity (86 vs. 81%) and the specificity (98 vs. 82%) compared to conventional WM [17]. Apical ischemia in septum at peak DSE is demonstrated in Figure 8 with mostly PSS and reduced strain rate /strain values.

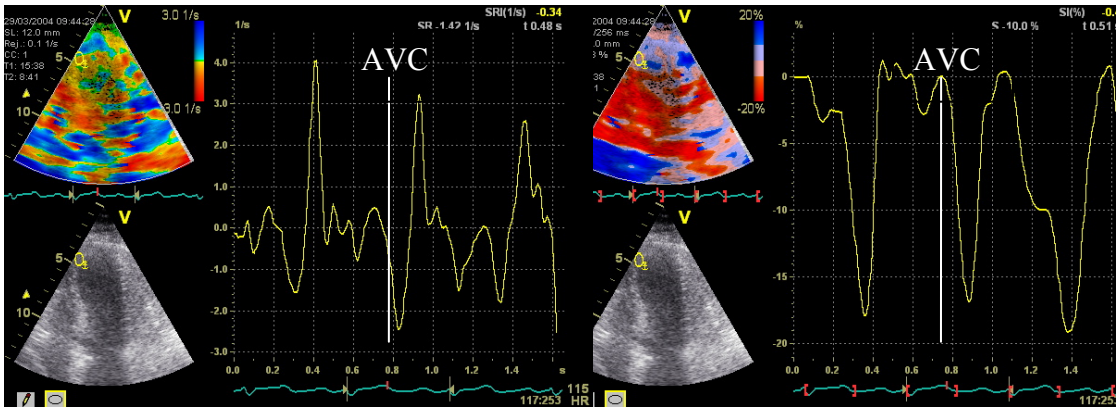

Figure 8. Strain rate (left image) and strain (right image) traces from apical septum at peak showing apical ischemia with reduced systolic values and mainly PSS.

Regional diastolic function is sensitive to ischemia, but both the reproducibility and the feasibility of the diastolic parameters are limited because of the merging of E and A waves at high heart rates at peak stress. This limits the applicability for the quantification of stress echocardiography and was not investigated in paper III or IV.

9.6 Application of DSE for prediction of mortality; WMSI versus SRI and optimal parameter

DSE is a reliable tool to predict cardiac events and mortality. WMSI at peak is used to quantify the extent and severity of ischemia and has been shown in several studies to be the strongest independent predictor of cardiac events [45, 94]. New wall motion abnormalities at peak and wall motion abnormalities at rest are other strong predictors with odds ratio between 2 and 4 [95, 96]. However the development of wall motion abnormalities is dependent on the achieved level of stress and a submaximal stress test might not provoke ischemia. Clinical independent predictors of total and cardiac mortality include age, hypertension, previous MI and heart failure [45, 46]. Rest WMSI and stress echo data add incremental information to clinical data [45, 46]. Paper IV examined patients undergoing DSE for evaluation of known or suspected coronary disease. Ischemia was detected in 43% of the patients and 39% had a previous MI. In agreement with others we demonstrated that age, hypertension and diabetes mellitus are predictors of mortality and the only independent predictor of these was diabetes. The number of ischemic or scarred segments, presence of ischemia and WMSI were the echo variables predictive of mortality. For SRI we compared the number of segments at risk per patient (using a cut-off) or the mean value; risk per patient with mean value (average of all segments measured) less than cut-off. The AUC for the optimal cut-offs was 0.73 for mean SR_s, 0.62 for mean S_{es}, 0.71 for segmental SR_s and for WMSI 0.62. They were all independent predictors of mortality, but in a multivariate analysis only mean SR_s (hazard ratio 2.5) was predictive with a cut-off value of cutoff >-2 s^{-1}. Cox models showed an increase in overall chi-square for clinical data (21), by adding WMSI (37) and mean SR_s (59). Both peak WMSI and mean SR_s reflect resting function as well as ischemia and reflect the global function. In contrast to paper III, where the accuracy of SRI in regional ischemia was evaluated, we here identified segments at high or low risk of mortality. Evaluation of the global function seems to be a stronger predictor for prediction of mortality compared to regional ischemia. Mean values identify patients with regional ischemia that lack the capacity of compensating with hyperkinesia in other segments. This may be the incremental information that is not derived by WMS. Mean values of SR_s also provided additional information for abnormal segments at peak.

9.7 Reference values and influence of hemodynamics in normal subjects during DSE for strain rate and strain

In paper III we studied 122 patients with a normal reaction to DSE. We found that age had no significant impact on the strain rate and strain values, neither at baseline nor at peak stress, although there was a tendency at age > 70 years (p=0.06) to a reduced SR_s at peak. Studies on tissue Doppler have on the contrary found an age-related decrease in systolic and early diastolic velocities with older age [55, 97], indicating that a decrease with age is present, and the lack of significance in this study may be due to lack of statistical power. In addition, heterogeneity of longitudinal shortening and lengthening exists, even in a normal young population. Strain rate and strain parameters are

relatively homogeneous throughout the myocardium. Normal values at baseline and peak are given in Table 5 (paper III). A normal response to DSE is illustrated in Figure 9 by curved strain rate CAMM and strain rate /strain traces.

The fibre structure in an aging heart is changed and the perfusion difficulties in the long axis fibres probably make them more vulnerable to early fibrosis, a lower deformation would thus be expected.

SR_s at peak was significantly reduced for systolic blood pressure >160 mmHg ($p<0.05$). This is probably an afterload effect as the heart pumps against an increased resistance with higher blood pressure due to an increased afterload. At peak stress, SR_s was significantly reduced ($p<0.01$) at heart rate <140 beats/min, but with no difference for strain. With higher heart rate, the ejection time shortens resulting in higher ejection velocity (rate). An increased contraction rate is the result. For an acceptable accuracy of the DSE test, the patients had to reach target heart rate. There were no significant differences in heart rate at baseline with age. A lower resting heart rate would be expected for younger persons, but could be explained by the elderly using more betablockers. The reason could be either some non-compliant patients with instructions on betablockers to be discontinued before the test or residual beta blockade remained even after 24 hours. This may have implications for the test itself, as this suggests a 48 hour-discontinuation before the test, if safe. Beta-blockade was the only independent predictor of SR_s.

The normal values at both baseline and peak are significantly reduced for the segment length method for both strain rate and strain compared to velocity gradient method (Table 5). The reason could be over-estimation in tissue Doppler because of noise, but might as well be under-estimation because of angular deviation. However for the segment length method which is angle-independent, noise appears to be a more important source of error than angular deviation.

Table 5. Normal values at baseline and peak DSE for velocity gradient method and segment length method

		Velocity gradient	Segment length	P-value
Baseline	SR_s s^{-1}	-1.4 (0.4)	-1.3 (0.3)	p <0.001
	S_{es} %	-18.4 (6.8)	-16.6 (5.0)	p <0.001
Peak	SR_s s^{-1}	-2.6 (0.7)	-2.3 (0.6)	p <0.001
	S_{es} %	-18.2 (8.4)	-15.6 (5.2)	p <0.001

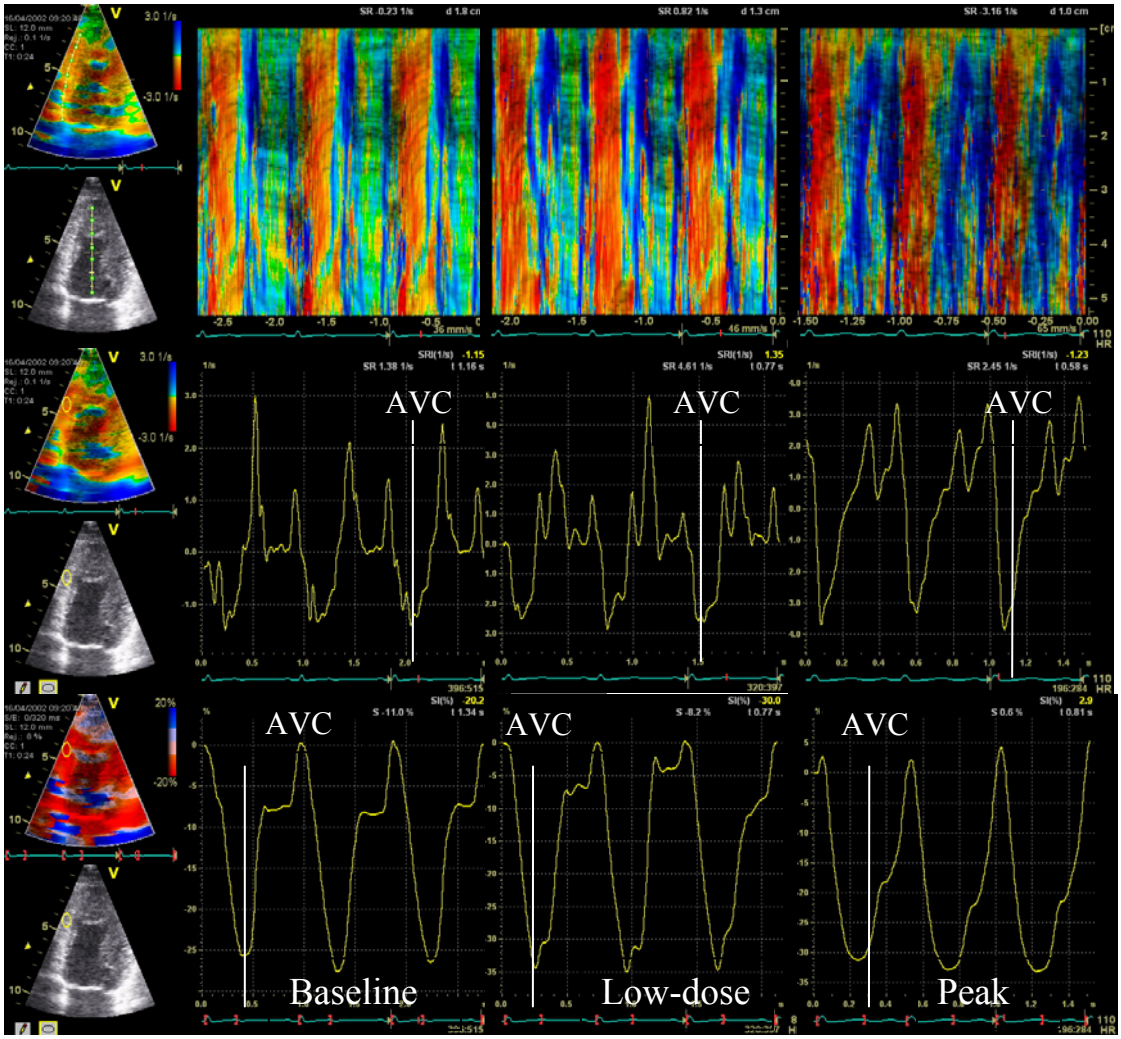

Figure 9. Normal response to DSE at baseline, low-dose and peak. Top figure shows curved M-modes by strain rate (SR) at the three stages, middle figure strain rate traces and lower figure strain traces.

9.8 Automated versus manual analysis and velocity gradient method with or without tracking versus segment length method

Our automated method combines tissue Doppler data and grey scale data allowing three different methods for calculation of the ultrasound derived deformation indices. The optimal method on which to base the calculation of strain rate and strain has not yet been established. Figure 10 illustrates the difference between the three methods in a normal, infarcted and remote segment. We found in the three last papers that both the velocity gradient and segment length method gave the same results, but slightly different values with a reduced value both at baseline and peak for segment length method. The velocity gradient method using a stationary ROI gave a lower reproducibility compared to tracking of the ROI, but with similar strain rate/strain values. Segmental method gave significantly reduced values and manual method in between the other methods. The disadvantage of the segmental method is the

dependency on the grey scale images and if one point fails to track properly, both segments have to be discarded. The calculation of strain rate/strain is one-dimensional compared to another commercially available speckle tracking method where the calculation is two-dimensional [33].

In order to be able to compare the tissue Doppler and speckle tracking strain rate values, Lagrangian strain rate must be converted to Eulerian strain rate (Appendix, equation 3). Eulerian and Lagrangian strain rate are approximately the same if the total strain is < 10%. However during ejection and filling the differences can be significant as the deformation usually is >10% [86].

Amundsen et al. showed that speckle tracking echocardiography provided accurate and angle-independent measurements of LV dimensions and strains in a comparison material of clinical data and MRI tagging and experimental data with sonomicrometry [24]. A combination of the two methods could be the optimal approach as speckle tracking is dependent on the quality of the B-mode images. There are several differences between the automated and manual method in filter and average settings; the temporal averaging in the manual method is done by either a Gaussian filter or a rectangle filter with default setting 40 ms Gaussian. The automated method uses a rectangle filter but only 10 ms in temporal averaging. For spatial averaging, the manual method uses information from several pixels in the ROI and linear regression is applied for the strain rate/strain calculation. Linear regression is not implemented in the automated method and v1 and v2 are measured at the end points of the ROI.

Second harmonic imaging has increased the quality of the B-mode images and in addition strain rate can be estimated using the second harmonic part of the signal. This would result in less stationary reverberations, a smaller variance and less bias because of the separation of the tissue signal from the stationary clutter. Aliasing will increase as the Nyquist velocity for strain rate is halved (Appendix, equation 8). However, there has been no published study on the beneficial effect of second harmonic strain rate and we choose not to implement it in our studies.

The time required for the DSE test was not prolonged by acquiring colour Doppler imaging data as this data together with grey scale imaging data are obtained at the same time. However our experience is that the sensitivity of conventional grey scale WM analysis might be reduced, which could have influenced the slightly lower sensitivity for WM (77%) than expected in paper III.

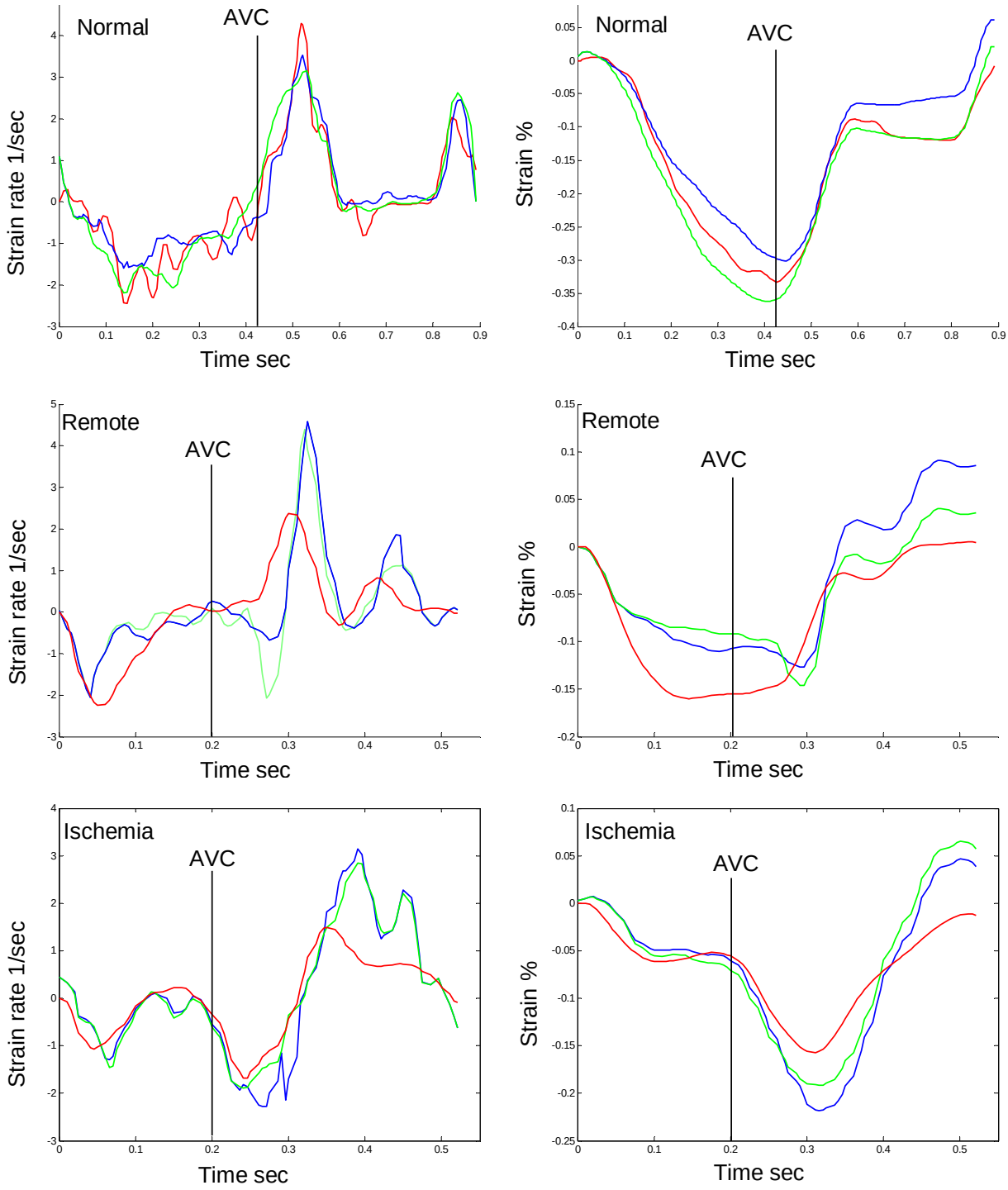

Figure 10. Strain rate (SR) and strain estimated with three different methods (red curve segment length method, blue curve dynamic velocity gradient method and green curve static velocity gradient method). SR traces are illustrated in the left images and strain traces in the right images. Top SR trace represents a normal trace at baseline from a 41 year old man with a normal response to DSE. Mid SR trace is from a remote mid lateral segment at peak from a patient with ischemia in apical septum represented in the lower SR trace. The traces in the lowest images show reduced SR_s values and mainly PSS. Note the differences in the curves, the red trace has in general reduced values and a different shape compared to the blue and green traces. The red trace is smoother probably due to lower temporal resolution. The green trace in the top image is noisier and could be an effect of no tracking throughout the cardiac cycle and information from non myocardium being picked up.

9.9 Feasibility and variability

An increase in heart rate at peak stress was not associated with a significant reduction in the number of interpretable segments for SR_s and S_{es} for non of the methods (velocity gradient and segment length). The price to pay for an automated method is the feasibility. Conventional visual WM assessment was possible in 98% of the segments at baseline and peak stress for paper II, III and for paper IV compared to 80-85% for SR_s in the automated methods. More segments could be quantified by the segment length method compared to velocity gradient method, as a result of being angle independent. A correlative study comparing deformation changes induced during stress echocardiography with angiographic and perfusion scintigraphy data, showed that deformation could be quantified in 85% of segments and visual assessment of changes in curved strain rate M-mode in 95% of all segments [17].

Reproducibility was highest in the segment length method (CV 15%) and lowest in the manual method (CV 21%), where the ROI can be placed in different positions in the segment. A stationary ROI compared to a tracked decreased reproducibility.

9.10 Clinical use, wide sector vs. narrow sector

We used a clinical applicable acquisition with wide sector as we sought to investigate the clinical use of SRI in DSE. Inclusion of narrow sectors of each wall increases the time use of the protocol. This is not realistic in clinical practice. However, SRI is sensitive to misalignment between the cardiac axis and the ultrasound beam. Therefore the optimal situation for accuracy of strain measurements would be a single wall with smallest possible sector recorded at a time. However, wall-by-wall analysis precludes the possibility of comparing synchronicity in opposite walls, as well as further image processing into for instance three dimensional or bull's eye.

The use of a narrow sector also increases the frame rate and the quality of the data. Adequate frame rate is crucial to resolve all systolic and diastolic strain rate events for the different stages of dobutamine infusion and a frame rate of at least 160 fps has been proposed [15]. A clinical study comparing the impact of different frame rates measured reduced strain values at low frame rates [98]. However applications that require long post-processing and optimal conditions with narrow sector are of limited relevance for the clinical use. It shows the potential use of the SRI method. Kowalski et al. studied the difference between narrow sector and wide sector and found no differences in the regional maximal systolic strain rate and strain values [15]. As the frame rate for wide sector was still high, 115 fps, a difference for systole would not be expected. However, the time to maximal systolic strain rate showed greater variability of the results between wide and narrow (>150 fps) sector angles. Paper I-III had a mean frame rate of 152 fps and 97 fps in paper IV. According to Lind et al. a frame rate of 100 fps in tissue Doppler velocity data would be sufficient to resolve the slower systolic and diastolic phases [99].

Great care has to be taken to ensure the quality of the data collected and the post-processing analysis must exclude segments due to misalignment, angle deviation and high signal noise.

9.11 Angiography as gold standard

Patients with angiographically verified total coronary occlusion with collaterals were included in paper III and IV as the functional significance of collaterals still is not clear. It has been shown that the presence of collaterals under these circumstances can sometimes prevent the development of a MI. The collaterals though only provide sufficient flow for maintenance of viability [100]. Clinical studies during PCI have shown an initial decrease in systolic strain rate /strain values by almost 50% compared with the baseline values in the segments at risk (i.e. those not supplied by collaterals). This is concomitant with the acute development of PSS in the segment at risk during balloon inflation with no measurable change in deformation in distal non-ischemic segments [90, 101]. In segments at risk supplied by collaterals balloon occlusion resulted in minor changes in systolic strain rate /strain and less PSS compared with non-collateralized segments at risk [101], indicating the protective nature of the collateral supply. The same study found peak systolic velocities unable to differentiate between collateralized and non-collateralized segments at risk [101]. However, this is an acute ischemia study and the same conditions cannot be applied to chronic ischemia.

Initially eyeballing was used to quantify coronary artery lesions in paper III, which resulted in a low sensitivity of WMS. All coronary angiograms were reanalysed by an invasive cardiologist blinded to the echocardiographic results and with use of a QCA programme. This changed the angiographic data in 14 patients.

9.12 Material

Only six patients were excluded due to poor image quality; five patients in paper IV and one patient in paper III because of emphysema and no window. The intention was to resemble the clinical situation as well as possible and they were all consecutively included. Not having optimal image quality compromises the feasibility of each study in terms of segments that can be analysed, but also the variability. An attempt to include 50% women in paper III was not successful as the inclusion time for the study would have been too long. In paper IV, 7% of the patients were lost to follow-up which is in accordance to other large prognostic studies [45, 46]. There is no central death register in Australia and the patients have to be followed up on the phone. Wrong telephone numbers or no phone numbers were the reasons for the failure to follow-up in most cases.

9.13 Discarding of segments

Some studies operate with a high feasibility of SRI in terms of segments. This can be achieved by selection of patients for optimal echogeneity, use of narrow sectors, extensive post processing or use of segments where artefacts have been included and interpreted as pathology. The automated method defines the ROI and objective traces are obtained as there is no possibility of searching for a suitable curve. In the manual method, in an attempt to avoid artefacts, a smaller region can be used for the measurements as the ROI can be reduced and moved as well as the strain length changed.

For the velocity gradient method, segments were discarded if the angular deviation exceeded 25 degrees. As a consequence of angle dependency only part of the apical segments were used for the measurements. Strain curves were discarded if they did not return to baseline at the end of the cycle. If the kernel region failed to properly track laterally and/or axially after adjustment, the segment was discarded. A displacement model was used to detect poor tracking. Using automated analysis, 20 – 25% of all segments had to be discarded, compared to only 8% by the manual method. Feasibility was least in the lateral and anterior wall, especially in mid-lateral and apical anterior segments. Reverberations were the major cause for rejection of 50% of the segments, followed by drop outs (no data), misalignment of the imaging plane, segmental angle deviation of >25º between the wall and the ultrasound beam and failure of tracking. However, as there was equal sensitivity and specificity for infracted segments in paper 2, it seems that a higher discard rate of segments does not change the utility of SRI analysis.

9.14 Limitations

Not holding the breath at end-expiration affected some of the traces, but three cardiac cycles were stored for all DSE studies and only the best quality cycles were included in the analysis. Averaging of three consecutive cardiac cycles will reduce random noise, which will not be repeated from cycle to cycle, but this was not applied, as respiration induces changes from one cycle to next.

When comparing accuracy between conventional WM and SRI, we are actually comparing radial wall motion with longitudinal. However, in semi quantitative analysis, they seem to be equivalent [74]. The acquisition of grey scale and TDI data were not made separately.

We have only used highest TDI frame rate, resulting in poor lateral resolution (16 or 20 lines in full sector), although it seem that a frame rate of 100 may be sufficient for systolic parameters, and this will generally result in better lateral resolution [102]. The temporal resolution of speckle tracking is a particularly difficult balance between under-sampling at low frame-rate (leading to reduced peak values and difficulty with tracking the speckle pattern because of excessive change from one frame to next), and reduced line density at high frame rate, compromising lateral resolution and giving poor

transverse tracking. Ultrasound data from two different scanners, Vivid 5 and Vivid 7 data was used, which give to some extent an inhomogeneous data set as the relation between grey scale and tissue Doppler data, are different with a 1:1 relation for Vivid 5 and 1:3-4 for Vivid 7. Paper I and II used both Vivid 5 and Vivid 7 data; paper III only Vivid 7 data and paper IV only Vivid 5 data. Speckle tracking has limitations due to the dependence of good image quality for the grey scale data. Tissue Doppler has disadvantages concerning reverberations, angle deviation, and noise (random and non-random). Thus, the SRI curve still requires interpretation in the context of the grey scale image, and uncritical use of SRI data may be misleading if the image is of poor quality and especially if the SRI waveform is suboptimal.

The automated method does not handle narrow sectors of each wall as the endocardial border detection is developed for a full apical view of both walls. This limited the frame rate, the possibility of avoiding reverberations and alignment. Although we applied an automated method of SRI measurement, this does not yet allow entirely objective assessment of regional myocardial function.

In Paper I, the sample size was small and not all patients were examined on admission. The time course was not blinded in the analysis.

Coronary angiography was used as the reference standard in paper III, but some discrepancies arise from the comparison of coronary anatomy and physiology. Coronary lesion severity can be over- and underestimated by angiography, and the physiological effect of stenoses varies with site, length and vessel size. Inter- and intraobserver variability was compared in the same images and most often the same loops.

The prognostic study in paper IV was set up in 1998, at which stage; tissue Doppler acquisitions were less sophisticated and informed than they are now. The frame rate both for tissue Doppler and B-mode images were low in some patients, and only one cineloop was stored. We followed patients for total mortality, in the belief that the definition of cardiac mortality is unreliable.

10. Conclusions

This thesis shows SRI to be a sensitive tool after myocardial infarction to measure recovery of function and during DSE for detection of ischemia as well as of prognostic value to differentiate patients of high and low risk of mortality. A proposed optimal SRI parameter to be measured has been established. We have also shown that an automated approach is feasible, time-saving and could potentially accelerate the clinical use of SRI in daily practice.

Conclusion paper I: SRI can demonstrate small changes in deformation rate from mid-infarct through the infarct and border zone to normal myocardium. It can also show changes over time, and be used to evaluate recovery of stunned myocardium.

Conclusions paper II: Automated analysis of strain rate and strain, with some manual adjustment, is feasible and quicker than manual analysis. Diagnostic accuracy was similar with all methods. Calculations from segment length variations had lower variability, and also reduced values.

Conclusions paper III: Automated analysis of SRI at DSE is feasible and accurate. SR_s appears to be the optimal variable and increases the sensitivity of expert conventional reading.

Conclusions paper IV: Average SR_s, derived from automated analysis of the SRI response to DSE, offers prognostic information on mortality that is independent and incremental to standard WMSI.

11. References

[1]. Isaaz K, Ethevenot G, Admant P, Brembilla B, Pernot C. A new Doppler method of assessing left ventricular ejection force in chronic congestive heart failure. *Am J Cardiol* 1989;64(1):81-7.

[2]. Isaaz K, Thompson A, Ethevenot G, Cloez JL, Brembilla B, Pernot C. Doppler echocardiographic measurement of low velocity motion of the left ventricular posterior wall. *Am J Cardiol* 1989;64(1):66-75.

[3]. McDicken WN, Sutherland GR, Moran CM, Gordon LN. Colour Doppler velocity imaging of the myocardium. *Ultrasound Med Biol* 1992;18(6-7):651-4.

[4]. Heimdal A, Stoylen A, Torp H, Skjaerpe T. Real-time strain rate imaging of the left ventricle by ultrasound. *J Am Soc Echocardiogr* 1998;11(11):1013-9.

[5]. Urheim S, Edvardsen T, Torp H, Angelsen B, Smiseth OA. Myocardial strain by Doppler echocardiography. Validation of a new method to quantify regional myocardial function. *Circulation* 2000;102(10):1158-64.

[6]. Edvardsen T. Quantitative assessment of intrinsic regional myocardial deformation by Doppler strain rate echocardiography in humans: validation against three-dimensional tagged magnetic resonance imaging. *Circulation* 2002;106(1):50-6.

[7]. Stoylen A, Heimdal A, Bjornstad K, Wiseth R, Vik-Mo H, Torp H et al. Strain rate imaging by ultrasonography in the diagnosis of coronary artery disease. *J Am Soc Echocardiogr* 2000;13(12):1053-64.

[8]. Jamal F. Can changes in systolic longitudinal deformation quantify regional myocardial function after an acute infarction? An ultrasonic strain rate and strain study. *J Am Soc Echocardiogr* 2002;15(7):723-30.

[9]. Kukulski T, Jamal F, Herbots L, D'hooge J, Bijnens B, Hatle L et al. Identification of acutely ischemic myocardium using ultrasonic strain measurements. A clinical study in patients undergoing coronary angioplasty. *J Am Coll Cardiol* 2003;41(5):810-9.

[10]. Hoffmann R, Altiok E, Nowak B, Heussen N, Kuhl H, Kaiser HJ et al. Strain rate measurement by doppler echocardiography allows improved assessment of myocardial viability inpatients with depressed left ventricular function. *J Am Coll Cardiol* 2002;39(3):443-9.

[11]. Hanekom L, Jenkins C, Jeffries L, Case C, Mundy J, Hawley C et al. Incremental value of strain rate analysis as an adjunct to wall-motion scoring for assessment of myocardial viability by dobutamine echocardiography: a follow-up study after revascularization. *Circulation* 2005;112(25):3892-900.

[12]. Koyama J, Ray-Sequin PA, Falk RH. Longitudinal myocardial function assessed by tissue velocity, strain, and strain rate tissue Doppler echocardiography in patients with AL (primary) cardiac amyloidosis. *Circulation* 2003;107(19):2446-52.

[13]. Weidemann F. Quantification of regional right and left ventricular function by ultrasonic strain rate and strain indexes in Friedreich's ataxia. *Am J Cardiol* 2003;91(5):622-6.

[14]. Weidemann F, Breunig F, Beer M, Sandstede J, Turschner O, Voelker W et al. Improvement of cardiac function during enzyme replacement therapy in patients with Fabry disease: a prospective strain rate imaging study. *Circulation* 2003;108(11):1299-301.

[15]. Kowalski M, Herregods M, Herbots L, Weidemann F, Simmons L, Strotmann J et al. The feasibility of ultrasonic regional strain and strain rate imaging in quantifying dobutamine stress echocardiography. *Eur J Echocardiogr* 2003;4(2):81-91.

[16]. Voigt J, Nixdorff U, Bogdan R, Exner B, Schmiedehausen K, Platsch G et al. Comparison of deformation imaging and velocity imaging for detecting regional inducible ischaemia during dobutamine stress echocardiography. *Eur Heart J* 2004;25(17):1517-25.

[17]. Voigt JU, Exner B, Schmiedehausen K, Huchzermeyer C, Reulbach U, Nixdorff U et al. Strain-rate imaging during dobutamine stress echocardiography provides objective evidence of inducible ischemia. *Circulation* 2003;107(16):2120-6.

[18]. Picano E, Lattanzi F, Orlandini A, Marini C, L'Abbate A. Stress echocardiography and the human factor: the importance of being expert. *J Am Coll Cardiol* 1991;17(3):666-9.

[19]. Kvitting JP, Wigström L, Strotmann JM, Sutherland GR. How accurate is visual assessment of synchronicity in myocardial motion? An In vitro study with computer-simulated regional delay in myocardial motion: clinical implications for rest and stress echocardiography studies. *J Am Soc Echocardiogr* 1999;12(9):698-705.

[20]. Weidemann F, Jamal F, Sutherland GR, Claus P, Kowalski M, Hatle L et al. Myocardial function defined by strain rate and strain during alterations in inotropic states and heart rate. *Am J Physiol Heart Circ Physiol* 2002;283(2):H792-9.

[21]. Heimdal A, Abraham T, Pislaru C, Belohlavek M. Angle dependency of strain rate imaging in an animal model. *J Am Soc Echocardiogr* 2000;13(5):484 Abstracts.

[22]. Bohs L, Trahey G. A novel method for angle independent ultrasonic imaging of blood flow and tissue motion. *IEEE Trans Biomed Eng* 1991;38(3):280-6.

[23]. Kaluzynski K, Chen X, Emelianov S, Skovoroda A, O'Donnell M. Strain rate imaging using two-dimensional speckle tracking. *IEEE Trans Ultrason Ferroelectr Freq Control* 2001;48(4):1111-23.

[24]. Amundsen BH, Helle-Valle T, Edvardsen T, Torp H, Crosby J, Lyseggen E et al. Noninvasive Myocardial Strain Measurement by Speckle Tracking Echocardiography Validation Against Sonomicrometry and Tagged Magnetic Resonance Imaging. *J Am Coll Cardiol* 2006;47(4):789-93.

[25]. Helle-Valle T, Crosby J, Edvardsen T, Lyseggen E, Amundsen BH, Smith HJ et al. New noninvasive method for assessment of left ventricular rotation: speckle tracking echocardiography. *Circulation* 2005;112(20):3149-56.

[26]. Notomi Y, Lysyansky P, Setser RM, Shiota T, Popovic ZB, Martin-Miklovic MG et al. Measurement of ventricular torsion by two-dimensional ultrasound speckle tracking imaging. *J Am Coll Cardiol* 2005;45(12):2034-41.

[27]. Notomi Y, Setser RM, Shiota T, Martin-Miklovic MG, Weaver JA, Popovic ZB et al. Assessment of left ventricular torsional deformation by Doppler tissue imaging: validation study with tagged magnetic resonance imaging. *Circulation* 2005;111(9):1141-7.

[28]. Langeland S, D'hooge J, Wouters PF, Leather HA, Claus P, Bijnens B et al. Experimental validation of a new ultrasound method for the simultaneous assessment of radial and longitudinal myocardial deformation independent of insonation angle. *Circulation* 2005;112(14):2157-62.

[29]. Mann DL, Gillam LD, Weyman AE. Cross-sectional echocardiographic assessment of regional left ventricular performance and myocardial perfusion. *Prog Cardiovasc Dis* 1986;29(1):1-52.

[30]. Pérez JE, Klein SC, Prater DM, Fraser CE, Cardona H, Waggoner AD et al. Automated, on-line quantification of left ventricular dimensions and function by echocardiography with backscatter imaging and lateral gain compensation. *Am J Cardiol* 1992;70(13):1200-5.

[31]. Lang RM, Vignon P, Weinert L, Bednarz J, Korcarz C, Sandelski J et al. Echocardiographic quantification of regional left ventricular wall motion with color kinesis. *Circulation* 1996;93(10):1877-85.

[32]. Fujino T, Ono S, Murata K, Tanaka N, Tone T, Yamamura T et al. New method of on-line quantification of regional wall motion with automated segmental motion analysis. *J Am Soc Echocardiogr* 2001;14(9):892-901.

[33]. Leitman M, Lysyansky P, Sidenko S, Shir V, Peleg E, Binenbaum M et al. Two-dimensional strain-a novel software for real-time quantitative echocardiographic assessment of myocardial function. *J Am Soc Echocardiogr* 2004;17(10):1021-9.

[34]. Reisner S, Lysyansky P, Agmon Y, Mutlak D, Lessick J, Friedman Z. Global longitudinal straon: a novel index of left ventricular systolic function. *J Am Soc Echocardiogr* 2004;17(6):630-3.

[35]. Toyoda T, Baba H, Akasaka T, Akiyama M, Neishi Y, Tomita J et al. Assessment of regional myocardial strain by a novel automated tracking system from digital image files. *J Am Soc Echocardiogr* 2004;17(12):1234-8.

[36]. Stoylen A, Heimdal A, Bjornstad K, Torp HG, Skjaerpe T. Strain Rate Imaging by Ultrasound in the Diagnosis of Regional Dysfunction of the Left Ventricle. *Echocardiography* 1999;16(4):321-9.

[37]. Voigt JU, Arnold MF, Karlsson M, Hubbert L, Kukulski T, Hatle L et al. Assessment of regional longitudinal myocardial strain rate derived from doppler myocardial imaging indexes in normal and infarcted myocardium. *J Am Soc Echocardiogr* 2000;13(6):588-98.

[38]. Jamal F, Kukulski T, Strotmann J, Szilard M, D'hooge J, Bijnens B et al. Quantification of the spectrum of changes in regional myocardial function during acute

ischemia in closed chest pigs: an ultrasonic strain rate and strain study. *J Am Soc Echocardiogr* 2001;14(9):874-84.

[39]. García-Fernández MA, Azevedo J, Moreno M, Bermejo J, Pérez-Castellano N, Puerta P et al. Regional diastolic function in ischaemic heart disease using pulsed wave Doppler tissue imaging. *Eur Heart J* 1999;20(7):496-505.

[40]. Cohen JL, Greene TO, Ottenweller J, Binenbaum SZ, Wilchfort SD, Kim CS. Dobutamine digital echocardiography for detecting coronary artery disease. *Am J Cardiol* 1991;67(16):1311-8.

[41]. Sawada SG, Segar DS, Ryan T, Brown SE, Dohan AM, Williams R et al. Echocardiographic detection of coronary artery disease during dobutamine infusion. *Circulation* 1991;83(5):1605-14.

[42]. Marwick T. Table 3.2. Stress Echocardiography: Its Role in the Diagnosis and Evaluation of Coronary Artery Disease. Norwell: Kluwer Academic Publishers; 2003, pp 76-7.

[43]. Hoffmann R, Lethen H, Marwick T, Arnese M, Fioretti P, Pingitore A et al. Analysis of interinstitutional observer agreement in interpretation of dobutamine stress echocardiograms. *J Am Coll Cardiol* 1996;27(2):330-6.

[44]. Hoffmann R, Marwick T, Poldermans D, Lethen H, Ciani R, van der Meer P et al. Refinements in stress echocardiographic techniques improve inter-institutional agreement in interpretation of dobutamine stress echocardiograms. *Eur Heart J* 2002;23(10):821-9.

[45]. Marwick T, Case C, Sawada S, Rimmerman C, Brenneman P, Kovacs R et al. Prediction of mortality using dobutamine echocardiography. *J Am Coll Cardiol* 2001;37(3):754-60.

[46]. Sicari R, Pasanisi E, Venneri L, Landi P, Cortigiani L, Picano E. Stress echo results predict mortality: a large-scale multicenter prospective international study. *J Am Coll Cardiol* 2003;41(4):589-95.

[47]. Geleijnse M. Cardiac outcome after normal stress echocardiograph. A multicenter study of 6,799 patients. *Circulation* 2000;102(II):381.

[48]. Bjørnstad K, Aakhus S, Torp HG. How does computer-assisted digital wall motion analysis influence observer agreement and diagnostic accuracy during stress echocardiography? *Int J Card Imaging* 1997;13(2):105-14.

[49]. Fathi R, Cain P, Nakatani S, Yu H, Marwick T. Effect of tissue Doppler on the accuracy of novice and expert interpreters of dobutamine echocardiography. *Am J Cardiol* 2001;88(4):400-5.

[50]. Tsutsui JM, Elhendy A, Anderson JR, Xie F, McGrain AC, Porter TR. Prognostic value of dobutamine stress myocardial contrast perfusion echocardiography. *Circulation* 2005;112(10):1444-50.

[51]. Elhendy A, O'Leary EL, Xie F, McGrain AC, Anderson JR, Porter TR. Comparative accuracy of real-time myocardial contrast perfusion imaging and wall motion analysis during dobutamine stress echocardiography for the diagnosis of coronary artery disease. *J Am Coll Cardiol* 2004;44(11):2185-91.

[52]. Ahmad M, Xie T, McCulloch M, Abreo G, Runge M. Real-time three-dimensional dobutamine stress echocardiography in assessment stress echocardiography in assessment of ischemia: comparison with two-dimensional dobutamine stress echocardiography. *J Am Coll Cardiol* 2001;37(5):1303-9.

[53]. Mor-Avi V, Vignon P, Koch R, Weinert L, Garcia MJ, Spencer KT et al. Segmental analysis of color kinesis images: new method for quantification of the magnitude and timing of endocardial motion during left ventricular systole and diastole. *Circulation* 1997;95(8):2082-97.

[54]. Fraser A, Payne N, Madler C, Janerot-Sjoberg B, Lind B, Grocott-Mason R et al. Feasibility and reproducibility of off-line tissue Doppler measurement of regional myocardial function during dobutamine stress echocardiography. *Eur J Echocardiogr* 2003;4(1):43-53.

[55]. Madler CF. Non-invasive diagnosis of coronary artery disease by quantitative stress echocardiography: optimal diagnostic models using off-line tissue Doppler in the MYDISE study. *Eur Heart J* 2003;24(17):1584-94.

[56]. Cain P, Marwick T, Case C, Baglin T, Dart J, Short L et al. Assessment of regional long-axis function during dobutamine echocardiography. *Clin Sci* 2001;Apr;100(4):423-32.

[57]. Hanekom L, Moir S, Jeffries L, MacNab D, Marwick T. Selection of optimal strain rate imaging parameter for the diagnosis of coronary artery disease during dobutamine stress echocardiography. An angiographic comparison. *Eur Heart J* 2005;26(abstract supplement):210.

[58]. Abraham TP, Belohlavek M, Thomson HL, Pislaru C, Khandheria B, Seward JB et al. Time to onset of regional relaxation: feasibility, variability and utility of a novel index of regional myocardial function by strain rate imaging. *J Am Coll Cardiol* 2002;39(9):1531-7.

[59]. Armstrong G, Pasquet A, Fukamachi K, Cardon L, Olstad B, Marwick T. Use of peak systolic strain as an index of regional left ventricular function: comparison with tissue Doppler velocity during dobutamine stress and myocardial ischemia. *J Am Soc Echocardiogr* 2000;13(8):731-7.

[60]. Jamal F, Strotmann J, Weidemann F, Kukulski T, D'hooge J, Bijnens B et al. Noninvasive quantification of the contractile reserve of stunned myocardium by ultrasonic strain rate and strain. *Circulation* 2001;104(9):1059-65.

[61]. Weidemann F, Broscheit J, Eberbach N, Steendijk P, Voelker W, Greim C et al. Dobutamine induces ineffective work in regional ischaemic myocardium: an experimental strain rate imaging study. *Clin Sci (Colch)* 2004;106(2):173-81.

[62]. Miyasaka Y, Haiden M, Kamihata H, Nishiue T, Iwasaka T. Usefulness of strain rate imaging in detecting ischemic myocardium during dobutamine stress. *Int J Cardiol* 2005;102(2):225-31.

[63]. Greenberg NL, Firstenberg MS, Castro PL, Main M, Travaglini A, Odabashian JA et al. Doppler-derived myocardial systolic strain rate is a strong index of left ventricular contractility. *Circulation* 2002;105(1):99-105.

[64]. Yip G, Khandheria B, Belohlavek M, Pislaru C, Seward J, Bailey K et al. Strain echocardiography tracks dobutamine-induced decrease in regional myocardial perfusion in nonocclusive coronary stenosis. *J Am Coll Cardiol* 2004;44(8):1664-71.

[65]. Weidemann F, Dommke C, Bijnens B, Claus P, D'hooge J, Mertens P et al. Defining the transmurality of a chronic myocardial infarction by ultrasonic strain-rate imaging: implications for identifying intramural viability: an experimental study. *Circulation* 2003;107(6):883-8.

[66]. Derumeaux G. Tissue Doppler imaging differentiates transmural from nontransmural acute myocardial infarction after reperfusion therapy. *Circulation* 2001;103(4):589-96.

[67]. Austen WG, Edwards JE, Frye RL, Gensini GG, Gott VL, Griffith LS et al. A reporting system on patients evaluated for coronary artery disease. Report of the Ad Hoc Committee for Grading of Coronary Artery Disease, Council on Cardiovascular Surgery, American Heart Association. *Circulation* 1975;51(4 SUPPL):5-40.

[68]. Lang RM, Bierig M, Devereux RB, Flachskampf FA, Foster E, Pellikka PA et al. Recommendations for chamber quantification: a report from the American Society of Echocardiography's Guidelines and Standards Committee and the Chamber Quantification Writing Group, developed in conjunction with the European Association of Echocardiography, a branch of the European Society of Cardiology. *J Am Soc Echocardiogr* 2005;18(12):1440-63.

[69]. Schiller NB. Recommendations for quantitation of the left ventricle by two-dimensional echocardiography. American Society of Echocardiography Committee on Standards, Subcommittee on Quantitation of Two-Dimensional Echocardiograms. *J Am Soc Echocardiogr* 1989;2(5):358-67.

[70]. Weidemann F, Kowalski M, D'hooge J, Bijnens B, Sutherland GR. Doppler myocardial imaging. A new tool to assess regional inhomogeneity in cardiac function. *Basic Res Cardiol* 2001;96(6):595-605.

[71]. Torp A, Rabben S, Stoylen A, Ihlen H, Andersen K, Brodin L. Automatic detection and tracking of left ventricular landmarks in echocardiography. *Proceedings IEEE Ultrasonics Symposium 2004* 2004;.

[72]. Aase S, Stoylen A, Bjork Ingul C, Frigstad S, Torp H. Automatic timing of aortic valve closure in apical tissue Doppler images. *Ultrasound Med Biol* 2006;32(1):19-27.

[73]. Stoylen A, Malm S, Aase S, Sagberg E. Aortic valve closure can be timed by tissue Doppler. *European Journal of Echocardiography* 2004;5(SUPPL 1):159.

[74]. Garot J. Quantitative systolic and diastolic transmyocardial velocity gradients assessed by M-mode colour Doppler tissue imaging as reliable indicators of regional left ventricular function after acute myocardial infarction. *Eur Heart J* 1999;20(8):593-603.

[75]. Derumeaux G. Assessment of nonuniformity of transmural myocardial velocities by color-coded tissue Doppler imaging: characterization of normal, ischemic, and stunned myocardium. *Circulation* 2000;101(12):1390-5.

[76]. Jamal F, Szilard M, Kukulski T, Liu XS, D'hooge J, Bijnens B et al. Changes in systolic and postsystolic wall thickening during acute coronary occlusion and reperfusion in closed-chest pigs: Implications for the assessment of regional myocardial function. *J Am Soc Echocardiogr* 2001;14(7):691-7.

[77]. Jennings R, Murry C, Steenbergen CJ, Reimer K. Development of cell injury in sustained acute ischemia. *Circulation* 1990;82((3 SUPPL)):II2-12.

[78]. Skulstad H, Edvardsen T, Urheim S, Rabben SI, Stugaard M, Lyseggen E et al. Postsystolic shortening in ischemic myocardium: active contraction or passive recoil? *Circulation* 2002;106(6):718-24.

[79]. Lyseggen E, Skulstad H, Helle-Valle T, Vartdal T, Urheim S, Rabben SI et al. Myocardial strain analysis in acute coronary occlusion: a tool to assess myocardial viability and reperfusion. *Circulation* 2005;112(25):3901-10.

[80]. Pislaru C, Anagnostopoulos PC, Seward JB, Greenleaf JF, Belohlavek M. Higher myocardial strain rates during isovolumic relaxation phase than during ejection characterize acutely ischemic myocardium. *J Am Coll Cardiol* 2002;40(8):1487-94.

[81]. Voigt JU, Lindenmeier G, Exner B, Regenfus M, Werner D, Reulbach U et al. Incidence and characteristics of segmental postsystolic longitudinal shortening in normal, acutely ischemic, and scarred myocardium. *J Am Soc Echocardiogr* 2003;16(5):415-23.

[82]. Pellikka PA, Roger VL, McCully RB, Mahoney DW, Bailey KR, Seward JB et al. Normal stroke volume and cardiac output response during dobutamine stress echocardiography in subjects without left ventricular wall motion abnormalities. *Am J Cardiol* 1995;76(12):881-6.

[83]. Urheim S. Myocardial strain by Doppler echocardiography. Validation of a new method to quantify regional myocardial function. *Circulation* 2000;102(10):1158-64.

[84]. Sutherland GR, Di Salvo G, Claus P, D'hooge J, Bijnens B. Strain and strain rate imaging: a new clinical approach to quantifying regional myocardial function. *J Am Soc Echocardiogr* 2004;17(7):788-802.

[85]. Weidemann F, Jamal F, Kowalski M, Kukulski T, D'Hooge J, Bijnens B et al. Can strain rate and strain quantify changes in regional systolic function during dobutamine infusion, B-blockade, and atrial pacing--implications for quantitative stress echocardiography. *J Am Soc Echocardiogr* 2002;15(5):416-24.

[86]. D'hooge J, Heimdal A, Jamal F, Kukulski T, Bijnens B, Rademakers F et al. Regional strain and strain rate measurements by cardiac ultrasound: principles, implementation and limitations. *Eur J Echocardiogr* 2000;1(3):154-70.

[87]. Storaa C, Aberg P, Lind B, Brodin LA. Effect of angular error on tissue Doppler velocities and strain. *Echocardiography* 2003;20(7):581-7.

[88]. Yuda S, Fang ZY, Leano R, Marwick TH. Is quantitative interpretation likely to increase sensitivity of dobutamine stress echocardiography? A study of false-negative results. *J Am Soc Echocardiogr* 2004;17(5):448-53.

[89]. Bjork Ingul C, Stoylen A, Slordahl S. Time to peak systolic strain rate is not a reliable index of regional myocardial function. *Eur J Echocardiography* 2003;4(supplement 1):373.

[90]. Jamal F, Kukulski T, D'hooge J, De Scheerder I, Sutherland G. Abnormal postsystolic thickening in acutely ischemic myocardium during coronary angioplasty: a velocity, strain, and strain rate doppler myocardial imaging study. *J Am Soc Echocardiogr* 1999;12(11):994-6.

[91]. Kukulski T. Acute changes in systolic and diastolic events during clinical coronary angioplasty: a comparison of regional velocity, strain rate, and strain measurement. *J Am Soc Echocardiogr* 2002;15(1):1-12.

[92]. Hosokawa H, Sheehan FH, Suzuki T. Measurement of postsystolic shortening to assess viability and predict recovery of left ventricular function after acute myocardial infarction. *J Am Coll Cardiol* 2000;35(7):1842-9.

[93]. Kukulski T. Identification of acutely ischemic myocardium using ultrasonic strain measurements. A clinical study in patients undergoing coronary angioplasty. *J Am Coll Cardiol* 2003;41(5):810-9.

[94]. Senior R, Soman P, Rajdeep S, Khattar S, Lahiri A. Prognostic value of Dobutamnie stress echocardiography in patients undergoing diagnostic coronary arteriography. *Am J Cardiol* 1997;79:1610-4.

[95]. Poldermans D, Fioretti PM, Boersma E, Cornel JH, Borst F, Vermeulen EG et al. Dobutamine-atropine stress echocardiography and clinical data for predicting late cardiac events in patients with suspected coronary artery disease. *Am J Med* 1994;97(2):119-25.

[96]. Poldermans D, Fioretti PM, Boersma E, Bax JJ, Thomson IR, Roelandt JR et al. Long-term prognostic value of dobutamine-atropine stress echocardiography in 1737 patients with known or suspected coronary artery disease: A single-center experience. *Circulation* 1999;99(6):757-62.

[97]. Cain P, Napier S, Haluska B, Short L, Marwick T. Influence of left ventricular size and hemodynamics on the systolic longitudinal myocardial Doppler velocity response to stress. *Am Heart J* 2002;143(1):169-75.

[98]. Storaa C, Lind B, Brodin LA. Distribution of left ventricular longitudinal peak systolic strain and impact of low frame rate. *Ultrasound Med Biol* 2004;30(8):1049-55.

[99]. Lind B, Nowak J, Dorph J, van der Linden J, Brodin LA. Analysis of temporal requirements for myocardial tissue velocity imaging. *Eur J Echocardiogr* 2002;3(3):214-9.

[100]. Koerselman J, van der Graaf Y, de Jaegere PP, Grobbee DE. Coronary collaterals: an important and underexposed aspect of coronary artery disease. *Circulation* 2003;107(19):2507-11.

[101]. Kukulski T, Jamal F, D'Hooge J, Bijnens B, De Scheerder I, Sutherland GR. Acute changes in systolic and diastolic events during clinical coronary angioplasty: a comparison of regional velocity, strain rate, and strain measurement. *J Am Soc Echocardiogr* 2002;15(1):1-2.

[102]. Hanekom L, Lundberg V, Leano R, Marwick T. Optimisation of strain rate imaging for application to stress echocardiography. Optimisation of strain rate imaging for application to stress echocardiography. *Ultrasound Med Biol* 2004;30(11):1451-60.

[103]. Beyar R, Shapiro EP, Graves WL, Rogers WJ, Guier WH, Carey GA et al. Quantification and validation of left ventricular wall thickening by a three-dimensional volume element magnetic resonance imaging approach. *Circulation* 1990;81(1):297-307.

[104]. Heimdal A. Doppler based ultrasound imaging methods for noninvasive assessment of tissue viability. Doctoral thesis. Trondheim: NTNU; 1999:77, pp 51.

[105]. Stoylen A. Strain rate imaging of the left ventricle by ultrasound. Feasibility, clinical validation and physiological aspects. Doctoral thesis. Trondheim: Bjærum AS; 2001, pp 64-9.

12. Appendix

12.1 Lagrangian versus Eulerian (natural strain) strain

Strain (S) is defined as the deformation of an object, relative to its original length.

$$S = \frac{L - L_O}{L_O} \tag{1}$$

L_0 is the original length and L the length of the myocardium after deformation. Instantaneous strain can be defined if the deformation before, during and at the end is known and is defined as:

$$S(t) = \frac{L(t) - L(t_0)}{L(t_0)} \tag{2}$$

The length of the myocardium is here known at a certain time L(t) and also at it's original length $L(t_0)=L_0$. Lagrangian strain is defined as the instantaneous shortening or lengthening in relation to the original length of the myocardium.

Eulerian strain (natural strain)(S_N) is defined as the instantaneous shortening or lengthening in relation to the instantaneous length of the myocardium. dt is an infinitesimally short time interval.

$$dS_N(t) = \frac{L(t+dt) - L(t)}{L(t)} = \frac{v2(t) - v1(t)}{L(t)} dt \tag{3}$$

where v1 and v2 are the endpoint velocities of the segment L. By adding all the infinitesimally small amounts of deformation the total natural strain is defined;

$$S_N(t) = \int_{t0}^{t} dS_N(t) \tag{4}$$

It has been shown that Lagrangian and Eulerian strain are related non-linearly [103];

$$S_N(t) = \ln(1 + S(t)) \quad \text{or} \quad S(t) = \exp(S_N(t)) - 1 \tag{5}$$

The relation between Lagrangian and Eulerian strain rate (SR) is given by

$$SR(t) = \frac{dS_N(t)/dt}{1 + S(t)} \tag{6}$$

12.2 Octave strain rate/strain (second harmonic imaging)

Octave strain is obtained when the second harmonic part of the signal is used. The advantage of octave strain is an estimate with less bias and smaller variance, due to fewer reverberations in the second harmonic signal [104]. However, the Nyquist limit

for strain rate will be halved with a potential increase of aliasing. Strain rate will not reach the critical value for aliasing and is of a less problem.

The relation between Nyquist velocity and the pulse repetition frequency (prf) is;

$$Nyquistvelocity = \frac{c \cdot prf}{4 f_0} \qquad (7)$$

c= 1540 m/sec (sound velocity), f_0= ultrasound frequency (2 MHz in cardiac application and 3.4 MHz in octave strain), prf= pulse repetition frequency, L=segment length

The Nyquist limit for strain rate is;

$$NyquistvelocitySR = \frac{c \cdot prf}{4 f_0 \cdot L} \qquad (8)$$

12.3 Algorithm for speckle tracking estimation

The speckle tracking algorithm used in this study combined speckle tracking (grey scale data) for lateral detection of motion and TDI for radial detection of velocity. The tracking method employed a two-dimensional search based upon the sum of absolute differences (SAD), which has been shown to track well-developed speckle patterns as accurately as normalized cross correlation [22]. The SAD tracking board performed a two-dimensional search according to the geometry shown in Figure 2. A small kernel region in one frame was compared to all possible translations with like-sized areas within larger search region in the next frame by calculating the sum of absolute differences over the kernel region for each possible translation. The displacement was found as the best match corresponding to minimum SAD

The size of the kernel defined the spatial velocity resolution while the size of the search region by the frame rate of grey scale (higher frame rate smaller search region). If the spatial averaging parameter was larger than zero, then the calculation of the SAD-matrix and cross correlation were repeated for further points along the ultrasound beam, and the result averaged. The algorithm made it possible to follow the displacement forth and back, and then averaging the results. Potential drift was therefore minimised.

12.4 Algorithms used for calculation of strain rate

Tissue Doppler measures velocity gradient, resulting in Eulerian strain rate:

$$SR = \frac{v(x) - v(x + \Delta x)}{\Delta x} \qquad [4] \qquad (9)$$

where v is the longitudinal velocity component of a point, x is the distance along the beam, and Δx is the offset between two points. This is the values given by scanner and EchoPAC analysis, and was the values used in this study. Strain is usually given as

Lagrangian strain, and to obtain this from Eulerian strain rate, a correction has to be applied:

$$S(t) = \exp\left\{\int_{t_0}^{t} SR(t)\,dt\right\} - 1 \quad [105] \qquad (10)$$

This is already implemented in analysis software, and was used in the study.

Paper I

Recovery of Stunned Myocardium in Acute Myocardial Infarction Quantified by Strain Rate Imaging: A Clinical Study

Charlotte Bjork Ingul, MD, Asbjorn Stoylen, MD, PhD, and
Stig A. Slordahl, MD, PhD, *Trondheim, Norway*

Background: **Strain rate (SR) imaging (SRI) is a tissue Doppler–based method of regional myocardial deformation imaging. The aim of this study was to see whether SRI could quantify changes in myocardial mechanical function after an acute myocardial infarction, and to follow the time course of these changes.**

Methods: **In all, 26 consecutive patients with first-time acute myocardial infarctions were examined on days 1, 7, and 90. Segments were analyzed with SRI and wall-motion score.**

Results: **Peak systolic SR in infarcted segments increased significantly in magnitude from day 1 to 7 (-0.45 to -0.68 s^{-1}, $P < .001$), but not after day 7. The deformation rate in border zone segments also increased significantly from day 1 to 7 (-0.8 to -0.95 s^{-1}, $P < .05$), with no further significant changes at 3 months. In normal segments, peak systolic SR decreased in magnitude during the first week. Systolic strain showed similar results as peak systolic SR.**

Conclusion: **SRI can demonstrate small changes in deformation rate from midinfarct through the infarct and border zone to normal myocardium. It can also show changes over time, probably as a result of recovery of stunned myocardium.** (J Am Soc Echocardiogr 2005;18:401-10.)

In the acute phase of myocardial infarction, regional contractility decreases because of necrosis and stunning, the latter being reversible.[1,2] Some later increase in contractility is, therefore, to be expected, at least in areas where reperfusion is present. Strain rate (SR) imaging (SRI) is a new tissue Doppler–based method that can quantify regional myocardial deformation.[3,4] It has been validated by ultrasonomicrometry.[5] SR (s^{-1})[3,6] is the rate of myocardial deformation, which is calculated from the spatial velocity gradient recorded between two neighboring tissue points (v_1 and v_2) as: $SR = (v_1 - v_2)/L$, where L is the distance between the points. Longitudinal SR is, therefore, negative in systole (shortening) and positive in diastole (lengthening). SR is a regional myocardial deformation parameter, closely related to contractility in normal myocardium. However, SR does not directly measure contractility, because it is load sensitive.[7,8] Increasing afterload decreases SR, and increasing preload increases it. Ischemia changes both systolic and diastolic function.[9-12] Earlier experimental and clinical studies have shown that peak systolic SR (SR_s) can differentiate not only between abnormally and normally contracting segments in the initial phase of an infarction,[3-5,13,14] but can also demonstrate subsequent recovery of transient ischemia.[5,13,14] In acute myocardial infarction (AMI), partial recovery of function after stunning should also be quantifiable by SRI, but this has not been studied previously. Our aim was, therefore, to see whether SRI could quantify changes in myocardial mechanical function after AMI, and follow the time course of these changes.

From the Department of Circulation and Medical Imaging, Norwegian University of Science and Technology

Supported by a grant from the Norwegian Research Council.

Reprint requests: Charlotte Bjork Ingul, MD, Department of Circulation and Medical Imaging, Faculty of Medicine, Norwegian University of Science and Technology, N-7489 Trondheim, Norway (E-mail: *charlotte.b.ingul@medisin.ntnu.no*).

0894-7317/$30.00

doi:10.1016/j.echo.2004.09.025

METHODS

Patients

In all, 30 consecutive patients with first-time AMI, admitted to the coronary care department at our hospital (which has both university and local functions), were asked to participate; all agreed. The inclusion criterion was first-time AMI, diagnosis of which was based on standard criteria of typical chest pain, electrocardiographic (ECG) changes, and increases in blood concentrations of the biochemical markers cardiac troponin T and creatine kinase-MB.[15] Patients who were hemodynamically unstable were excluded. None were excluded because of poor image quality. A total of 4 patients were excluded during the study; 3 had coronary artery bypass operation and 1 died during the observation period, thus, the final study population was 26 patients. The study was approved by the regional ethical committee, and all

Table 1 Baseline characteristics of the 26 patients

Age (y)	65 (48-81)
Male/female sex	16/10
Height (cm)	172 (158-187)
Weight (kg)	77 (55-105)
Peak troponin T (μg/L)	7.2 (0.85-25)
Peak creatine kinase MB (μg/L)	244.5 (48->500)
Q wave/non-Q wave myocardial infarction	19/7
S-T elevation	26
Anterior/inferior myocardial infarction	10/16
Thrombolytic therapy	6
Primary angioplasty	11
Thrombolytic therapy and primary angioplasty	3
Infarct-related artery patent/occluded*	14/5

Data presented as mean (range) or number of patients if no unit indicated.
*In 7 patients, no angiography was done.

patients gave written informed consent. Patient characteristics are given in Table 1.

Echocardiography Data Acquisition

Examinations were performed with scanners (Vivid 7 [55 examinations] or Vivid 5 [20 examinations], GE Vingmed Ultrasound, Horten, Norway) using a phased-array transducer. Single cine loops were recorded from 3 standard apical planes: 4-chamber, 2-chamber, and long-axis. In some patients several recordings were done from the same plane for quality reasons, and the best recording was chosen for analysis. The cineloops were recorded in tissue second-harmonic mode with a frame rate of 35 to 50 frames/s, and in Doppler tissue mode with a mean frame rate of 154 frames/s (range: 109-208). Pulse repetition frequency was 1000 Hz. A complete echocardiographic Doppler study was also recorded, including parasternal long- and short-axis views.

Echocardiography Data Analysis

Recordings were stored digitally and analyzed offline with software (Echopac PC, GE Vingmed Ultrasound). All segments were analyzed with SRI and wall-motion score (WMS) by 2-dimensional echocardiography, according to the American Society of Echocardiography 16-segment model[16] in a 1-to-4 scale: 1 = normal, 2 = hypokinesia, 3 = akinesia, 4 = dyskinesia, x = assessment not possible. Normal, infarcted, and border zone segments were identified by WMS and anatomic location (from ECG and coronary angiography), and were studied on days 1 and 7, and at 3 months. WMS index (WMSI) was calculated as the average WMS of segments studied for each patient. The number of infarcted segments per patient varied. A sub-analysis was done, in which the anatomic midinfarct segment of each patient was compared with a remote control segment.

For each segment, a stationary region of interest (ROI) was manually set in early systole in the middle of the myocardium. The ROI was extended longitudinally and adjusted if possible, to the same length (mean 20 mm) as the analyzed segment, and 5 mm laterally. The velocity gradient was calculated based on many velocities within the ROI and the offset length was 10 to 12 mm, depending on the noise level. In the basal segments, the ROI was set to avoid the aortic valve plane, and in apical segments the lower third was used to avoid unsuitable angle deviation exceeding 30 degrees. Aortic valve closure was used as a time marker for end systole. Aortic valve closure was derived from Doppler tissue velocity, pulsed wave, and a sample volume was placed in the basal septal segment in an apical 4-chamber view (Figure 1).[13,17] Ejection fraction was calculated as the percentage change in left ventricular (LV) chamber volumes between diastole and systole from apical 4-chamber and 2-chamber or long-axis views, using Simpson's method.

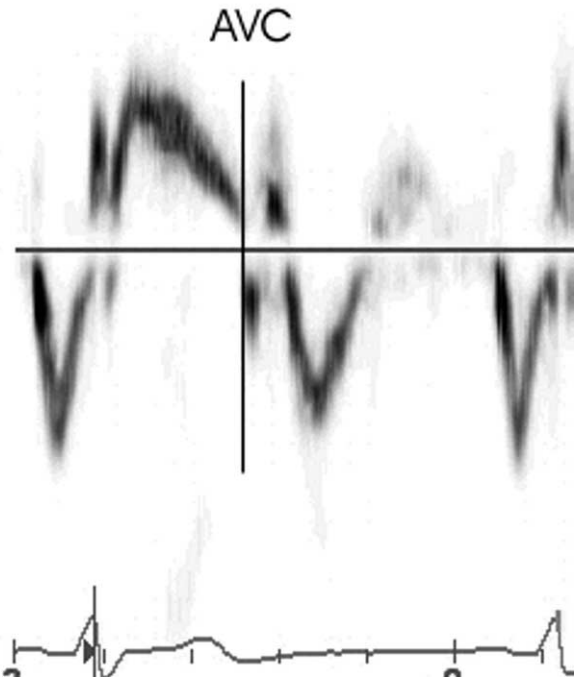

Figure 1 Pulsed wave tissue Doppler with sample volume positioned at base of basal septal segment to determine aortic valve closure (AVC). AVC was timed at beginning of isovolumic relaxation time as indicated.

Parameters Measured and Definitions of Segments

SR_s was chosen as the primary parameter for measuring myocardial deformation rate. The values of SR_s and strain are described in absolute magnitude in the "Results" and "Discussion" sections. A change from, for example, -1.0 to -0.5 s^{-1} will, thus, be described as a decrease. Peak strain rate of early diastolic filling (SR_e) was measured at the peak of the first positive wave after isovolumic relaxation. If more than one peak was seen, they were compared with mitral flow, and the SR_e peak consistent in time with the E wave of mitral flow was chosen as the correct. The onset of diastole (early filling), E wave, was measured by pulsed wave Doppler

Table 2 Two-dimensional and Doppler echocardiographic characteristics, blood pressure and heart rate, longitudinal segmental peak strain rate for systole, diastole, and systolic strain

	Day 1	Day 7	3 mo
Heart rate (beats/min)	72 (11)	64 (11)‡	63 (11)
Systolic BP (mm Hg)	119 (18)	130 (20)*	151 (20)‡
Diastolic BP (mm Hg)	70 (9)	73 (11)	83 (7)†
EF (%)	50.5 (8.6)	51.5 (8.9)	54.2 (7.9)*
LVEDV (mL)	116.6 (22)	118.9 (24)	117.1 (24)
WMSI	1.5 (0.19)	1.43 (0.22)	1.28 (0.23)†
Infarcted segments (n = 119)			
SRs (s^{-1})	−0.45 (0.28)	−0.68 (0.45)‡	−0.77 (0.53)
SRe (s^{-1})	0.90 (0.5)	1.04 (0.62)	1.16 (0.67)
SRa (s^{-1})	0.91 (0.68)	1.07 (0.85)	1.14 (0.92)
Ses (%) (n = 104)	−4.0 (6.0)	−7.4 (6.8)‡	−8.4 (9.6)
Midinfarct segments (n = 26)			
SRs (s^{-1})	−0.25 (0.2)	−0.51 (0.31)‡	−0.51 (0.31)
SRe (s^{-1})	0.91 (0.38)	1.03 (0.46)	1.05 (0.40)
SRa (s^{-1})	0.82 (0.57)	0.85 (0.51)	0.84 (0.53)
Ses (%) (n = 26)	−2.7 (3.3)	−6.7 (4.4)†	−6.5 (8.8)
Border zone (n = 38)			
SRs (s^{-1})	−0.80 (0.27)	−0.95 (0.38)*	−0.91 (0.33)
SRe (s^{-1})	1.08 (0.55)	1.30 (0.63)	1.13 (0.49)
SRa (s^{-1})	1.01 (0.70)	1.27 (0.82)	1.21 (0.78)
Ses (%) (n = 24)	−9.6 (4.1)	−14.1 (6.1)†	−13.6 (7.1)
Normal segments (n = 238)			
SRs (s^{-1})	−1.41 (0.48)	−1.31 (0.5)*	−1.26 (0.46)§
SRe (s^{-1})	1.63 (0.70)	1.60 (0.80)	1.56 (0.82)
SRa (s^{-1})	1.66 (0.92)	1.52 (0.99)	1.54 (0.86)
Ses (%) (n = 175)	−16.6 (7.6)	−16.6 (7.1)	−17.5 (7.4)

BP, Blood pressure; *EF*, ejection fraction; *LVEDV*, left ventricular end-diastolic volume; *Ses*, systolic strain; *SRa*, late diastolic strain rate; *SRe*, early diastolic strain rate; *SRs*, peak systolic index (16 segments scored 1–4/16 segments; 1 = normal, 2 = hypokinesia, 3 = akinesia, 4 = dyskinesia); *SRs*, peak systolic strain rate; *WMSI*, wall motion score index (16 segments scored 1–4/16 segments; 1 = normal, 2 = hypokinesia, 3 = akinesia, 4 = dyskinesia).
*$P < .05$.
†$P < .01$.
‡$P < .001$.
§day 1–3 months $P < .001$.

of mitral flow, with the cursor positioned at the level of the tip of the mitral valve leaflets in the apical 4-chamber view. Peak strain rate of late diastolic filling, the A wave (SR_a), was measured as the first positive wave occurring after the P wave on ECG. Postsystolic shortening (PSS) was defined as myocardial segment shortening after end systole. Peak postsystolic SR was measured as the first negative wave after end systole, and the cutoff between normal and pathologic peak postsystolic SR was empirically chosen as $-0.2\ s^{-1}$. Systolic strain (S_{es}) was measured at end systole. Peak strain (S_{peak}) was measured as the greatest value after end systole. Postsystolic strain was calculated as the difference between S_{peak} and S_{es}. A postsystolic strain index (PSI) was calculated for all segments; $(S_{peak} - S_{es})/S_{peak}$.[18]

Infarcted segments were defined as segments with WMS greater than 1, corresponding to a location defined by ECG and angiography. The border zone was defined as segments with normal WMS and SR_s less than $-0.5\ s^{-1}$ and greater than $-1.0\ s^{-1}$, localized between normal and infarcted segments. With exception of excluded ones, the remaining segments were defined as normal. In all, 16 were defined as infarcted only by SR_s and anatomic location, because of poor 2-dimensional echocardiographic images. Midinfarct segments were defined as the central part of the infarction.

In previous studies of an infarct population, we found that SR_s in normal segments was $-1.2\ s^{-1}$ and in segments with WMS of 2 was $-0.75\ s^{-1}$.[4] The cut-off for the normal segments in this study was placed between these numbers, as SR has a high variability, and normal values have to be defined in rather wide confidence intervals. Return to normalization of SR_s was, therefore, defined as SR_s $-1.0\ s^{-1}$ or less.

Statistics

All measurements are presented as mean ± SD. Student *t* test was used for comparison of two variables. Time series were analyzed by repeated measurements of analysis of variance, with pairwise post hoc analysis by Bonferroni's method. For assessing the relationship between variables, Pearson's correlation coefficient was used, and validity of parametric analysis was confirmed by Spearman rank correlation coefficient. Multiple linear regression was used to test predictors of

Table 3 Postsystolic shortening in normal, border zone, and infarcted segments over time; peak postsystolic strain rate, postsystolic strain index, and number of segments

Segment	Day 1	Day 7	3 mo
Infarcted			
SRps, mean PSS all infarct segments s^{-1}	−0.74 (0.4)	−0.56 (0.51)†	−0.39 (0.45)*
Infarcted segments with PSS	73	51	41
Mean PSS in segments with PSS at time of measurement	−0.74 (0.4)	−0.79 (0.42)	−0.68 (0.38)
PSI	0.57 (0.33)	0.51 (0.33)	0.46 (0.33)
Infarcted segments with postsystolic strain	55	41	24
Border zone			
SRps, mean PSS all border segments s^{-1}	−0.64 (0.32)	−0.14 (0.23)‡	−0.09 (0.21)
Border zone segments with PSS	12	4	2
Mean PSS in segments with PSS at time of measurement	−0.64 (0.32)	−0.41 (0.18)	−0.51 (0.021)
PSI	0.25 (0.14)	0.14 (0.06)	0.25 (0.07)
Border zone segments with postsystolic strain	14	3	4
Normal			
SRps, mean PSS all normal segments s^{-1}	−0.71 (0.34)	−0.32 (0.52)‡	−0.27 (0.61)
Normal segments with PSS	13	4	4
Mean PSS in segments with PSS at time of measurement	−0.71 (0.34)	−0.96 (0.43)	−1.03 (0.49)
PSI	0.19 (0.14)	0.2 (0.11)	0.2 (0.12)
Normal segments with postsystolic strain	49	23	17

Data presented as mean (SD).
PSI, Postsystolic strain index; *PSS*, postsystolic shortening; *SRps*, peak postsystolic strain rate were followed in the same segments at day 1, day 7, and after 3 months.
*$P < .05$.
†$P < .01$.
‡$P < .001$.
Data presented as mean (SD).

recovery of myocardial function. A value of $P < .05$ was considered statistically significant. For intraobserver and interobserver variability, we used Bland and Altman 95% limits of agreement.

RESULTS

A total of 1248 segments were analyzed; SR_s could be assessed in 1152 (92.3%). The number of interpretable segments on basal, mid, and apical level was 93.6%, 96.1%, and 95.2%, respectively ($P < .05$ basal-mid, $P < .01$ basal-apical). Fewer segments were adequate for analysis of S_{es} (77%). Basic hemodynamic, global, and regional systolic and diastolic measurements are given in Table 2. Heart rate decreased from day 1 to 7 ($P < .01$) with no further changes. Systolic blood pressure increased significantly over time. Ejection fraction increased from day 7 to 3 months ($P < .05$), but LV end-diastolic volume showed no significant changes during the study.

Systolic Function

SR_s was less in midinfarct segments than the mean of all infarcted segments (−0.25 vs −0.45 s^{-1}, $P < .001$), and less than in border zone segments (−0.8 s^{-1}, $P < .001$), which in turn were less than in normal segments (−1.41 s^{-1}, $P < .001$). SR_s increased in infarcted segments during the first week ($P < .001$), but not thereafter. Midinfarct segments recovered less, as measured by SR_s increase, than the mean of all infarcted segments. SR_s exceeded −1 s^{-1} in 26 (22%) of all infarcted segments at 3 months. Such segments had a greater SR_s initially, which increased from −0.68 at day 1 to −1.49 s^{-1} at 3 months ($P < .001$). In the remaining infarcted segments, SR_s was initially lower, −0.38 s^{-1}, and increased only to −0.56 s^{-1} at day 7 and 3 months (Table 2).

In the border zone, SR_s was initially reduced, but had increased after 1 week ($P < .05$), with no further significant changes. Normal segments showed an initial hyperkinesia (−1.41 s^{-1}) that decreased significantly after 1 week (−1.31 s^{-1}, $P < .05$), paralleling the increase in SR_s in the infarcted segments. At day 1, of 119 infarcted segments, SR_s was zero in 3 (akinesia) and positive in 6 (dyskinesia). There was a biphasic response with an initial positive SR value, and thereafter a negative systolic peak in 15 segments. The remaining 94 infarcted segments were hypokinetic, with a negative SR_s (Table 2).

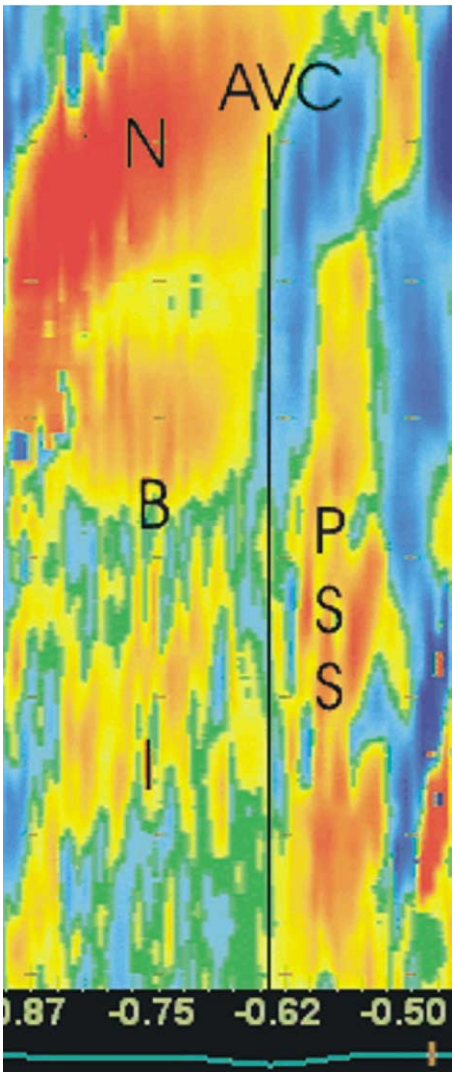

Figure 2 Longitudinal strain rate. Curved anatomic M-mode of inferior wall, with acute inferior infarction, showing gradient of deformation rate from normal (*N*) to border zone (*B*) to infarcted (*I*) segment. Postsystolic shortening (*PSS*) extends into normal segment.

There was no initial difference in SR_s between Q wave and non-Q wave infarctions (-0.44 s^{-1} vs -0.45 s^{-1}), but there was at 3 months (SR_s -0.71 s^{-1} vs -0.95 s^{-1}, $P < .05$). S_{es} showed similar patterns as SR_s, increasing after 1 week in infarcted ($P < .001$), midinfarct ($P < .05$), and border zone segments ($P < .05$). In normal segments there were no significant changes in S_{es} (Table 2).

Diastolic Function

In infarcted segments, SR was reduced both in early (SR_e) and late (SR_a) diastole (day 1; SR_e 0.9 s^{-1}, SR_a 0.91 s^{-1}), with border zone values (day 1; SR_e 1.08 s^{-1}, SR_a 1.01 s^{-1}) between those of infarcted and normal segments. Peak strain rate during early and late filling only increased slightly in infarcted segments during 3 months ($P = .054$, $P = .053$). There were no significant changes in early or late diastole in normal and border zone segments during follow-up (Table 2).

PSS

PSS was most pronounced in the infarcted segments, both in magnitude and extent. It was present in 60% of infarcted segments, compared with 29% in the border zone and 5% of normal segments (Table 3). The frequency of PSS was greatest in midinfarct segments (73%). PSS disappeared in almost all normal and border zone segments during the first week. There were 73 infarcted segments with PSS at day 1 and 41 at 3 months.

There was no difference in SR_s at any time between infarcted segments without (n = 46) or with (n = 73) PSS (-0.49 s^{-1} vs -0.42 s^{-1} at day 1, -0.74 s^{-1} vs -0.65 s^{-1} at day 7, and -0.77 s^{-1} vs -0.77 s^{-1} at 3 months, respectively, all nonsignificant). Mean PSI in the infarcted segments at day 1 was 0.57, decreasing to 0.46 at 3 months. The initial values were much lower in normal and border zone segments (0.25 vs 0.19) (Table 3).

WMS

Mean SR_s at day 1 was as follows: for segments with WMS = 1 (n = 287), -1.29 (0.52) s^{-1}; WMS = 2 (n = 65), -0.76 (0.49) s^{-1}; and WMS = 3 (n = 62) and WMS = 4 (n = 1), -0.39 (0.35) s^{-1}. WMSI was 1.5 at day 1, decreasing from day 7 to 3 months (1.43 vs 1.28, $P = .001$; Table 2). WMSI and SR_s were correlated at day 1 ($r = 0.63$, $P < .01$). WMS for midinfarct segments was 2 in 7 patients and 3 in 19.

Reproducibility

We reanalyzed 104 segments for intraobserver variability. A total of 4 segments (1 normal and 3 infarcted) were randomly selected from each patient, and the infarcted ones were reanalyzed at the different time steps. For assessment of interobserver variability, 251 segments were randomly selected and analyzed by a second experienced observer. The 95% limits of agreement for the intraobserver analysis were ± 0.38 s^{-1} and bias was -0.001 (nonsignificant). The mean for all segments was -0.82 s^{-1}. For interobserver analysis, the corresponding numbers were ± 0.69 s^{-1} and -0.02 (nonsignificant). The mean for all segments was 1.0 s^{-1}.

DISCUSSION

SR_s and S_{es}

This study showed that SR_s and S_{es} can quantify changes in regional myocardial mechanical function

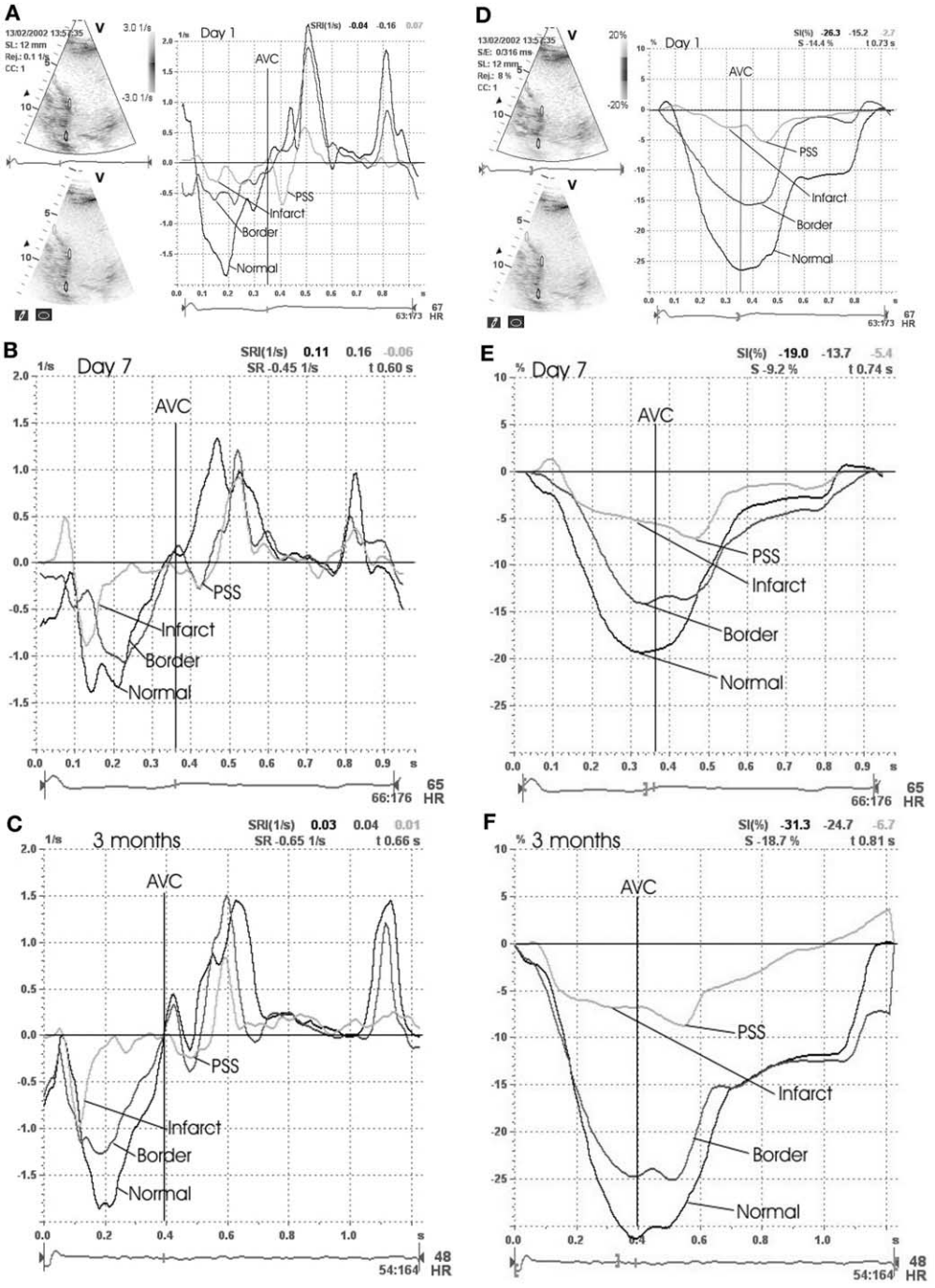

Figure 3 Inferior wall of 65-year-old man with acute apical infarction, treated with prehospital thrombolysis. Coronary angiography showed proximal left anterior descending coronary artery stenosis. *Upper curves* show strain rate values, *lower curves* show strain values, over time. Day 1 peak systolic strain rate (SR_s) was $-0.2\ s^{-1}$ in infarcted segment and $-0.7\ s^{-1}$ in border zone segment. Normal segment showed hyperkinesia and SR_s was $-1.8\ s^{-1}$. On day 7, infarcted segment showed improved SR_s ($-0.9\ s^{-1}$) and border zone normalization of SR_s ($-1.0\ s^{-1}$). After 3 months there were no major changes. Infarcted segment showed initial postsystolic shortening, decreasing over time. Measuring only SR_s showed normalized value at 3 months, but strain rate curves (day 7 and 3 months) suggest short-lasting initial peak value, without lasting shortening, and strain curves confirm that function had not returned to normal, with still low end-systolic strain at 3 months.

after AMI. Hence, SRI can quantify the recovery of stunned myocardium in both infarcted and border zone segments. However, the degree of variation is greater than desirable for clinical use.

The main increases in SR_s and S_{es} occurred during the first week. Other studies demonstrate that delayed recovery because of stunning occurs during a period of weeks rather than months. Several studies of LV WMS in patients receiving reperfusion treatment for AMI have shown delayed return of regional LV function.[19] We were also able to identify reduced function in border zone segments, indicating that SR_s can potentially detect changes in contractility not yet demonstrable by WMS. Our data demonstrate a clear gradient of systolic deformation rate from midinfarct to normal segments, as exemplified in Figure 2, taken from a patient with an inferior infarction.

The method also seems sensitive enough to detect initial hyperkinesia in noninfarcted segments, as shown by the time course of systolic SR. The deformation rate decreased in normal segments during the first week, possibly indicating decreasing compensatory hyperkinesia. A greater initial SR_s value in the acute phase was the best predictor of improvement in LV systolic function. Figures 3 and 4 show the time course of SR and strain from patients with AMI. Figure 3 illustrates the potential pitfall; whereas SR_s has almost returned to normal by day 7, albeit with a short peak and limited contraction, S_{es} is still reduced, confirming that function has not yet recovered. On the other hand, Figure 4 shows a SR_s curve with a longer lasting peak and a normalized value at day 7; strain gives the same information. The differences of the SR and strain curves in Figures 3 and 4 can be explained thus: SR only measures the rate of lengthening or shortening (deformation), whereas strain measures the relative amount of deformation.

Peak Early Diastolic SR

Experimental and clinical studies using Doppler tissue imaging show depressed early diastolic function in acute ischemia.[20,21] Earlier echocardiographic studies have reported similar findings with Doppler measurements of mitral flow velocity.[22] Doppler tissue imaging, however, is less load-dependent than standard Doppler measurements.[23] The time course of depressed early diastolic filling, post-AMI, has previously been studied by traditional Doppler methods,[24] but not, to our knowledge, using SRI.

We found that, in the acute phase, early diastolic function was relatively less affected than systolic function in the infarcted segments, possibly because of increased LV filling pressure. However, our data also indicate less subsequent recovery of early diastolic function. This lack of significant recovery of diastolic function 3 months post-AMI, judged by standard Doppler measurements, has been reported elsewhere.[24] During the study period, we found that SR_e was unchanged in the normal segments, as did Smalling[9] in an AMI animal experiment. In that study, standard Doppler measurements showed reduced early diastolic filling, and the compensatory effect of increased diastolic function in normal segments was less pronounced than the systolic compensation.

We found that the SR_e was more reduced in the infarcted segments than in the border zone. Diastolic filling is influenced by the amount of necrotic myocardium.[25] Only 19 of 26 infarctions in our study were transmural, which could explain the relatively less depressed diastolic function we observed.

Feasibility of SR and Strain

There were 15% more analyzable segments with SR compared with strain. Segments were excluded because of artifacts, poor gray-scale visibility, or unsuitable angle deviation. Feasibility was lower in strain mainly because of drift in the curves.

PSS and PSI in Different Segments

PSS is a sensitive marker of ischemia.[10,11,17,26,27] However, as PSS is found in 30% of myocardial segments in control subjects,[28] its specificity is low. In our study, only 5% of normal segments showed PSS, and significantly fewer at 3 months, in accordance with earlier findings from our group.[29] Our material consisted of normal segments in an infarcted population, which might explain the differences between our study and those with only normal segments. Differences in the definition of PSS may also cause discrepancies; hence, we used a strict definition, with a cut-off value between normal and pathologic PSS of $-0.2\ s^{-1}$. We choose this cutoff since Voigt et al[28] suggested that PSS is not pathologic unless it exceeds 20% of total myocardial shortening, which would correspond to our SR limit.

Other indices have been suggested as markers of ischemia, as PSS in itself is not sufficiently sensitive. Pislaru et al[30] suggested an index of PSS/SR_s greater than 1 to differentiate ischemic segments from nonischemic ones in segments with a reduced deformation rate. In an experimental study, Kukulski[18] proposed a PSI with a cutoff of 0.25 (for longitudinal strain) for identification of acutely ischemic segments. In our study, PSI distinguished well between ischemic (PSI 0.57), border zone (PSI 0.25), and normal (PSI 0.19) segments in the acute phase. Most of the PSS, as measured by peak postsystolic SR, disappeared after 1 week in all types of segments. Normalization of longitudinal function was defined as $SR_s -1.0\ s^{-1}$ or less, and different predictors were tested. The degree of PSS in infarcted segments did not seem to predict recovery of function, as our data showed no difference over time in SR_s between segments with or without PSS.

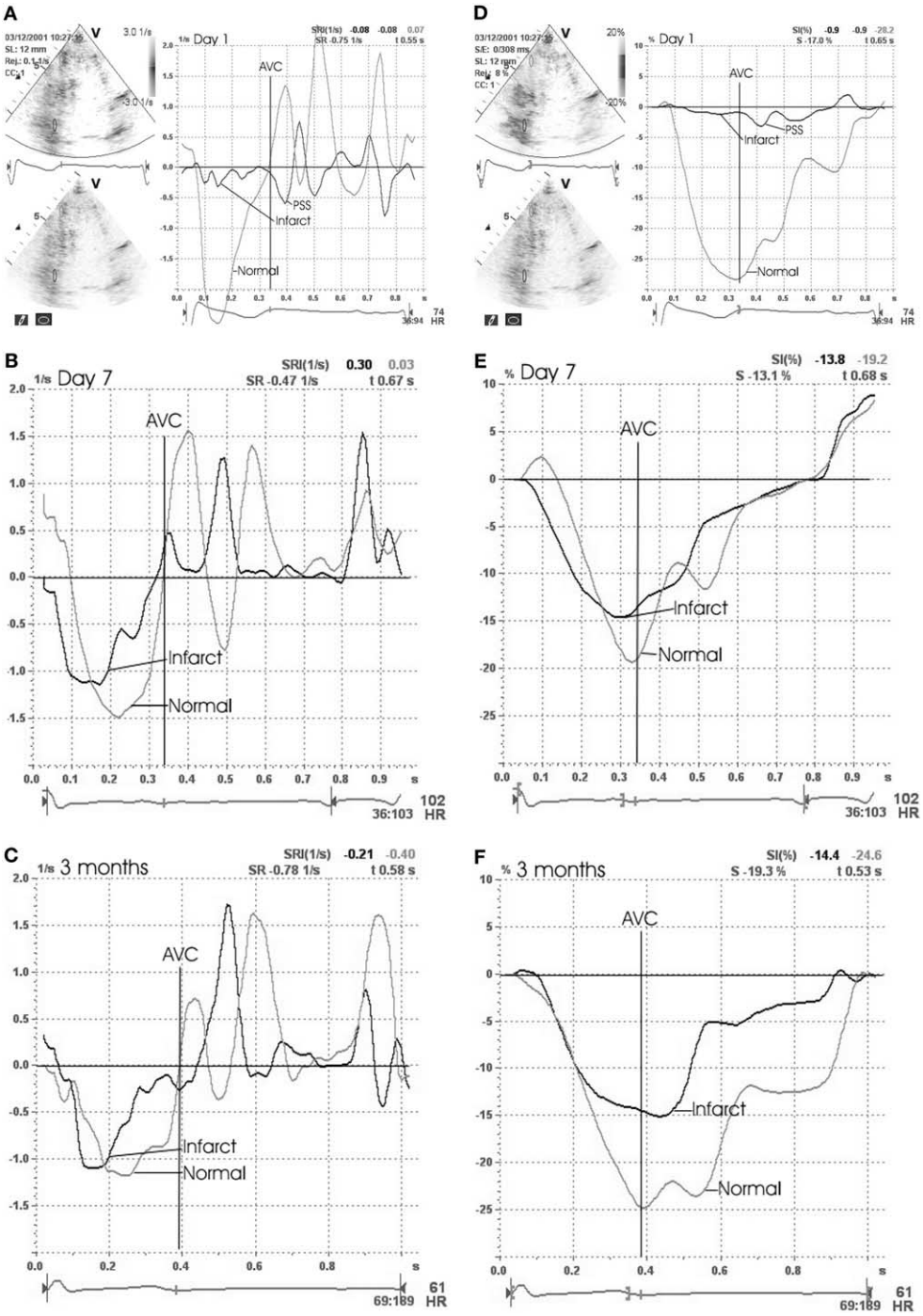

Figure 4 A 75-year-old man with acute inferior infarction treated with percutaneous coronary intervention and 3 stents in occluded right coronary artery. On day 1, peak systolic strain rate (SR_s) in infarcted segment was $-0.3\ s^{-1}$ and there was initial hyperkinesia in normal segment, SR_s $-2.0\ s^{-1}$. By day 7, function had recovered in infarcted segment (SR_s $-1.0\ s^{-1}$) and hyperkinesia in normal segment normalized (SR_s $-1.5\ s^{-1}$). Postsystolic shortening disappeared in infarcted segment after 3 months. End-systolic strain confirmed normalization of function.

The Effect of WMS and the Transmural Extent of Infarction on SR

This study showed that SR_s is a more sensitive index than WMS for quantifying regional changes over time in localized myocardial areas. Unlike SR_s, WMSI provides information on global ventricular changes, and showed an increase at 3 months. Conventional assessment of wall motion is based on endocardial excursion and wall thickening, qualitative methods that have well-known limitations, such as echo quality, and being subjective and experience-dependent.[31] SR_s is lower in transmural than nontransmural infarctions.[32] Our study showed no difference in SR_s between Q and non-Q in SR_s day 1 and 7, but at 3 months function had almost recovered for non-Q but not for Q wave infarctions. This is consistent with the finding of Schinkel et al,[33] who showed no difference in the residual viability of infarcted regions between Q wave and non-Q wave infarctions. In our study, Q wave infarctions were small and generally had few akinetic segments.

SR and Strain Give Different Information

Even with a negative SR_s, there may be initial or late dyskinesia during systole. Important information about systole will be missed if only SR_s is used. Figure 3 illustrates this clearly. Strain takes all of systole into account and, being an integration of SR, is less influenced by random noise. However, it does not provide the same information about diastole; a combination of strain and SR_s might offer a better solution.

Reproducibility

Intraobserver variability was high; the 95% limits of agreement were $\pm 0.38\ s^{-1}$, ie, the smallest significant change in repeated measurement in a single patient was 0.38 (repetition coefficient). The mean changes in our patients were smaller than that, thus, this method for SRI is slightly too insensitive for follow-up of individual patients. Variability might be reduced by averaging more cineloops. Interobserver variability was even higher with 95% limits of agreement of $\pm 0.69\ s^{-1}$.

Limitations

The curves were not studied independently, as the same researcher set the ROI of the segments and, therefore, wall motion was visible, possibly influencing the objectivity of the researcher. There was no independent method of function; coronary angiography and ECG were used to distinguish the segments. The sample size was small and not all patients were examined on admission, some being seen the day after. In all, 7 patients had no coronary angiography. The technique of SRI still has many limitations such as random noise, nonrandom noise, and angle dependency.[34] The anterior and lateral walls in particular give some uncertainty in SR measurement. The poor lateral resolution gives uncertainty about the exact localization of the ROI. Time course was not blinded in the analysis.

Conclusion

We have shown that SRI can demonstrate small changes in contractility from midinfarct through to the border zone and normal myocardium, and changes over time, probably as a result of recovery of stunned myocardium. PSS in infarcted segments did not predict improvement of function.

We wish to thank Profs Liv Hatle and Tom Marwick for constructive criticism and helpful comments of the manuscript.

REFERENCES

1. Braunwald E. The stunned myocardium: prolonged, postischemic ventricular dysfunction. Circulation 1982;66:1146-9.
2. Dorge H. Pathophysiology of hibernation, stunning, and ischemic preconditioning. Thorac Cardiovasc Surg 1998;46:255-62.
3. Stoylen A, Heimdal A, Bjornstad K, Torp HG, Skjaerpe T. Strain rate imaging by ultrasound in the diagnosis of regional dysfunction of the left ventricle. Echocardiography 1999;16:321-9.
4. Stoylen A. Strain rate imaging by ultrasonography in the diagnosis of coronary artery disease. J Am Soc Echocardiogr 2000;13:1053-64.
5. Urheim S. Myocardial strain by Doppler echocardiography: validation of a new method to quantify regional myocardial function. Circulation 2000;102:1158-64.
6. Heimdal A, Stoylen A, Torp H, Skjaerpe T. Real-time strain rate imaging of the left ventricle by ultrasound. J Am Soc Echocardiogr 1998;11:1013-9.
7. Leone BJ. Effects of progressive myocardial ischemia on systolic function, diastolic dysfunction, and load dependent relaxation. Cardiovasc Res 1992;26:422-9.
8. Weidemann F, Jamal F, Sutherland GR, Claus P, Kowalski M, Hatle L, et al. Myocardial function defined by strain rate and strain during alterations in inotropic states and heart rate. Am J Physiol Heart Circ Physiol 2002;283:H792-9.
9. Smalling RW. Comparison of early systolic and early diastolic regional function during regional ischemia in a chronically instrumented canine model. J Am Coll Cardiol 1983;2:263-9.
10. Safwat A. Pressure-length loop area: its components analyzed during graded myocardial ischemia. J Am Coll Cardiol 1991; 17:790-6.
11. Lowenstein E. Regional ischemic ventricular dysfunction in myocardium supplied by a narrowed coronary artery with increasing halothane concentration in the dog. Anesthesiology 1981;55:349-59.
12. Cerisano G. Echo-Doppler evaluation of left ventricular diastolic dysfunction during acute myocardial infarction: methodological, clinical and prognostic implications. Ital Heart J 2001;2:13-20.
13. Jamal F, Kukulski T, Strotmann J, Szilard M, D'hooge J, Bijnens B, et al. Quantification of the spectrum of changes in

regional myocardial function during acute ischemia in closed chest pigs: an ultrasonic strain rate and strain study. J Am Soc Echocardiogr 2001;14:874-84.
14. Jamal F. Can changes in systolic longitudinal deformation quantify regional myocardial function after an acute infarction? An ultrasonic strain rate and strain study. J Am Soc Echocardiogr 2002;15:723-30.
15. Alpert JS. Myocardial infarction redefined–a consensus document of the joint European Society of Cardiology/American College of Cardiology committee for the redefinition of myocardial infarction. J Am Coll Cardiol 2000;36:959-69.
16. Schiller NB. Recommendations for quantitation of the left ventricle by two-dimensional echocardiography: American Society of Echocardiography committee on standards, subcommittee on quantitation of two-dimensional echocardiograms. J Am Soc Echocardiogr 1989;2:358-67.
17. Weidemann F, Kowalski M, D'hooge J, Bijnens B, Sutherland GR. Doppler myocardial imaging: a new tool to assess regional inhomogeneity in cardiac function. Basic Res Cardiol 2001;96:595-605.
18. Kukulski T. Identification of acutely ischemic myocardium using ultrasonic strain measurements: a clinical study in patients undergoing coronary angioplasty. J Am Coll Cardiol 2003;41:810-9.
19. Kloner RA, Jennings RB. Consequences of brief ischemia: stunning, preconditioning, and their clinical implications; part 1. Circulation 2001;104:2981-9.
20. Derumeaux G. Doppler tissue imaging quantitates regional wall motion during myocardial ischemia and reperfusion. Circulation 1998;97:1970-7.
21. García-Fernández MA, Azevedo J, Moreno M, Bermejo J, Pérez-Castellano N, Puerta P, et al. Regional diastolic function in ischaemic heart disease using pulsed wave Doppler tissue imaging. Eur Heart J 1999;20:496-505.
22. Wind BE, Snider AR, Buda AJ, O'Neill WW, Topol EJ, Dilworth LR. Pulsed Doppler assessment of left ventricular diastolic filling in coronary artery disease before and immediately after coronary angioplasty. Am J Cardiol 1987;59:1041-6.
23. Nagueh SF, Middleton KJ, Kopelen HA, Zoghbi WA, Quiñones MA. Doppler tissue imaging: a noninvasive technique for evaluation of left ventricular relaxation and estimation of filling pressures. J Am Coll Cardiol 1997;30:1527-33.
24. Poulsen SH, Jensen SE, Egstrup K. Longitudinal changes and prognostic implications of left ventricular diastolic function in first acute myocardial infarction. Am Heart J 1999;137:910-8.
25. Pipilis A, Meyer TE, Ormerod O, Flather M, Sleight P. Early and late changes in left ventricular filling after acute myocardial infarction and the effect of infarct size. Am J Cardiol 1992;70:1397-401.
26. Barletta G. Post-ejection thickening as a marker of viable myocardium: an echocardiographic study in patients with chronic coronary artery disease. Basic Res Cardiol 1998;93:313-24.
27. Urheim S. Postsystolic shortening of ischemic myocardium: a mechanism of abnormal intraventricular filling. Am J Physiol Heart Circ Physiol 2003;284:H2343-50.
28. Voigt JU, Lindenmeier G, Exner B, Regenfus M, Werner D, Reulbach U, et al. Incidence and characteristics of segmental postsystolic longitudinal shortening in normal, acutely ischemic, and scarred myocardium. J Am Soc Echocardiogr 2003; 16:415-23.
29. Stoylen A, Ingul CB, Torp H. Strain and strain rate parametric imaging: a new method for post processing to 3-/4-dimensional images from three standard apical planes; preliminary data on feasibility, artefact and regional dyssynergy visualization. Cardiovasc Ultrasound 2003;1:11.
30. Pislaru C, Anagnostopoulos PC, Seward JB, Greenleaf JF, Belohlavek M. Higher myocardial strain rates during isovolumic relaxation phase than during ejection characterize acutely ischemic myocardium. J Am Coll Cardiol 2002;40:1487-94.
31. Picano E, Lattanzi F, Orlandini A, Marini C, L'Abbate A. Stress echocardiography and the human factor: the importance of being expert. J Am Coll Cardiol 1991;17:666-9.
32. Weidemann F, Dommke C, Bijnens B, Claus P, D'hooge J, Mertens P, et al. Defining the transmurality of a chronic myocardial infarction by ultrasonic strain-rate imaging: implications for identifying intramural viability; an experimental study. Circulation 2003;107:883-8.
33. Schinkel AF, Bax JJ, Boersma E, Elhendy A, Vourvouri EC, Roelandt JR, et al. Assessment of residual myocardial viability in regions with chronic electrocardiographic Q-wave infarction. Am Heart J 2002;144:865-9.
34. D'hooge J, Heimdal A, Jamal F, Kukulski T, Bijnens B, Rademakers F, et al. Regional strain and strain rate measurements by cardiac ultrasound: principles, implementation and limitations. Eur J Echocardiogr 2000;1:154-70.

Paper II

Automated Analysis of Strain Rate and Strain: Feasibility and Clinical Implications

Charlotte Bjork Ingul, MD, Hans Torp, Dr Tech, Svein Arne Aase, MS, Sigrid Berg, MS, Asbjorn Stoylen, MD, PhD, and Stig A. Slordahl, MD, PhD, *Trondheim, Norway*

Background: **This study evaluated 3 new automated methods, based on a combination of speckle tracking and tissue Doppler, for the analysis of strain rate (SR) and strain. Feasibility and values for peak systolic strain rate (SR_s) and end-systolic strain (S_{es}) were assessed.**

Methods: **Thirty patients with myocardial infarction and 30 normal subjects were examined. Customized software with automatic definition of segments was used for automated measurements. SR_s and SR_{es} were measured over each segment simultaneously and identified automatically. The study compared tissue Doppler–based SR and strain measurements without (method 1) and with segment tracking (method 2) to speckle tracking–based measurements (method 3). For tracking, speckle tracking and tissue Doppler were used in combination. Standard manual analysis was used as a reference.**

Results: **The automated analysis (16 segments, 3 apical views) required 2 minutes; manual analysis took 11 minutes. Accuracy was compared in 56 segments (28 mid-infarcted and 28 normal) from 28 patients and was 93.9% for method 1, 93.8% for method 2, 95.8% for method 3, and 96.2% for the manual method. In the normal group, mean SR_s ($0.27\ s^{-1}$) was less with method 3 than with the other methods ($P < .001$).**

Conclusions: **Our findings indicate that automated analysis of SR and strain, with some manual adjustment, is feasible and quicker than manual analysis. Diagnostic accuracy was similar with all methods. SR_s was lower in the speckle tracking–based method than in the Doppler-based methods.** (J Am Soc Echocardiogr 2005;18:411-8.)

Strain rate (SR) and strain are new methods for quantifying regional deformation rate and deformation by either tissue Doppler[1] or speckle tracking.[2] Manual analysis is time-consuming, and the postprocessing required for acceptable results requires experience. Further, strain rate imaging (SRI) has a high variability and thus is currently of limited clinical use. The new scanner technology simultaneously acquires not only high-quality 2-dimensional images with adequate frame rates for gray-scale imaging, but also high-frame-rate tissue Doppler data, enabling applications that use both modalities.[3,4]

Both tissue Doppler–based and speckle tracking–based SR have strengths and weaknesses. Doppler-based ultrasound techniques quantify only the axial component of motion (ie, motion along the direction of the transmitted ultrasound wave) and thus are angle-dependent.[5-8] They are also prone to errors induced by random noise. Other errors can occur because although conventional SRI measures the SR at a fixed point in space, deformation occurs in myocardial segments displaced during the cardiac cycle. The importance of tracking the region of interest (ROI) through the cardiac cycle has been emphasized,[9] although not yet documented.

In gray-scale images, interference by backscattered ultrasound from neighboring structures results in a random speckled pattern. This gives each small area a unique pattern that remains relatively constant from 1 frame to the next. Hence a suitable pattern-matching algorithm can identify the displacement from 1 frame to the next, allowing the motion of the myocardium to be followed in 2 dimensions.[2,10] Time-domain speckle tracking techniques are effective for quantifying tissue velocities.[11,12] However, the low frame rate of gray-scale images may lead to undersampling, reducing peak values. If the frame rate is too low, then the speckle pattern will change too much from one frame to the next, preventing the myocardial region from being followed precisely. In contrast, increasing the frame rate will reduce line density, reducing lateral resolution and yielding poor transverse tracking.[13]

From the Department of Circulation and Medical Imaging, Norwegian University of Science and Technology, Trondheim, Norway.

Supported by a grant from the Norwegian University of Science and Technology.

Hans Torp and Asbjorn Stoylen have received honoraria from GE Vingmed for lecturing.

Reprint requests: Charlotte Bjork Ingul, MD, Department of Circulation and Medical Imaging, Faculty of Medicine, Norwegian University of Science and Technology, N-7489 Trondheim, Norway (E-mail: *charlotte.b.ingul@ntnu.no*).

0894-7317/$30.00

doi:10.1016/j.echo.2005.01.032

We developed methods for automatic segmental analysis by combining speckle tracking and tissue Doppler in various combinations. The purposes of the study were (1) to assess the feasibility of automated analysis compared with manual analysis, and (2) to evaluate diagnostic accuracy and compare measurement values of 3 different automated methods of measuring SR and strain (using speckle tracking and tissue Doppler in 3 different ways) in comparison with standard manual analysis.

METHODS

Study Population

The main study examined 30 patients (mean age 65 ± 9 years; 11 women) with a first myocardial infarction (17 inferior/13 anterior, 23 Q-wave, mean creatine kinase MB 266 μg/L, mean troponin T 7.4 μg/L) and 30 subjects (mean age 57 ± 12 years; 15 women) with normal ventricles, coronary angiography, and dobutamine stress echocardiography. Finally, to evaluate the influence of B-mode frame rate on undersampling and precision in speckle tracking (method 3), further analysis was done in 10 healthy individuals (mean age 28 ± 6 years; 5 women). No patient was excluded due to poor acoustic window. The approval of the regional ethics committee was obtained, and all subjects gave written informed consent.

Echocardiography Image Acquisition

The main study examinations were performed with either a Vivid 5 scanner (12 examinations) or a Vivid 7 scanner (58 examinations) (GE Vingmed Ultrasound, Horten, Norway), using a phased-array transducer. The frame rate study was performed on a Vivid 7. Three cine loops from the 3 standard apical planes (4-chamber, 2-chamber, and long-axis) were recorded simultaneously in both tissue second harmonic mode and tissue Doppler mode. The mean frame rate on the Vivid 7 was 155 frames per second (FPS) (range, 109-209 FPS) for tissue Doppler and 49 FPS (range, 36-70 FPS) for B-mode. The mean frame rate on the Vivid 5 was 133 FPS (range, 130-147 FPS) for both tissue Doppler and B-mode. The pulse repetition frequency was 1000 Hz.

In the additional B-mode frame rate study, recordings were made at 70 FPS and reduced to 35 FPS in gray-scale data in apical 4-chamber, 2-chamber, and long-axis views. The sector angle was set to 60 degrees, with equal frame rates for B-mode and tissue Doppler images.

Echocardiography Data Analysis

Automated identification of myocardial segments. For the automated measurements, we used customized software (GcMat; GE Vingmed Ultrasound), a postprocessing system that runs under Matlab (MathWorks, Natick, Mass). For each apical view, the apex, mitral ring, and the endocardial border were identified automatically[4] and the myocardium was divided into 6 equal segments (Figure 1), subject to manual adjustment.

A speckle tracking method, using minimum SAD (sum of absolute differences) of the B-mode pixel data[14] combined with tissue Doppler velocities, was used to track the position of a kernel region (a chosen region of the myocardium with a unique speckle pattern) of the segment borders throughout the cardiac cycle. Tracking was done axially by tissue Doppler data and laterally by speckle tracking. Tracking by tissue Doppler along the ultrasound beam limited the search area to a sector extending in the lateral direction and thus reduced the time for the speckle search. To avoid drift, the tracking algorithm was applied both forward and backward, and the results were averaged. The position of the kernel regions could be adjusted manually if tracking was poor. This search procedure enabled tracking of segment position, segment orientation, and segment length throughout the cycle. The following parameters were used for GcMat analysis: axial averaging, 1 mm; temporal averaging, 10 ms. The distance for SR calculation was 15 mm (for methods 1 and 2).

Aortic valve closure. The timing of aortic valve closure (AVC) was defined from the Doppler spectrum of aortic flow, pulsed wave, in the apical 4-chamber view. The value was stored and displayed automatically in all curves, adjusted to the heart rate in the actual image being analyzed.

Methods. In method 1, a stationary ROI was placed automatically in the center of the defined segment at end-diastole. SR was calculated from the velocity gradient along the ultrasound beam[1] at a fixed position in space, as illustrated in Figure 1 between p1 and p2. Tracking was not used in this method; only automated segmentation and ROI placement are used.

In method 2, a dynamic ROI was placed automatically in the center of the segment at end-diastole, and the midpoint of the segment was tracked throughout the cardiac cycle. Axial movement was measured by tissue Doppler; lateral movement, by speckle tracking. SR and strain measurements were calculated as in method 1 by tissue Doppler.

In method 3, strain was calculated directly from the variation of the segment length using the tracked end points: strain = $(L-L_0)/L_0$, as illustrated in Figure 1 between p3 and p4. SR was calculated as the temporal derivative of strain, with correction to Eulerian SR. This enabled angle-independent measurements of SR and strain. Segment tracking was done as in method 2. In the automated analysis, measurements from a segment were only accepted or discarded. Thus if the kernel region failed to properly track laterally and/or axially after adjustment, then the segment was discarded. The segment also was discarded if the B-mode image showed regions with missing ultrasound data (dropouts) or larger reverberations. For methods 1 and 2, segments were discarded if the angular deviation exceeded 25 degrees.

For standard manual measurements of tissue Doppler, we used commercial software, EchoPAC PC (GE Vingmed Ultra-

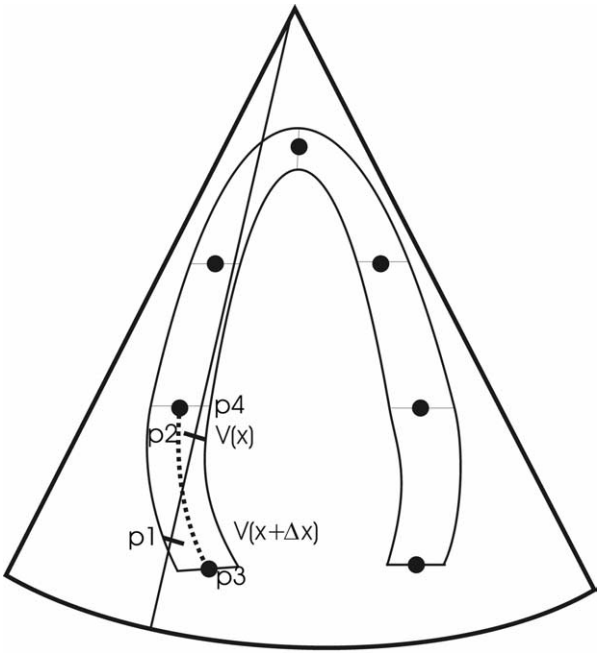

Figure 1 Ultrasound sector with 1 beam and an apical view of the left ventricle. Seven material points (1 apical, 2 in the atrioventricular plane, and 2 in each wall between the apex and the basis) are set automatically by an edge detector algorithm. These points divide the ventricle into 6 segments. The differences between the strain rate calculations are illustrated in the basal segment on the left side. For the speckle-based method, strain is calculated between p3 and p4 defining the segment (as shown by dotted line), independent of the angle to the beam. For tissue Doppler–based methods, SR is calculated along the ultrasound beam between the marked lines for offset, p1 to p2. In the stationary method (method 1), the ROI is set in space rather than in the myocardium. *SR*, strain rate; *ROI*, region of interest.

sound). A stationary ROI was placed manually in the center of a segment at mid-systole with an offset of 12 mm for SR calculation. The size of the ROI was adjusted to cover the segment length. If artifacts were seen on the B-mode image, then the size and position of the ROI was adjusted to avoid them. For the apical segments, only the lower third was used. In manual analysis, the segmental ROI could be adjusted, which reduced the number of discarded segments. Segments were also discarded if the SR curve was very noisy, if the peak of the SR curve came close to aortic valve opening or closing, or if the curve was flat and lacked E- and A-waves. Segments were also discarded if the angular deviation exceeded 25 degrees. Strain curves were discarded if they did not return to baseline at the end of the cycle.

Measurements. Peak systolic strain rate (SR_s) and end systolic strain (S_{es}) were chosen as the primary parameters and were measured in 18 segments from 3 apical views. Two apical segments were excluded according to the standard 16-segment model of the American Society of Echocardiography.[15] Figure 2 illustrates the automatically generated SR curves. Mean values and standard deviation (SD) were analyzed in all segments for all 60 subjects. For comparison of diagnostic accuracy between the 4 methods, we analyzed 28 patients with a first myocardial infarction; 2 patients with negligible infarct size were excluded. SR_s was measured in 1 infarct segment from the central part of the infarction area (from ECG and coronary angiography) and in 1 remote (normal) segment from each patient, for a total of 28 infarcted and 28 normal segments. The normal value for SR_s was defined as a value $\leq -1\ s^{-1}$, based on earlier studies in which we found that SR_s was $-1.2\ s^{-1}$ in normal segments and $-0.75\ s^{-1}$ in segments with wall motion score 2.[16] The cutoff for the normal segments was in between these numbers, because SR has a high variability and normal values must be defined with a wide confidence interval.

Intraobserver and interobserver variability was tested in 16 patients, 8 with normal dobutamine stress echocardiography and coronary angiography and 8 with acute myocardial infarction. We reanalyzed 18 segments from each, for a total of 288 segments. For the manual method, 251 infarcted and normal segments were randomly selected from the infarct population for intraobserver and interobserver variability.

Statistical Analysis

Measurements are presented as mean ± SD. One-way analysis of variance was used to compare mean values between the 4 methods, with post hoc analysis done using Scheffe's test. Area under the receiver operating characteristic (ROC) curve was used to compare sensitivity and specificity between methods. A P value $< .05$ was considered statistically significant. For intraobserver and interobserver variability, the Bland and Altman 95% limits of agreement and coefficient of variation (COV) were used.

RESULTS

Feasibility Data

In all, 799 segments (665 normal and 134 infarcted) were analyzed by all 4 methods. Between 20% and 25% of all segments analyzed using automated methods had to be discarded, compared with only 8% of segements analyzed manually (Table 1). Method 3 yielded the greatest number of analyzable segments for both SR_s and S_{es} (81.5% and 80.3%, respectively) of the automated methods, but still fewer than manual analysis (92.3% and 90.3%, respectively) (Table 1). Feasibility was lowest in the lateral and anterior wall, especially in the mid-lateral and apical anterior segments (Table 2).

Reverberation was the major cause for discarding segments, accounting for 50% of the discards in methods 1 and 2 and 54% of the discards in method 3. Dropouts (no data) were the second-leading cause, accounting for 21% of the discards in all methods. Misalignment of the imaging plane caused 10% of the discards in methods 1 and 2, and 9% of

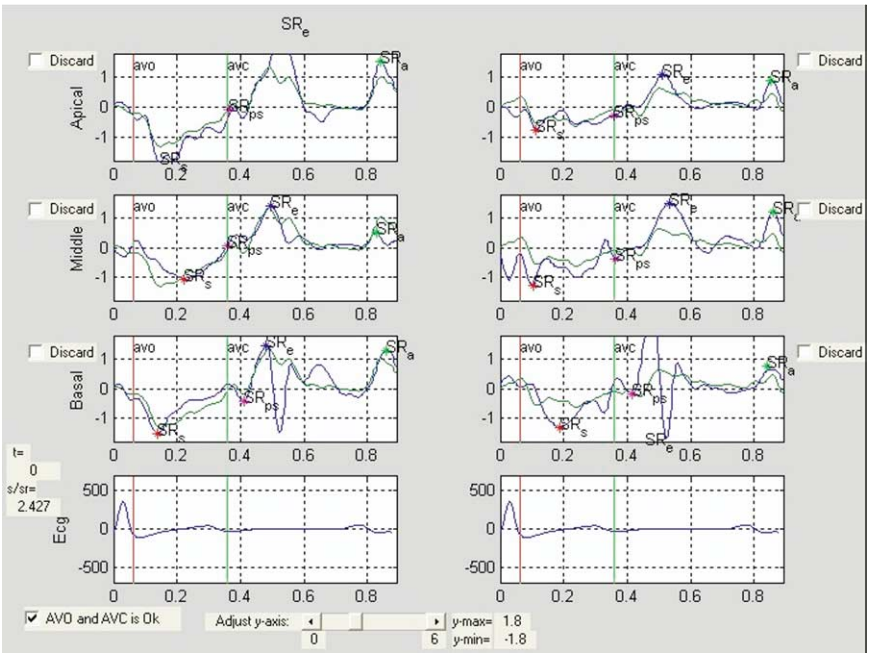

Figure 2 User interface for display and correction of the automated analysis results. The application shows SR or strain curves from all 6 segments simultaneously, in this case from a 4-chamber view, with septal segments to the left; lateral segments to the right; apical, mid-wall, and basal segments from the top downward; and the ECG waveform at the bottom. The darker curve is from the segment; the lighter curve is the average of the 3 segments in the wall for comparison. Timing of aortic valve opening (AVO) and closure (AVC) is imported from the Doppler recordings. Points representing SR_s, postsystolic strain rate (SR_{ps}), and peak strain rate during E and A waves (SR_e and SR_a, respectively) are suggested by the software, subject to manual correction. Finally, the segment can simply be discarded by ticking the appropriate boxes.

Table 1 Mean values for SR_s and S_{es} in normal and infarcted segments, for the 4 methods

	Method 1	Method 2	Method 3	Manual method
Normal segments SR_s (s^{-1})	−1.45 (0.53)	−1.48 (0.52)	−1.15 (0.32)***	−1.32 (0.44)
Normal segments S_{es} (%)	−18.3 (7.4)	−18.9 (7.6)	−16.9 (4.9)*	−17.3 (6.8)
Infarcted segments SR_s (s^{-1})	−0.60 (0.42)	−0.61 (0.45)	−0.61 (0.37)	−0.46 (0.27)**
Infarcted segments S_{es} (%)	−2.9 (8.3)	−3.3 (8.7)	−4.5 (6.1)	−4.0 (5.8)

A 16-segment model was used, and 988 normal segments and 169 infarcted segments were analyzed. In the normal group, mean SR_s for method 3 was significantly lower than in the other methods ($P < .001$). For S_{es}, there was a significant difference between methods 1 and 3 ($P < .05$). In the infarcted group, mean SR_s was significantly lower than in the other methods ($P < .01$). There were no differences for S_{es}.
S_{es}, End systolic strain rate; *SR_s*, peak systolic strain rate.
*$P < .05$; **$P < .01$; ***$P < .001$.

the discards in method 3. Segmental angle deviation of > 25 degrees between the wall and the ultrasound beam caused 9% of the discards in methods 1 and 2. Finally, tracking of the kernels was evaluated visually, and segments were discarded if the tracking did not follow the myocardium, even when any of the aforementioned problems were not visibly present. This was the case in 12% of the discarded segments in method 3.

Time Difference Manual/Automated Method

Full patient analysis, AVC, SR_s, postsystolic SR, peak early diastolic SR, peak late diastolic SR, S_{es}, and postsystolic strain of 16 segments from 3 apical views took about 2 minutes by automated analysis and 11 minutes by manual analysis.

Mean Values for the Different Methods

In the normal group, the mean SR_s was less in method 3 than in the other methods ($P < .001$) (Table 1). The difference for S_{es} was much smaller and not significant between method 3 and manual (Table 1). In the infarcted segments, SR_s was greater ($P < .01$) for the automated methods than manually, with no significant differences between the auto-

Table 2 Number of segments in which SR_s could be analyzed by the 4 methods

Segment level/wall	Number segments/ method	Method 1	Method 2	Method 3	Manual method
Basal	288	194	210	219	270
Mid	288	194	186	179	263
Apical	192	129	96	169	168
Septal	144	112	101	130	139
Lateral	144	77	81	100	134
Inferior	144	114	109	131	142
Anterior	144	83	80	86	116
Inferior lateral	96	66	58	64	89
Anterior septal	96	65	63	60	81

SR_s, Peak systolic strain rate.

mated methods. There was no difference between the methods for S_{es} in the infarcted segments (Table 1).

Frame Rate for B-Mode Images

In the B-mode frame rate study (frame rates of 70 FPS and 35 FPS), we analyzed 160 segments. SR_s was analyzable in 134 (84%) and 132 segments (83%), respectively. Slightly fewer segments were analyzable for S_{es} (128 and 129, respectively). Mean SR_s was -1.12 (0.31) s^{-1} at 70 FPS and -1.13 (0.42) s^{-1} at 35. Mean *Ses* was -18.7% (5.1%) and -19.1% (5.3%), respectively.

Sensitivity/Specificity/Accuracy/Receiver Operating Characteristic

In all, 56 segments (28 mid-infarcted and 28 normal) were analyzed by all methods (Figure 3). The normal value for SR_s was defined as ≤ -1 s^{-1}. Sensitivity was greatest for method 3 (100%), and specificity was greatest for method 3 and the manual method (96%) (Table 3). Accuracy was 96.2% for the manual method and 95.8% for method 3 (Table 3). The area under the ROC curve was 0.989 for method 1, 0.987 for method 2, 1.0 for method 3, and 0.994 for the manual method (Figure 4).

Reproducibility Data

The COV between the 3 automated methods was 15%–20%, with method 3 the lowest. The COV was almost the same for intraobserver and interobserver measurements. Reproducibility was the lowest in manual analysis, with the highest COV for interobserver analysis (Table 3).

DISCUSSION

The present study has demonstrated that automated analysis methods are feasible and faster than standard manual analysis, but they enable analysis of fewer segments. The automated methods still require some manual adjustments.

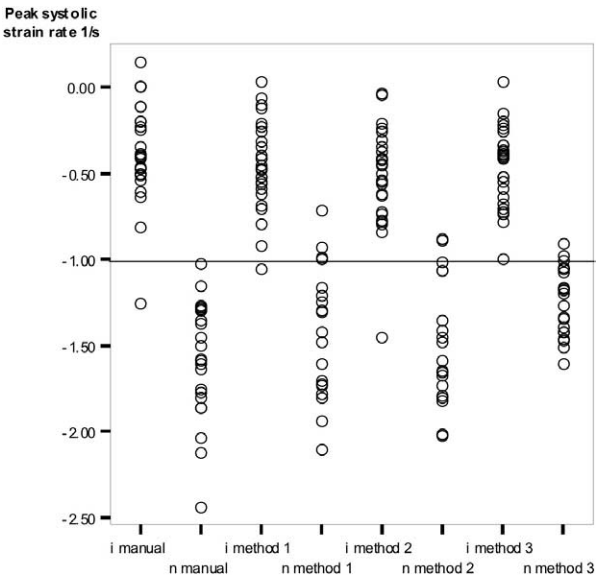

Figure 3 Scatterplot with SR_s values of 28 mid-infarcted segments (i) and 28 normal remote segments (n) of the same patient. All 4 methods used in the study are represented; the normal value for SR_s was defined as a value of ≤ -1 s^{-1}.

Feasibility of the Different Methods and Reasons for Exclusion

Method 3 had the greatest feasibility of the automated methods. Because of its angle independence, it was as feasible as manual analysis at the apex. Tracking the ROI (method 2) did not increase feasibility compared with stationary ROI (method 1). The major reason for exclusion of normal segments was reverberations, a difficult factor to improve in image quality. Angular deviation exceeding 25 degrees was of less importance. Manual analysis was the most feasible, probably because it was possible to adjust the ROI to avoid reverberations and unsuitable angular deviation.

Table 3 Sensitivity, specificity, accuracy and variability for normal and infarcted segments for SR_s

	Method 1	Method 2	Method 3	Manual method
Sensitivity %	96.4	96.3	100	96.4
Specificity %	90.5	90.5	95.8	96
Accuracy %	93.9	93.8	95.8	96.2
Intraobserver				
COV (%)	20	16	15	21
Total mean SR_s (s^{-1})	−1.36	−1.43	−1.30	−0.92
95% limits of agreement (lower, upper)	−0.54, 0.56	−0.42, 0.48	−0.38, 0.41	−0.38, 0.38
Bias	0.014	0.031	0.012	−0.001
Interobserver				
COV (%)	28	17	15	30
Total mean, SR_s (s^{-1})	−1.36	−1.38	−1.32	−1.1
95% limits of agreement (lower, upper)	−0.52, 0.55	−0.45, 0.51	−0.40, 0.40	−0.69, 0.67
Bias	0.016	0.034	0.001	−0.02

For sensitivity, specificity, and accuracy, 28 mid-infarcted and 28 remote normal segments were chosen with a cutoff value for normal segments of $SR_s \leq -1\ s^{-1}$. For intraobserver and interobserver variability for the manual method, only the patients with infarct were reanalyzed, not the normal group. For the other methods, segments were randomly selected from both groups; hence the differences in total mean values.
COV, Coefficient of variation; *SR_s*, peak systolic strain rate.

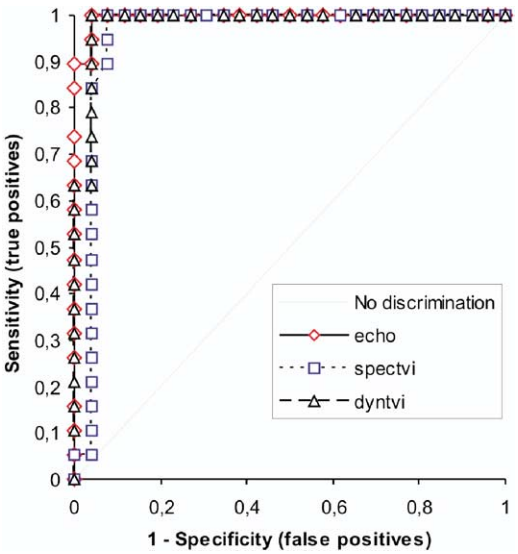

Figure 4 ROC curve of method 2 (dyntvi), method 3 (spectvi), and the manual method (echo). *ROC*, Reciever operating system.

Differences in Mean Values Among Methods

There were no differences in SR_s and S_{es} between methods 1 and 2, probably because of the poor spatial resolution of SRI based on tissue Doppler. Comparing the stationary ROI with the location of the Doppler beams, it was evident that the values calculated could include information from the other segments inside the ventricle or from the pericardium. However, the possible advantages of a dynamic ROI could not be verified in this study and may be of minor importance.

In normal segments, the mean value of SR_s was lowest in method 3. Because there were few differences between frame rates of 35 and 70 in the B-mode frame rate study, this finding probably was not due to undersampling. Noise spikes in the tissue Doppler–derived SR could result in excessively high values. The S_{es} measurements are little influenced by random noise, because negative noise and positive noise cancel out during integration. This is also indicated in the results; the mean value in normal segments was similar in method 3 and the manual method.

In the infarcted segments, SR_s was significantly greater for the automated methods than the manual method. This could be an effect of bias in placing the ROI, because the manual analysis was unblended. S_{es} was the same for method 3 and the manual method in both normal and infarcted segments. This lack of difference may be due to overestimation in tissue Doppler because of noise; speckle tracking–based SR may give more accurate values. On the other hand, the angle dependency of tissue Doppler–based SR is considered to be a problem. Angle deviation often results in underestimation. But method 3, which is angle-independent, results in the lowest values, and thus noise appears to be a more important source of error than angle deviation.

Advantages and Disadvantages of the Automated Methods

Table 4 summarizes the features of the different methods. Method 1 is not dependent on tracking but is based on a stationary ROI set in space, and thus is unable to follow the myocardium through the cardiac cycle. Methods 2 and 3 do not track well in walls with poor B-mode data, in which the unique speckle pattern of each point defining the segments in the myocardium cannot be repeated perfectly from frame to frame. This necessitates manual adjustment in about 25% of the total points. The

Table 4 Features of the different methods

Method	Feasibility in % for SR_s/S_{es}	Advantages	Disadvantages	Reproducibility (1 = highest; 4 = least)
Method 1	75.2% (SR_s)	B-mode independent	ROI fixed in space, not in myocardium	3
	66.9% (S_{es})	Time-saving	Angle-dependent	
Method 2	75.5% (SR_s)	ROI follows myocardium	Tracking dependent on B-mode data	2
	68.0% (S_{es})	Time-saving	Angle-dependent	
Method 3	81.5% (SR_s)	ROI follows myocardium	Tracking dependent on B-mode data and frame rate	1
	80.3% (S_{es})	Time-saving, Angle-independent		
Manual	92.3% (SR_s)	ROI can be adjusted within segment	Time-consuming, Angle-dependent	4
	90.3% (S_{es})		Fixed ROI	

ROI, Region if interest; S_{es}, end systolic strain; SR_s, peak systolic strain rate.

advantage of methods 2 and 3 is that the ROI stays in the same position relative to the myocardium. Methods 1 and 2 are angle-dependent, because SR is calculated along the ultrasound beam. The effect of the cosine of the insonation angle and/or the use of pericardial or cavity velocity could lead to either underestimation or overestimation.

The advantage of method 3 is that strain and SR can be measured directly by changes in segmental length and by tracking in 2 directions along the direction of the wall, rather than along the ultrasound beam; that is, it is angle-independent and measures longitudinal strain. The disadvantage of method 3 is if the algorithm fails to track one of the segment boundary points, then the measured strain values will be wrong for 2 segments (the 2 segments adjacent to the point). Method 3 is dependent on B-mode frame rate, but this is more important when measuring peak values in diastole and isovolumic phases. There was no difference in SR_s and S_{es} at 70 FPS compared with 35 FPS.

The manual method is extremely time-consuming and less objective compared with the automated methods. The ROI is fixed in space, not in the myocardium, and large lateral movements will influence measurements. However, reverberations can be avoided.

Infarcted Versus Normal Segments

Even though we used preselected segments to establish the accuracy of the methods, our findings demonstrate that the automated methods are as good as the manual method in distinguishing between infarcted and normal segments.

Reproducibility

Intraobserver and interobserver variability were greater than expected for automated analysis, with little difference seen among the methods. The manual method had the least reproducibility, probably because the ROI can be placed differently in the same segment.

Conclusion

Automated analysis methods are faster than and as accurate as manual analysis, but they cannot analyze as many segments as can be done manually. Automated analysis thus may increase the clinical feasibility of SRI. SR based on speckle tracking yielded lower SR_s, which, due to lower noise sensitivity, may be more accurate than tissue Doppler–based measurements. This possibility requires further study.

REFERENCES

1. Heimdal A, Stoylen A, Torp H, Skjaerpe T. Real-time strain rate imaging of the left ventricle by ultrasound. J Am Soc Echocardiogr 1998;11:1013-9.
2. Kaluzynski K, Chen X, Emelianov S, Skovoroda A, O'Donnell M. Strain rate imaging using two-dimensional speckle tracking. IEEE Trans Ultrasonogr Ferroelectr Freq Control 2001; 48:1111-23.
3. Kirkhorn J, Bjaerum S, Olstad B, Kristoffersen K, Torp H. A new technique for improved spatial resolution in high-frame-rate color Doppler imaging. Proc IEEE Ultrason Symp 2003; 1:1947-50.
4. Torp A, Rabben S, Stoylen A, Ihlen H, Andersen K, Brodin L, et al. Automatic detection and tracking of left ventricular landmarks in echocardiography. Proc IEEE Ultrason Symp 2004 (In press).
5. Heimdal A. Doppler-based ultrasound imaging methods for noninvasive assessment of tissue viability. Doctoral thesis, Norwegian University of Science and Technology, Norway, 1999.
6. Stoylen A. Strain rate imaging by ultrasonography in the diagnosis of coronary artery disease. J Am Soc Echocardiogr 2000;13:1053-64.
7. Castro PL, Greenberg NL, Drinko J, Garcia MJ, Thomas JD. Potential pitfalls of strain rate imaging: angle dependency. Biomed Sci Instrum 2000;36:197-202.
8. Rabben S, Irgens F, Haukanes A, Smiseth O. An analysis of the angle dependence in strain (rate) imaging of the left ventricle. Proc IEEE Ultrason Symp 2003;1:13-6.
9. D'Hooge J, Bijnens B, Thoen J, Van de Werf F, Sutherland GR, Suetens P. Echocardiographic strain and strain-rate imaging: a new tool to study regional myocardial function. IEEE Trans Med Imaging 2002;21:1022-30.

10. Bohs L, Geiman B, Anderson M, Gebhart S, Trahey G. Speckle tracking for multi-dimensional flow estimation. Ultrasonics 2000;38:369-75.
11. Bonnefous O, Pesque P. Time domain formulation of pulse-Doppler ultrasound and blood velocity estimation by cross-correlation. Ultrason Imaging 1986;8:73-85.
12. Trahey G, Hubbard S, von Ramm O. Angle-independent ultrasonic blood flow detection by frame-to-frame correlation of B-mode images. Ultrasonics 1988;26:271-6.
13. Stoylen A. Problems and pitfalls of strain rate imaging. Available at: *http://www.ntnu.no/~stoylen/strainrate/Howto/Pitfalls.html*; Accessed on September 3, 2004.
14. Bohs L, Trahey G. A novel method for angle-independent ultrasonic imaging of blood flow and tissue motion. IEEE Trans Biomed Eng 1991;38:280-6.
15. Schiller NB. Recommendations for quantitation of the left ventricle by two-dimensional echocardiography. American Society of Echocardiography Committee on Standards, Subcommittee on Quantitation of Two-Dimensional Echocardiograms. J Am Soc Echocardiogr 1989;2:358-67.
16. Stoylen A, Heimdal A, Bjornstad K, Wiseth R, Vik-Mo H, Torp H, et al. Strain rate imaging by ultrasonography in the diagnosis of coronary artery disease. J Am Soc Echocardiogr 2000;13:1053-64.

Paper III and IV are not included due to copyright restrictions.